

ROBUST ADAPTIVE CONTROL OF ELECTRO-
HYDRAULIC SERVO SYSTEM SUBJECT TO
DISTURBANCE AND PARAMETER
UNCERTAINTY

BY

AYINDE BABAJIDE ODUNITAN

A Thesis Presented to the
DEANSHIP OF GRADUATE STUDIES

KING FAHD UNIVERSITY OF PETROLEUM & MINERALS

DHAHRAN, SAUDI ARABIA

In Partial Fulfillment of the
Requirements for the Degree of

MASTER OF SCIENCE

In

SYSTEMS ENGINEERING

FEBRUARY 2015


KING FAHD UNIVERSITY OF PETROLEUM & MINERALS
DHAHRAN 31261, SAUDI ARABIA

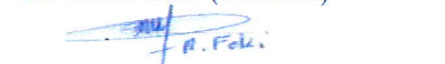
DEANSHIP OF GRADUATE STUDIES

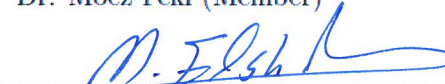
This thesis, written by **AYINDE BABAJIDE ODUNITAN** under the direction of his thesis adviser and approved by his thesis committee, has been presented to and accepted by the Dean of Graduate Studies, in partial fulfillment of the requirements for the degree of **MASTER OF SCIENCE IN SYSTEMS ENGINEERING**.


Thesis Committee



Dr. Sami El Ferik (Advisor)



Dr. Salim Ibrir (Member)


Dr. Moez Feki (Member)


Dr. Moustafa Elshafei (Member)


Dr. AbdulWahid Al-Saif (Member)


Dr. Adel Ahmed
For Department Chairman


Dr. Salam A. Zummo
Dean of Graduate Studies

Date

25/2/15



©Ayinde Babajide Odunitan
2015

To

My Father, my late Mother, Felicia Mojisola Ayinde, My beloved wife, Ajoke Ayinde and my siblings.

ACKNOWLEDGMENTS

I would like to express my gratitude to my supervisor, Dr. Sami El Ferik for his valuable contributions, guidance and support towards the completion of this thesis. My appreciation also goes to Dr Salim Ibrir for his heart of gold and all the knowledge impacted and also for being one of my thesis committee members.

I also want to thank Dr. AbdulWahid Al-Saif, Dr. Moustafa Elshafei and Dr. Moez Feki, for their suggestions on this work. I am forever indebted to my father for his love, to my wife for her encouragements and patience at all time and to my siblings for their support. I am grateful to all my friends and colleagues at KFUPM for the nice and tough times we shared together. A big thank you to everybody who contributed in one way or the other to the success of this thesis.

TABLE OF CONTENTS

LIST OF TABLES	vi
LIST OF FIGURES	vii
LIST OF ABBREVIATIONS	xi
ABSTRACT (ENGLISH)	xii
ABSTRACT (ARABIC)	xiv
CHAPTER 1 INTRODUCTION	1
1.1 Motivation	3
1.2 Thesis Objectives	4
1.3 Thesis Outline	5
CHAPTER 2 LITERATURE REVIEW	6
2.1 Modeling of Electrohydraulic Servo System	6
2.2 Control of Electrohydraulic Servo System	8
CHAPTER 3 NOTATION AND BASIC KINEMATICS OF ELECTRO HYDRAULIC SERVO VALVE	13
3.1 Model of a spool Valve Controlled Piston	15
3.2 Electrohydraulic Servo Valve Dynamic Equations	19
CHAPTER 4 BACKSTEPPING BASED CONTROLLER DESIGN	20
4.1 Controller Design with a Constant Gain	23
4.2 Controller Design with a Time-Varying Gain	27

4.3	Controller Design using Sliding Mode Control with Discontinuous Surface	34
4.3.1	Controller Design using Classical Sliding Surface	34
4.3.2	Controller Design with Discontinuous Surface	38
4.4	Results and Discussion	41
CHAPTER 5 OBSERVER DESIGN		47
5.1	Backstepping based Observer Design	49
5.2	Results and Discussion	57
CHAPTER 6 ROBUST ADAPTIVE CONTROL DESIGN		60
6.1	Results Discussion	67
6.2	High-Gain Adaptive Observer Design	69
6.3	Simulation Results for the High-Gain Adaptive Observer Design .	76
6.3.1	Results Discussion	79
6.4	Results and Discussion	88
CHAPTER 7 CONCLUSIONS AND FUTURE WORK		93
7.1	Conclusions	93
7.2	Future works	94
REFERENCES		96
VITAE		103

LIST OF TABLES

3.1	Nomenclature	16
4.1	Numerical value for simulations	46
6.1	Numerical value for simulating the high gain adaptive observer . .	77
6.2	Numerical values for simulations	89

LIST OF FIGURES

1.1	Vibrator-ground schematic	1
1.2	Seismic survey process	2
1.3	A cross-section of a deployed vibrator	3
3.1	Basic circuit of a hydraulic seismic vibrator.	14
3.2	Basic circuit of a hydraulic seismic vibrator.	15
3.3	Electro-hydraulic System	15
4.1	Closed-loop controller scheme	23
4.2	Backstepping controller with constant feedback gain, using constant reference ($r = 20\text{cm}$) and under constant disturbance ($d(t) = 0.1$)	28
4.3	Backstepping controller with constant feedback gain, using constant reference ($r = 20\text{cm}$) and under sinusoidal disturbance ($d(t) = 0.1\sin(t)$)	29
4.4	Backstepping controller with constant feedback gain, using sinusoidal reference ($r = 0.05\sin(t)\text{m}$) and under constant disturbance ($d(t) = 0.1$)	30
4.5	Backstepping controller with constant feedback gain, using sinusoidal reference ($r = 0.05(\sin(t) + \sin(2t) + \sin(3t))\text{m}$) and under constant disturbance ($d(t) = 0.1$)	31
4.6	Backstepping controller with time-varying feedback gain, using constant reference ($r=0.2\text{m}$) and under constant disturbance ($d(t) = 0.1$)	35
4.7	Backstepping controller with time-varying feedback gain, using constant reference($r = 0.3\text{m}$) and under constant disturbance($d(t) = 0.1$)	36

4.8	Backstepping controller with time-varying feedback gain, for sinusoidal reference ($r = 0.05(\sin(t))\text{m}$) and under constant disturbance ($d(t) = 0.1$)	37
4.9	Backstepping Controller with time-varying feedback gain, using sum of sinusoids reference($r = 0.05(\sin(t) + \sin(2t) + \sin(3t))\text{m}$) and under constant disturbance ($d(t) = 0.1$)	38
4.10	Backstepping controller for reference ($0.05\sin(2\pi ft)\text{m}$) with sweep frequency $f=5$ Hz	39
4.11	Backstepping controller for reference ($0.05\sin(2\pi ft)\text{m}$) with sweep frequency $f=10$ Hz	40
4.12	Backstepping controller for reference ($0.05\sin(2\pi ft)\text{m}$) with sweep frequency $f=15$ Hz	41
4.13	Backstepping controller for reference ($0.05\sin(2\pi ft)\text{m}$) with sweep frequency $f=17$ Hz	42
4.14	SMC under constant disturbance[$d(t) = 0.1$]	43
4.15	SMC and Backstepping controller with time-varying feedback gain, using constant reference ($r = 0.2\text{m}$) and under constant disturbance ($d(t) = 0.1$)	44
4.16	SMC and Backstepping controller with time-varying feedback gain, using constant reference ($r = 0.3\text{m}$) and under Constant disturbance($d(t) = 0.1$)	45
4.17	SMC and Backstepping controller with time-varying feedback gain, using constant reference ($r = 0.3\text{m}$) and under time-varying disturbance ($d(t) = 0.3\sin(t)$)	46
5.1	Controller using estimated states	49
5.2	Behavior of the observer and hydraulic servo system using a constant feedback gain (λ) and under a constant disturbance	55
5.3	Behavior of the observer and hydraulic servo system under a sinusoidal disturbance using a constant feedback gain (λ)	56

5.4	Behavior of the observer and hydraulic servo system under a constant disturbance using a constant feedback gain (λ). Reference($r = 10\sin(t)$ cm)	57
5.5	Behavior of the observer and hydraulic servo system under a constant disturbance using a constant feedback gain (λ). Reference($r = 10\sin(t)$)cm)	58
5.6	Behavior of the observer and hydraulic servo system under a constant disturbance using a constant feedback gain (λ). Reference($r = 0.05(\sin(t) + \sin(2t) + \sin(3t))m$)	59
5.7	Behavior of the observer and hydraulic servo system under a constant disturbance using a constant feedback gain (λ). Reference($r = 0.05(\sin(t) + \sin(2t) + \sin(3t))m$)	59
6.1	Adaptive Control Scheme	61
6.2	Behavior of the hydraulic servo system under a constant disturbance, Reference($r = 30$ cm)	68
6.3	The error plots	69
6.4	Behavior of the hydraulic servo system under a constant disturbance, Reference($r = 10\sin(t)$)cm)	70
6.5	The error using Reference($r = 10\sin(t)$)cm)	71
6.6	Behavior of the hydraulic servo system under a constant disturbance, Reference($r = 0.05(\sin(t) + \sin(2t) + \sin(3t))m$)	72
6.7	The error using Reference($r = 0.05(\sin(t) + \sin(2t) + \sin(3t))m$)	73
6.8	Schematic of Adaptive Output Feedback Control.	74
6.9	Behavior of the observer and hydraulic servo system under a constant disturbance using a constant feedback gain (λ). Reference($r = 0.3m$)	77
6.10	Estimation error when $r = 0.3m$	77

6.11 Behavior of the observer and hydraulic servo system under a constant disturbance using a constant feedback gain (λ). Reference($r = 10\sin(t)$ cm)	78
6.12 Estimation error when $r = 10\sin(t)$ cm	78
6.13 Tracking error when $r = 10\sin(t)$ cm	79
6.14 Behavior of the observer and hydraulic servo system under a constant disturbance using a constant feedback gain (λ). Reference($r = 0.05(\sin(t) + \sin(2t) + \sin(3t))$ m)	80
6.15 Estimation error when ($r = 0.05(\sin(t) + \sin(2t) + \sin(3t))$ m) . .	81
6.16 Tracking error when ($r = 0.05(\sin(t) + \sin(2t) + \sin(3t))$ m) . . .	82
6.17 A more detailed vibrator-ground model prototype [1].	83
6.18 Behavior of the hydraulic servo system with $r = 30$ cm	90
6.19 Behavior of the hydraulic servo system with $r = 10\sin(t)$ cm . . .	90
6.20 Behavior of the hydraulic servo system $r = 0.05(\sin(t) + \sin(2t) + \sin(3t))$ m	91
6.21 Behavior of the perturbed hydraulic servo system under an adaptive control with time-varying gain.	92

LIST OF ABBREVIATIONS

<i>EHSS</i>	Electro-Hydraulic Servo System
<i>SMC</i>	Sliding Mode Control
<i>PID</i>	Proportional-Integral-Derivative
<i>ABC</i>	Artificial Bee Colony
<i>DPSO</i>	Dynamic Particle Swarm Optimization.
<i>AI</i>	Artificial Intelligence
<i>MR</i>	Reaction mass
<i>MB</i>	Baseplate mass

THESIS ABSTRACT

NAME: Ayinde Babajide Odunitan

TITLE OF STUDY: Robust Adaptive Control of Electro-hydraulic Servo System Subject to Disturbance and Parameter Uncertainty.

MAJOR FIELD: SYSTEMS ENGINEERING

DATE OF DEGREE: FEBRUARY 2015

This thesis addresses the control of hydraulic servo system rod subject to uncertainty in parameters and to an unknown but bounded disturbance. The proposed backstepping-based robust controller guarantees a uniformly ultimately bounded tracking error leading to practical stability of the closed loop system. Three schemes are proposed. First, a constant gain-based controller that achieves a good tracking accuracy with a steady state error in the millimeter range, but induces control input oscillations in transient. To improve such behavior, a second controller with time varying gain is proposed. Both controllers assure robustness against perturbations and uncertainties in the dynamics of the system. A high gain observer is designed using backstepping approach to estimate the immeasurable states of the system. Lastly, a robust adaptive backstepping based controller is developed. The tracking error between reference input and the output of the

system is the performance metric used. The state observer is also employed to estimate the states of the system under the adaptive feedback. The proposed robust adaptive backstepping-based controller guarantees a uniformly ultimately bounded tracking error leading to practical stability of the closed loop system.

ملخص الرسالة

الاسم الكامل: أيندى باباجيدى اوديتون

عنوان الرسالة: تحكم متأقلم متين لنظام أتمتى الكترو هيدروليكي بهدف الأضطرابات وعدم الثبات فى المتغيرات

التخصص: هندسة نظم وتحكم

تاريخ الدرجة العلمية: فبراير 2015

هذة الأطروحة تناقش التحكم فى عمود لنظام أتمتى هيدروليكي تستند الى عدم ثبات فى قيم العناصر بالإضافة الى أضرابات محدودة و غير معروفة. متحكم التراجع المتين المقترح يضمن تتبع الخطأ حول حدود محددة تؤدي لأتزان النظام فى الدورة المغلقة. ثلاثة مخططات سوف تقترح. الأول عنصر ربح ثابت يصل الى دقة تتبع مقبولة مع حالة ثبات الخطأ بحدود المليميتر لكن مع تذبذب فى إشارة الدخل. لتحسين هذا السلوك تم اقتراح متحكم مع ثابت ربح متغير مع الوقت. كلا من المتحكمين يضمنان الثبات ضد الأضرابات و المتغيرات العشوائية فى النظام المتحرك. ثابت ربح مراقب عالى مصمم بإستخدام نهج متحكم متراجع لتقييم حالات النظام الغير مقاسة. أخيرا تحكم متأقلم تراجعى متين سيصمم. اداء قياسى أستخدم لتحديد الخطأ التتبعى بين أصل الدخل وخرج النظام. مراقب الحالة أستخدم أيضا لتقييم حالات النظام بإستخدام المتحكم المتأقلم. المتحكم المقترح المتأقلم المتين التراجعى يضمن انتظام حدود تتبع الخطأ التى تؤدي لأتزان النظام فى الدورة المغلقة.

CHAPTER 1

INTRODUCTION

Electro-hydraulic servo systems (EHSS) are ubiquitous in the industries due to their inherent ability to deliver fast and power responses. They have been found useful in many industrial applications ranging from aerospace to manufacturing. EHSS also find applications in safety critical missions such as flight control. Moreover, this type of system is an integral part of the equipment called the vibroseis used for soil testing in Seismic applications [2]. The efficiency of the vibroseis depends greatly on the ability of the vibrator to synchronously generate repeated ground-force sweep over a broad range of frequency [1]. The ground and baseplate of the vibrator has the configuration shown in Fig. 1.1.

The notion of using vibroseis method in seismic data acquisition is to radiate

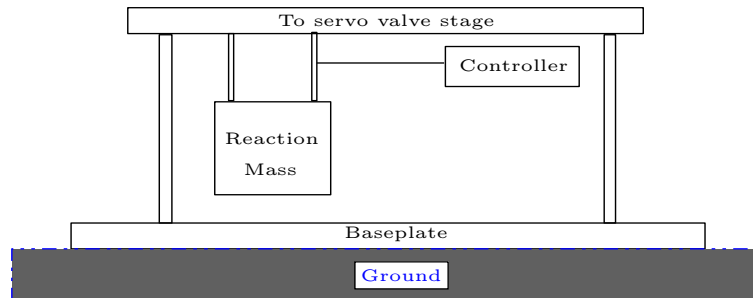


Figure 1.1: Vibrator-ground schematic

a theoretically prescribed frequency modulated signal into the earth. The the-

oretical sweep can easily be created using electronic generator and transformed into oscillations of the baseplate. Typically, the transformation is done using the hydraulic supply and servo-valve [3]. Due to low rigidity of the vibrator baseplate and the surface unevenness, the contact stiffness between the ground and the baseplate varies greatly. Fig. 1.2 emphasizes the detailed steps in the survey [4]. Consequently, the variation in the contact stiffness yields a nonlinear and unpredictable distortion of the original sweep signal. A cross section of the vibrator in contact with the ground is shown in Fig. 1.3.

In order to mitigate the discrepancy between the theoretical sweep (the input

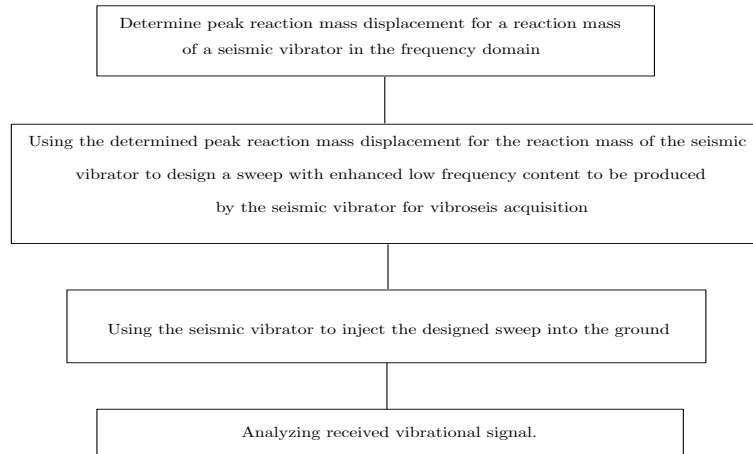


Figure 1.2: Seismic survey process

to the system) and the actual motion of the baseplate (output of the vibroseis system), a sophisticated vibrator control system has to be employed. It has been established in [3] that displacement is a better feature of the baseplate motion that represents the seismic signal entering the earth over its counterpart, the ground force. One of the many advantages of using displacement as the source signature is its measurability unlike the ground force that has to be estimated with significant

and unknown uncertainty [3].

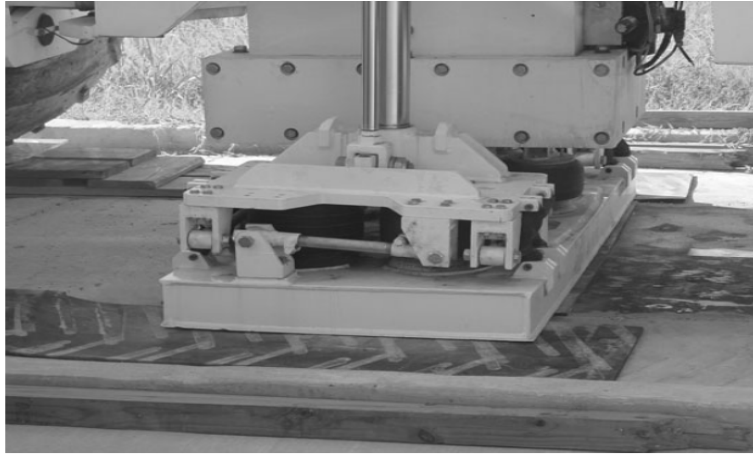


Figure 1.3: A cross-section of a deployed vibrator

1.1 Motivation

The primary motivation behind this work is to design a control strategy for EHSS that can be implemented on a vibroseis. The model of the servovalve used in this thesis, describes the fluid flow without neglecting the occurrence of leakage due to fabrication imperfections. Owing to the fact that the system's model is highly nonlinear, the control design for these type of system is never trivial. Due to the nature of applications this system is used for, the model is susceptible to parameter variations, component failures and disturbances. Hence, robust control laws are generally opted for.

One of the major drawbacks of all state-feedback control methodologies is that the feedback is dependent on the states of the system under control. Practically, availability of the states measurements may be inconceivable because sometimes

either the measurements are impossible or are possible, but too expensive [5]. In the case of electrohydraulic servo systems, measuring the differential pressure is a costly task and requires high technology procedure to avoid additional leakage [6]. To circumvent around this problem, a robust adaptive observer that can estimate states is required. Subsequently, the estimated states from the observer can be used to compute the control signal. For the sake of simplicity, the observer is designed separately from the controller.

1.2 Thesis Objectives

In this thesis, an adaptive backstepping-based robust controller is proposed that guarantees a uniformly ultimately bounded tracking error leading to a practical stability of the closed loop system. This thesis is structured in three folds. First, we propose a constant gain backstepping-based robust controller that can achieve a good tracking accuracy with a steady state error in the millimeter range, but induces control input oscillations in transient. To improve on such undesired behavior, a second controller with time varying gain is proposed. Both controllers assure robustness against perturbations and uncertainties in the dynamics of the system. The results of these two aforementioned proposed controllers are benchmarked with a recently proposed sliding mode controllers with discontinuous surfaces. Secondly, an observer was constructed to estimate the states of the system that are not available.

Furthermore, a robust adaptive output feedback control based on backstepping

technique is proposed that adapts to parameter changes and external disturbance. Finally, the stability analysis of all the aforementioned controllers is proved using the Lyapunov approach.

1.3 Thesis Outline

- Chapter 2 presents the literature about the modeling and control of the EHSS model that will be used throughout this thesis..
- Chapter 3 gives the notation, basic kinematics and Dynamical Equations of the Electrohydraulic servo valve.
- Chapter 4 presents both the constant-gain and time-varying gain controller design based on the backstepping method and the simulation results. Also in this section, the results of the controllers are benchmarked with other recent controllers in the literature.
- Chapter 5 presents the observer design for the EHSS and the simulation results.
- Chapter 6 presents the robust adaptive feedback control and observer design based on backstepping technique and the simulation results as well.
- Chapter 7 concludes the thesis .

CHAPTER 2

LITERATURE REVIEW

All the applications mentioned in the introduction however, demand an extremely high precision position control of the spool valve. Due to the fluid inflow and outflow in the servo valve, friction on the actuators, as well as the moving part of the valve, the dynamics of these systems are highly nonlinear. Also, phenomena such as entrapment of air inside the hydraulic valve, parameters variations (due to temperature changes), unknown model errors and perturbations all contribute to the challenges faced in various attempts to control such systems. This type of system exhibits a high degree of nonlinearity and non-differentiability due to inherent characteristics such as leakage, friction and the fluid flow in and out of the valve [7].

2.1 Modeling of Electrohydraulic Servo System

An accurate model of the electrohydraulic system is necessary to implement various control strategies for high precision position control. System identification

is used in [8] to model the electro-hydraulic actuator servo system dynamics using a linear model approximation. The advantage of this method is that an apriori knowledge of the system is not necessarily required. Also in [9], Hao et al. use the simulative data and theory to model the main spool flow field of the servo valve.

The importance of friction effects in modeling an hydraulic servo system cannot be over-emphasized since, friction is an inherent feature of all machine incorporating parts with relative motion [10]. By considering all the difficulties involved in accurately modeling the friction, authors in [11] presented a LuGre model-based adaptive control scheme which gives a better estimation of the friction, good disturbance rejection and general robustness to uncertainties in parameters.

In [12], authors implemented a novel variable structure controller which lumps both the friction and load as external disturbances. System model identification coupled with an adaptive Fuzzy PID control can also be used to obtain a more accurate model and controller for the electro-hydraulic servo system [13]. The most accurate model used in this work incorporates leakages in the servo valve and nonlinear friction compensation at the load end [6].

2.2 Control of Electrohydraulic Servo System

Despite the high level of nonlinearities involved in the dynamics of electrohydraulic servo systems, linear control theory and concepts are often used to simplify the complexity involved in the control analysis. In [14], system's linearization around an operating condition followed by pole placement methods were used to control the system. Susceptibility to poor performance is one of the major drawbacks of the closed-loop system whenever the system strays from the desired operating condition due parameter changes.

In addition, linear control design methods cannot guarantee the same performance of the closed loop control system all over the operating range [15]. In order to improve the precision and robustness of a linear PID, a feedback-feedforward iterative learning controller was developed in [11]. The feedforward part of the controller aims at improving the precision while the feedback makes the closed-loop system more robust.

Auto-disturbance rejection and feedback controller was used for position control of an electro-hydraulic system with both internal and external disturbances [16]. Also a nonlinear adaptive feedback linearization position control with load disturbance rejection and friction compensation was proposed in order to mitigate the effect of external load variation and coulomb friction [17].

Artificial intelligent (AI) approaches are also used for nonlinear friction compensation. In [10], a neuro-fuzzy approach which is based on support vector machine friction compensation. This technique was used to enhance the position

tracking and also to reduce the high steady state error and overshoot problems which tend to surface whenever there is nonlinearity in the friction. Dynamic particle swarm optimization (DPSO) based algorithm has also been used to improve the precision of position control [18].

In an attempt to compensate for the negative effects of fluid leakage across a faulty actuator piston seal, a fractional order controller based on micro artificial bee colony (ABC) algorithm was developed by authors to control a servo-hydraulic position system. Non-model based adaptive control scheme with high tracking accuracy even in the presence of disturbance, parameter variations and uncertain nonlinearities was developed. The controller works well even without any apriori knowledge of the model of the system [15].

In [6, 19, 20], sliding mode techniques are employed in controlling the position of the hydraulic servo. The results by these authors show a high precision in position tracking even when the plant is subjected to external disturbance. Adaptive sliding mode approach was used in [21] to mitigate the effect of uncertainties in the system. One of the shortcomings of implementing sliding mode controller is that the control law is discontinuous, and due to the rapid switching, there are tendencies to observe phenomena such as input discontinuity and fast chattering.

Backstepping is a design strategy that employs a recursive approach in formulating the control law [22] and it is often used for designing stabilizing controls for some class of dynamical nonlinear systems. This method is developed by inserting new variables that depends on the state variables, controlling parameters

and the stabilizing functions. The essence of this stabilizing function is to redress any nonlinearity that can impede the stability of the system. Due to the recursive nature of the control design, formulation of the controller generally starts with a well known stable system. Subsequently, virtual controllers are employed to help stabilize the outer subsystems progressively. The process of using the virtual controllers in the stabilization of the subsystem continues until the external control is accessible. In fact, it has been shown that backstepping technique can be used to force nonlinear systems to behave like a linear system transformed into a new set of coordinates [23].

One of the numerous advantages of using backstepping technique in designing a controller is its ability to avoid useful nonlinearity cancelation. The objective of backstepping gravitates towards stabilization and tracking in contrast with its corresponding feedback linearization method. Furthermore, backstepping approach has been found to relax matching conditions on perturbations. This helps facilitate controller designs for perturbed nonlinear system even if the perturbation is nowhere around the equation containing the input.

Backstepping method is generally used for tracking and regulation problems [22]. Authors in [24] use backstepping based neural adaptive technique to control the velocity of the electro hydraulic system subject to internal friction, flow nonlinearity and noise. Combination of 3 different types of controllers were used to stabilize the system.

Most importantly, electrohydraulic system's parameters are subject to variation

due to temperature rise. For instance, bulk modulus viscous friction coefficients are prone to variation due to temperature fluctuations. Owing to the fact that backstepping controller design relies on actual system's parameters, the need arises to design a controller that adapts to these changes.

To overcome the problem of variation in parameters, authors in [25–27] employed adaptive control schemes. In controlling electro-hydraulic systems, adaptive schemes suffer a serious setback if the uncertain parameter is the supply pressure difference which happens to appear in a square-root in the dynamics of the system. This setback is because traditional adaptive schemes demand the system to be linear in uncertain parameters. Lyapunov approach was used in [2] to design an enhanced feedback linearization-based controller for electro-hydraulic servo systems with supply pressure uncertainties/changes.

In [28], an adaptive position control of an electrohydraulic system with variations in supply pressure is proposed. The gradient method based on the augmented error is used to estimate the unknown parameters and the control was able to achieve a closed loop stability. Position control has also been tackled using indirect adaptive backstepping technique and the influences aside chattering and saturation effects of the tuning parameters of the error dynamics. A part of the dynamics of the hydraulic system was considered a norm-bounded uncertainty in [29,30] and two backstepping based adaptive controllers that force the tracking error converges to zero are designed.

Each of these aforementioned controllers has its inherent weakness, for in-

stance in sliding mode control, the control law is discontinuous, and fast switching (chattering) is possible. For the feedback linearization, the linearization becomes incorrect and create unstable closed loop system, if there is parameter changes present in the system. For the backstepping technique, it is easier to find a Lyapunov function and the feedback can easily be formulated if all state variables are measurable. A nonlinear observer can be used to estimate the immeasurable states and parameter variations can be easily dealt with by . Based on this, we developed an adaptive nonlinear output feedback control for the electrohydraulic system that overcomes all the disadvantages using nonlinear adaptive backstepping techniques.

CHAPTER 3

NOTATION AND BASIC KINEMATICS OF ELECTRO HYDRAULIC SERVO VALVE

The fundamental step in dynamic system analysis, design and control is obtaining a mathematical model. The general dynamics and kinematics equations for EHSS are presented in this section. As earlier mentioned in the introductory part of this work, one of the key applications of EHSS is the vibrator system used in seismic data acquisition. The schematic of the hydraulic seismic vibrator is as shown in Fig. 3.1. The flow of hydraulic fluid is supplied by the variable displacement pressure-compensated piston pump which is driven by the engine in Fig. (3.1). Particles that enter the system through hose interior or seals are removed through the use of filters [31]. The flow through the servo valve drives the reaction mass (MR) upward thereby generating a reaction force that is applied to a piston that is coupled to the earth with the help of the baseplate (MB). Simultaneously, the fluid in the upper chamber of the piston leaves through the lower chamber back into the servo-valve and subsequently back into the pump.

All the flow losses as a result of leakage are compensated for with the help

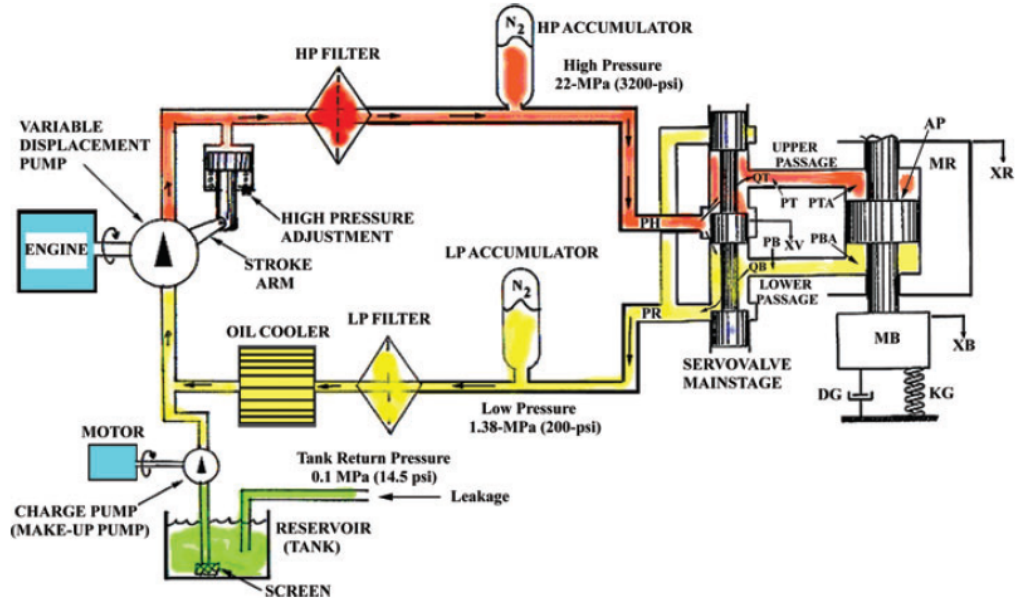


Figure 3.1: Basic circuit of a hydraulic seismic vibrator.

of the charge pump. In order to maintain a good contact between the baseplate and the load (earth) while is dynamically driven, a hold-down system is used. The system pressure is maintained using the accumulators whenever transient flow occurs. These accumulators must be placed very close to the servo valve to effectively damp all the transient effect [31].

The passage of the spool valve system is analogous to a transmission line in the electrical sense where the hydraulic flow is like the current and the pressure is like the voltage as depicted in Fig. 3.2 below. Using similar analogy, a capacitor represents the combined effect of the fluid compressibility and passage compressibility, an inductor is seen as the mass of the fluid and the resistance as the passage flow resistance.

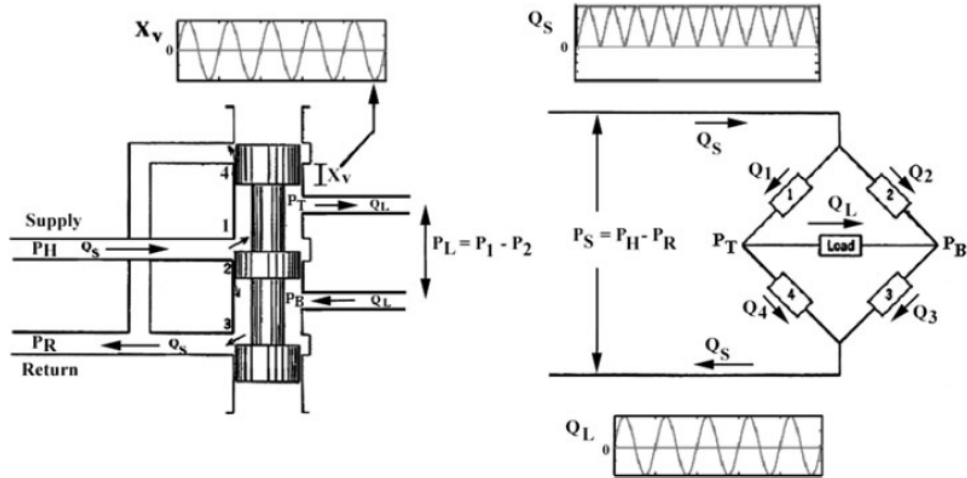


Figure 3.2: Basic circuit of a hydraulic seismic vibrator.

3.1 Model of a spool Valve Controlled Piston

Pistons are referred to as linear hydraulic actuation devices. Depending on what controls the actuation devices, they can be categorized into either pump controlled or valve controlled [32]. In this section of the thesis, we focus on the valve-controlled pistons.

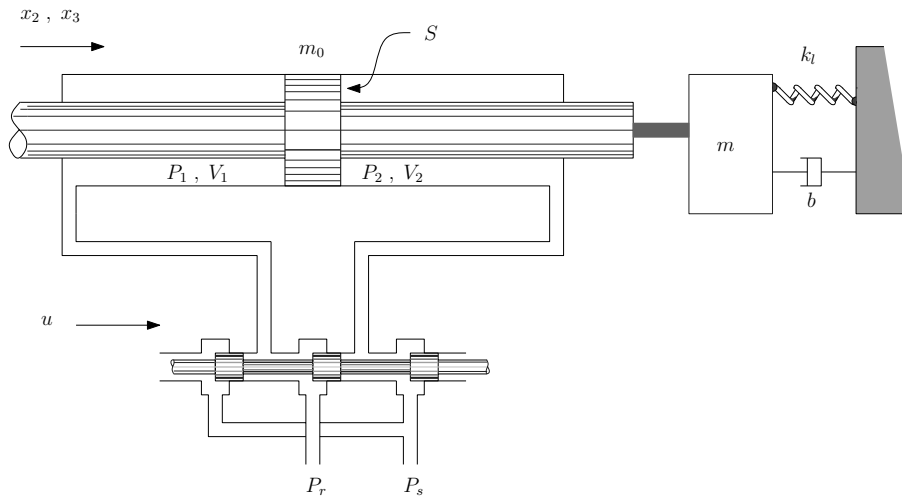


Figure 3.3: Electro-hydraulic System

Symbol	Definition
V_1	volume of the forward chamber (includes valve, connecting hose and piston), m^3
V_2	volume of the return chamber (includes valve, connecting hose and piston), m^3
V_{10}	initial volume of forward chamber, m^3
V_{20}	initial volume of return chamber, m^3
S_1, S_2	piston surface area of each side, m^2
x_p	piston position relative to the middle of the stroke, m
l_p	full stroke length of the piston, m
v	velocity of the piston, m/s
m_o	mass of the piston
m	mass of the load, kg
i	input current, mA
k_l	Load spring gradient, N/m
b	viscous damping coefficient, Ns/m
k	flow gain constant, Ns/m
P_s, P_r	supply and return pressure, Nm^{-2}
P_s, P_r	pressures in upper and lower chambers, Nm^{-2}

Table 3.1: Nomenclature

The dynamics of the EHSS depicted in Fig. 3.3 can be represented by the set of ordinary nonlinear differential [32] in Eq. (3.1). The spool consists of a four-way spool valve, supplying a double effect linear cylinder with a double rodded piston. The piston exerts a force on a load modeled by a mass, spring and a sliding viscous friction.

$$\begin{aligned}
\frac{dP_1}{dt} &= \frac{B}{V_o + Sx_p}(Q_1(i, P_1) - S_1v), \\
\frac{dP_2}{dt} &= \frac{B}{V_o - Sx_p}(Q_2(i, P_2) - S_2v), \\
\frac{dv}{dt} &= \frac{1}{m+m_o}(S_1P_1 - S_2P_2 - bv - k_l(x_p - x_{po})), \\
\frac{dx_p}{dt} &= v + d(t).
\end{aligned} \tag{3.1}$$

with

$$Q_1(i, P_1) = \begin{cases} ki\sqrt{P_s - P_1} + \frac{\alpha}{1+\gamma i}(P_s - P_1) - \frac{\alpha}{1+\gamma i}(P_1 - P_r), & \text{if } i \geq 0 \\ ki\sqrt{P_1 - P_r} + \frac{\alpha}{1-\gamma i}(P_s - P_1) - \frac{\alpha}{1-\gamma i}(P_1 - P_r), & \text{if } i < 0 \end{cases}$$

$$Q_2(i, P_2) = \begin{cases} -ki\sqrt{P_2 - P_r} + \frac{\alpha}{1+\gamma i}(P_s - P_2) - \frac{\alpha}{1+\gamma i}(P_2 - P_r), & \text{if } i \geq 0 \\ -ki\sqrt{P_s - P_2} + \frac{\alpha}{1-\gamma i}(P_s - P_2) - \frac{\alpha}{1-\gamma i}(P_1 - P_r), & \text{if } i < 0 \end{cases}$$

For symmetric piston, $S_1 = S_2 = S$ and by setting $m + m_0 = m_t$, then the third equation in Eq. (3.1) can be simplified to:

$$m_t \frac{dv}{dt} = S(P_1 - P_2) - bv - k_l(x_p - x_{po}), \quad (3.2)$$

and also, choosing,

$$P_L = P_1 - P_2, \quad (3.3)$$

$$Q_L = \frac{Q_1 - Q_2}{2}$$

After thorough manipulations of these equations, Q_L is then given as

$$Q_L = S \frac{dx_p}{dt} + \frac{V_0}{2B} \frac{d}{dt}(P_1 - P_2) + \frac{Sx_p}{2B} \frac{d}{dt}(P_1 + P_2) \quad (3.4)$$

Also,

$$P_1 = \frac{P_s + P_r + P_L}{2}, \quad (3.5)$$

$$P_2 = \frac{P_s + P_r - P_L}{2}$$

Again, for simplicity, we can make $V_t = 2V_o$, where V_t is the total volume of the cylinder. Then,

$$Q_L = Sv + \frac{V_t}{4B} \frac{dP_L}{dt} \quad (3.6)$$

$Q_1(i, P_1)$ and $Q_2(i, P_2)$ can then be expressed in terms of Q_L as given in below:

$$Q_L = \begin{cases} \frac{ki}{2} \sqrt{P_s - P_1} + \sqrt{P_2 - P_r} - \frac{\alpha}{1+\gamma i} P_L, & \text{if } i \geq 0 \\ \frac{ki}{2} \sqrt{P_s - P_1} + \sqrt{P_2 - P_r} - \frac{\alpha}{1+\gamma i} P_L, & \text{if } i < 0 \end{cases}$$

Inserting the values P_1 and P_2 into the equation of Q_L above yields:

$$Q_L = ki \sqrt{\frac{P_s - P_r - \text{sign}(i)P_L}{2}} - \frac{\alpha}{1+\gamma|i|} P_L \quad (3.7)$$

Therefore, the overall system model is as given in (5.4)

$$\begin{aligned} \frac{dP_L}{dt} &= \frac{4B}{V_t} (ki \sqrt{P_s - P_r - \text{sign}(i)P_L} - \frac{\alpha}{1+\gamma|i|} P_L - Sv), \\ \frac{dv}{dt} &= \frac{1}{m_t} (SP_L - bv - k_l(x_p - x_{po})), \\ \frac{dx_p}{dt} &= v + d(t). \end{aligned} \quad (3.8)$$

3.2 Electrohydraulic Servo Valve Dynamic Equations

The jack in a hydraulic system consists of a four-way spool valve supplying a double effect linear cylinder with a double rodded piston. The piston drives a load modeled by mass, spring and a sliding viscous friction.

The electro-hydraulic system subjected to parameters uncertainty and external disturbance at the level of the output can be modeled by the dynamics [6] given in Eq. (3.9) and as depicted in Figure 3.3: Choosing $P_L = x_1$, $v = x_2$, $x_p = x_3$ and $i = u$, we have

$$\begin{aligned}
 \dot{x}_1 &= \frac{4B}{V_t} (ku\sqrt{P_d - \text{sign}(u)x_1} - \frac{\alpha x_1}{1+\gamma|u|} - Sx_2), \\
 \dot{x}_2 &= \frac{1}{m_t} (Sx_1 - bx_2 - \beta x_3), \\
 \dot{x}_3 &= x_2 + d(t).
 \end{aligned} \tag{3.9}$$

where $\beta = (k_l + \Delta k_l)$.

CHAPTER 4

BACKSTEPPING BASED CONTROLLER DESIGN

In this section, control design is presented based on nonlinear backstepping method for electro hydraulic servo system subject to bounded disturbance and parameter uncertainties. As mentioned earlier, one key feature of the backstepping technique in designing a controller is its ability to avoid useful nonlinearity cancelation. The objective of employing backstepping method gravitates towards the stabilization and tracking in contrast with its corresponding feedback linearization method. Furthermore, backstepping approach has been found to relax matching conditions on perturbations. This helps facilitate controller designs for perturbed nonlinear system even if the perturbation is nowhere around the equation containing the input.

Considering the EHSS modeled by the dynamics [6] given in Eq. (4.1) below:

$$\begin{aligned}\dot{x}_1 &= \frac{4B}{V_t}(ku\sqrt{P_d - \text{sign}(u)x_1} - \frac{\alpha x_1}{1+\gamma|u|} - Sx_2), \\ \dot{x}_2 &= \frac{1}{m_t}(Sx_1 - bx_2 - \beta x_3), \\ \dot{x}_3 &= x_2 + d(t).\end{aligned}\tag{4.1}$$

where $\beta = (k_l + \Delta k_l)$. The following assumptions hold:

Assumption 4.1 1. $d(t)$ is an unknown but bounded disturbance with $|d(t)| <$

d_{max} .

2. Δk_l is unknown and bounded with $|\Delta k_l| < \Delta k_l^{max}$.

3. The dynamic of the spool-valve is assumed fast enough so it can be ignored in the dynamic model.

4. The states of the system are available.

5. Reference input($r(t)$) is a known continuously differentiable bounded trajectory.

As earlier mentioned, the nonlinearities with respect to the input "u" in the dynamics of the system make it an intricate task in trying to control the output of the system. We are able to circumvent this challenge by designing a backstepping based controller that will drive the position of the rod to a desired reference "r(t)".

Remark 4.1 One should note that $u > 0$ is equivalent to the spool valve moving to the right allowing $x_1 < 0$. Likewise, $u < 0$ is equivalent to the spool valve moving to the left prompting $x_1 > 0$. Therefore, $sign(u) = -sign(x_1)$ and consequently, $\sqrt{P_d - sign(u)x_1} = \sqrt{P_d + |x_1|}$ and thus $\sqrt{P_d - sign(u)x_1}$ is always a nonzero real valued function.

In order to use the backstepping method to design the controller, a re-indexing of the states variables is needed to transform the system into its standard strict

feedback form. Let

$$\begin{aligned}
 \xi_1 &= x_3, \\
 \xi_2 &= x_2, \\
 \xi_3 &= x_1.
 \end{aligned} \tag{4.2}$$

The dynamics of the transformed system is then given below in Eq. (4.3)

$$\begin{aligned}
 \dot{\xi}_1 &= \xi_2 + d(t), \\
 \dot{\xi}_2 &= \frac{1}{m_t}(S\xi_3 - b\xi_2 - \beta\xi_1), \\
 \dot{\xi}_3 &= \frac{4B}{V_t}(ku\sqrt{P_d - \text{sign}(u)\xi_3} - \frac{\alpha\xi_3}{1+\gamma|u|} - S\xi_2).
 \end{aligned} \tag{4.3}$$

Let

$$\begin{aligned}
 e_1 &= \xi_1 - r, \\
 e_2 &= \xi_2 - \dot{r}, \\
 e_3 &= f(\xi) - \ddot{r},
 \end{aligned} \tag{4.4}$$

where $f(\xi) = \dot{\xi}_2$.

Then, the error dynamics satisfies

$$\begin{aligned}
 \dot{e}_1 &= e_2 + d, \\
 \dot{e}_2 &= e_3, \\
 \dot{e}_3 &= \left(\frac{\partial f(\xi)}{\partial \xi}\right)^T \dot{\xi} - \ddot{r}.
 \end{aligned} \tag{4.5}$$

The rest of this section presents two controller designs using the backstepping approach. The first controller employs a constant feedback gain while in the second controller, the gain of the feedback is modified to a time-varying exponential function. The controller with the time-varying feedback is then benchmarked with one of the recent method in the literature which utilizes sliding mode control method with discontinuous sliding surfaces. The schematic of the proposed controller is as shown in Figure 4.1.

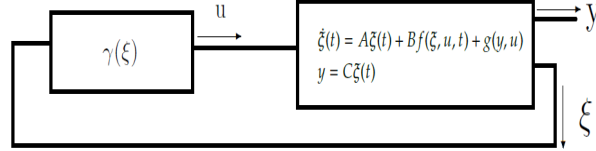


Figure 4.1: Closed-loop controller scheme

4.1 Controller Design with a Constant Gain

Let λ_c and k_o be constant design parameters ≥ 1 ,

$$u = \frac{m_t V_t}{4SBk_1 k \min(\sqrt{P_d - \xi_3}, \sqrt{P_d + \xi_3})} v \quad (4.6)$$

$$v = -k_o(\alpha_1 e_1 + \alpha_2 e_2 + \alpha_3 e_3) - (d_{max}|c_1| + |f_1| + |f_2|) \quad (4.7)$$

where

$$g(u) = \frac{4Bk}{V_t} \sqrt{P_d - \text{sign}(u)\xi_3}, \quad (4.8)$$

$$c_1 = \lambda_c + \frac{3}{2} - \frac{\beta}{\lambda_c^4 m_t}, \quad (4.9)$$

$$\begin{aligned} f_1 = & e_2 + \lambda_c e_1 + (\lambda_c + \frac{3}{2})e_2 + (1 + \frac{\lambda_c + \frac{\lambda_c^3}{2}}{\lambda_c^4})e_3 \\ & + \frac{-\beta(e_2 + \dot{r})}{m_t \lambda_c^4} - \frac{b m_t (e_3 - \ddot{r}) + b^2 (e_2 + \dot{r}) + b\beta(e_1 + r)}{m_t^2 \lambda_c^4} \end{aligned} \quad (4.10)$$

$$- \frac{b(e_2 + \dot{r}) + \beta(e_1 + r)}{m_t^2 \lambda_c^4} - \frac{S^2}{m_t \lambda_c^4} (e_2 + \dot{r}) - \frac{1}{\lambda_c^4} \ddot{r}$$

$$f_2 = \frac{-\alpha S (\frac{m_t (e_3 - \ddot{r})}{S} + \frac{b(e_2 + \dot{r}) + \beta(e_1 + r)}{S})}{\lambda_c^4 m_t} \quad (4.11)$$

$$\alpha_1 = \frac{3}{2} + \lambda_c, \quad \alpha_2 = 1 + \frac{1}{\lambda_c^3} + \frac{1}{2\lambda_c}, \quad \alpha_3 = \frac{1}{\lambda_c^4}. \quad (4.12)$$

Theorem 4.1 *The system with kinematic model (4.3) and controller (4.6)-(4.12) is practically stable and the solution of the error dynamic (4.5) is globally uniformly ultimately bounded with ultimate bound satisfying the following condition*

$$|(\alpha_1 e_1 + \alpha_2 e_2 + \alpha_3 e_3)^2 + \frac{\lambda_c}{2} e_1^2 + (e_2 + \lambda_c e_1)^2| \leq \sqrt{(\frac{1}{2\lambda_c} + \frac{1}{2\lambda_c^5})} d_{max}^2$$

Proof. We use the following Lyapunov function candidate

$$V_1 = \frac{1}{2} e_1^2, \quad (4.13)$$

Calculating the derivative of $V(x)$ along the trajectories of the perturbed EHSS, we obtain

$$\begin{aligned}\dot{V}_1 &= -\lambda_c e_1^2 + e_1(e_2 + \lambda_c e_1) + e_1 d. \\ \dot{V}_1 &\leq -\lambda_c e_1^2 + e_1(e_2 + \lambda_c e_1) + \frac{1}{2\lambda_c} d^2 + \frac{\lambda_c}{2} e_1^2, \\ &\leq -\frac{\lambda_c}{2} e_1^2 + \frac{1}{2\lambda_c} d^2 + e_1(e_2 + \lambda_c e_1).\end{aligned}\tag{4.14}$$

we have used the Young's inequality (also sometimes called the PeterPaul inequality) with $\lambda_c > 0$

$$e_1 d \leq |e_1| |d| \leq \frac{1}{2\lambda_c} d^2 + \frac{\lambda_c}{2} e_1^2\tag{4.15}$$

Let $V_2 = \frac{1}{2\lambda_c^4} (e_2 + \lambda_c e_1)^2$, then

$$\dot{V}_2 = \frac{1}{\lambda_c^4} (e_2 + \lambda_c e_1) (e_3 + \lambda_c (e_2 + d))\tag{4.16}$$

Therefore,

$$\dot{V}_1 + \dot{V}_2 \leq -\frac{\lambda_c}{2} e_1^2 + \frac{1}{2\lambda_c} d^2 + \frac{1}{\lambda_c^4} (e_2 + \lambda_c e_1) [e_3 + \lambda_c e_2 + \lambda_c^4 e_1 + \lambda_c d]\tag{4.17}$$

But,

$$\begin{aligned}\frac{1}{\lambda_c^3} (e_2 + \lambda_c e_1) d &\leq \frac{1}{\lambda_c^3} |d| |e_2 + \lambda_c e_1|, \\ &\leq \frac{1}{\lambda_c^3} \left[\frac{1}{2\lambda_c^2} d^2 + \frac{\lambda_c^2}{2} (e_2 + \lambda_c e_1)^2 \right]\end{aligned}\tag{4.18}$$

Inserting Eq. (4.18) into Eq. (4.17), we have

$$\dot{V}_1 + \dot{V}_2 \leq -\frac{\lambda_c}{2}e_1^2 + \left(\frac{1}{2\lambda_c} + \frac{1}{2\lambda_c^5}\right)d^2 + (e_2 + \lambda_c e_1)\left[\frac{1}{\lambda_c^4}(e_3 + \lambda_c e_2 + \lambda_c^4 e_1) + \frac{\lambda_c^2}{2}(e_2 + \lambda_c e_1)\right]. \quad (4.19)$$

$$\dot{V}_1 + \dot{V}_2 \leq -\frac{\lambda_c}{2}e_1^2 + \left(\frac{1}{2\lambda_c} + \frac{1}{2\lambda_c^5}\right)d^2 - (e_2 + \lambda_c e_1)^2 + (e_2 + \lambda_c e_1)[\alpha_1 e_1 + \alpha_2 e_2 + \alpha_3 e_3] \quad (4.20)$$

Choosing $V_3 = \frac{1}{2}(\alpha_1 e_1 + \alpha_2 e_2 + \alpha_3 e_3)^2$, then,

$$\begin{aligned} \dot{V} &= \dot{V}_1 + \dot{V}_2 + \dot{V}_3 \\ &\leq -\frac{\lambda_c}{2}e_1^2 + \left(\frac{1}{2\lambda_c} + \frac{1}{2\lambda_c^5}\right)d^2 - (e_2 + \lambda_c e_1)^2 + (e_2 + \lambda_c e_1)[\alpha_1 e_1 + \alpha_2 e_2 + \alpha_3 e_3] \\ &\quad + (\alpha_1 e_1 + \alpha_2 e_2 + \alpha_3 e_3)[\alpha_1 \dot{e}_1 + \alpha_2 \dot{e}_2 + \alpha_3 \dot{e}_3] \end{aligned} \quad (4.21)$$

$$\begin{aligned} \dot{V} &\leq -\frac{\lambda_c}{2}e_1^2 + \left(\frac{1}{2\lambda_c} + \frac{1}{2\lambda_c^5}\right)d^2 - (e_2 + \lambda_c e_1)^2 \\ &\quad + (\alpha_1 e_1 + \alpha_2 e_2 + \alpha_3 e_3)[e_2 + \lambda_c e_1 + \alpha_1 \dot{e}_1 + \alpha_2 \dot{e}_2 + \alpha_3 \dot{e}_3] \end{aligned} \quad (4.22)$$

$$\begin{aligned} \dot{V} &\leq -\frac{\lambda_c}{2}e_1^2 + \left(\frac{1}{2\lambda_c} + \frac{1}{2\lambda_c^5}\right)d^2 - (e_2 + \lambda_c e_1)^2 \\ &\quad + (\alpha_1 e_1 + \alpha_2 e_2 + \alpha_3 e_3)\left[g(u).u + f_1(e) + c_1 d + \frac{f_2}{1+\gamma|u|}\right] \end{aligned} \quad (4.23)$$

After algebraic manipulation of Eq. (4.23) and considering that:

$$\frac{1}{1+\gamma|u|} \leq 1; \quad (4.24)$$

$$c_1 d(\alpha_1 e_1 + \alpha_2 e_2 + \alpha_3 e_3) \leq d_{max} |c_1| |\alpha_1 e_1 + \alpha_2 e_2 + \alpha_3 e_3| \quad (4.25)$$

$$(\alpha_1 e_1 + \alpha_2 e_2 + \alpha_3 e_3)f_2 \leq |f_2| |\alpha_1 e_1 + \alpha_2 e_2 + \alpha_3 e_3| \quad (4.26)$$

then,

$$\begin{aligned} \dot{V} &\leq -\frac{\lambda_c}{2}e_1^2 + \left(\frac{1}{2\lambda_c} + \frac{1}{2\lambda_c^5}\right)d^2 - (e_2 + \lambda_c e_1)^2 + (\alpha_1 e_1 + \alpha_2 e_2 + \alpha_3 e_3)g(u).u \\ &\quad + |\alpha_1 e_1 + \alpha_2 e_2 + \alpha_3 e_3|(d_{max} |c_1| + |f_1| + |f_2|) \end{aligned} \quad (4.27)$$

Therefore,

$$\dot{V} \leq -\frac{\lambda_c}{2}e_1^2 - (e_2 + \lambda_c e_1)^2 - (\alpha_1 e_1 + \alpha_2 e_2 + \alpha_3 e_3)^2 + \left(\frac{1}{2\lambda_c} + \frac{1}{2\lambda_c^5}\right)d_{max}^2 \quad (4.28)$$

The right-hand side of the foregoing inequality is not negative because of the disturbance and uncertainty terms. Near the origin where e_i , for $i = 1, 2, 3$, is almost zero $\dot{V} > 0$ pushing the trajectories away from 0.

However,

$$\begin{aligned} \dot{V} &\geq 0 \\ &\Rightarrow \frac{\lambda_c}{2}e_1^2 + (e_2 + \lambda_c e_1)^2 + (\alpha_1 e_1 + \alpha_2 e_2 + \alpha_3 e_3)^2 \\ &\geq \left(\frac{1}{2\lambda_c} + \frac{1}{2\lambda_c^5}\right)d_{max}^2 \end{aligned} \quad (4.29)$$

Hence, if we start within the set defined by e_i , ($i = 1, 2, 3$) such that $V_3 = (\alpha_1 e_1 + \alpha_2 e_2 + \alpha_3 e_3)^2 > \left(\frac{1}{2\lambda_c} + \frac{1}{2\lambda_c^5}\right)d_{max}^2$, then $\dot{V} < 0$ and the solution will remain in that set for all future time.

Remark 4.2 *The design parameter λ_c should be selected as big as possible to make decrease the ultimate bound in the tracking error dynamic. The larger is λ the more oscillatory is the transient and higher is the control input. In order, to allow λ to take large values and avoid transient problems, one should allow λ to be function of time rather than a constant. In the next section, the design of the controller for such case is presented.*

4.2 Controller Design with a Time-Varying Gain

In this section, we will design a backstepping-based controller and allow the Young's inequality parameter λ to be function of time. The objective is to al-

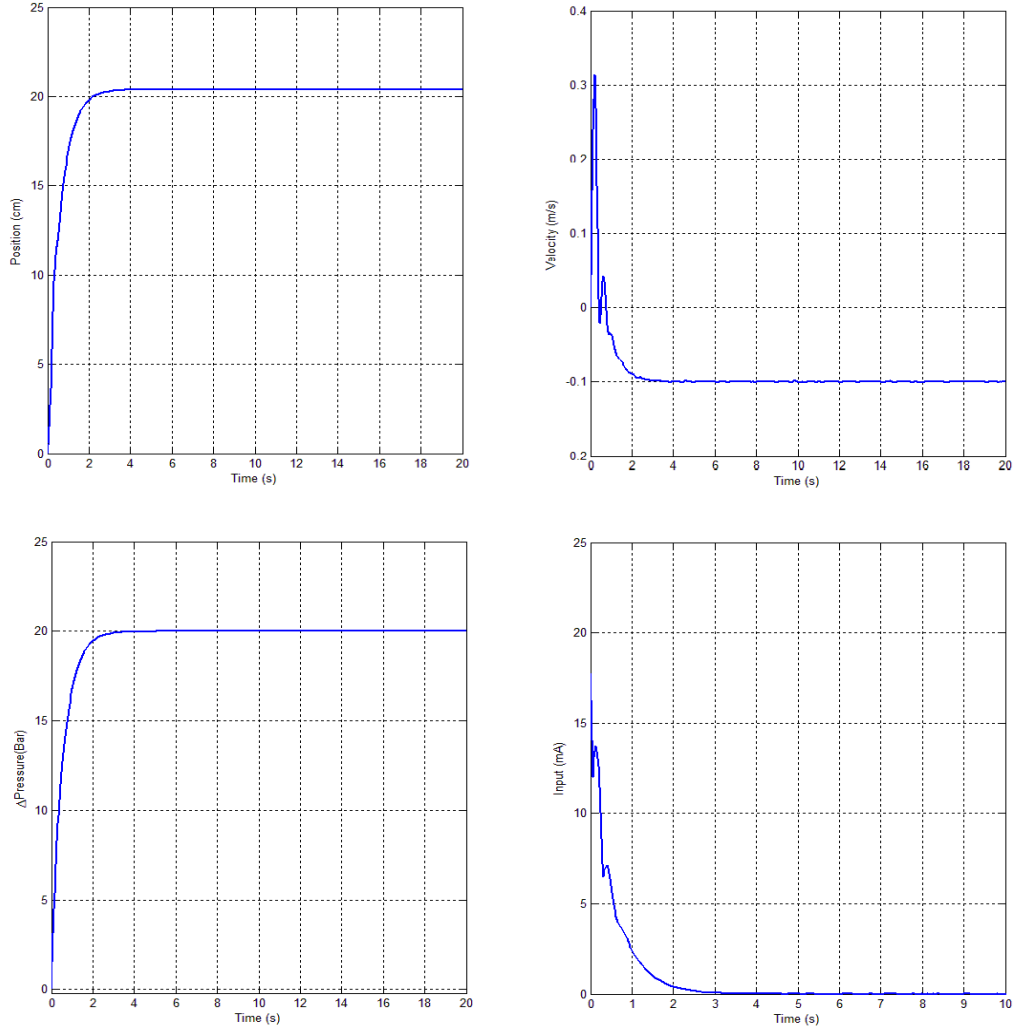


Figure 4.2: Backstepping controller with constant feedback gain, using constant reference ($r = 20\text{cm}$) and under constant disturbance ($d(t) = 0.1$)

low λ to take large values while avoiding transient performance issues. Define

$$\lambda = \lambda_{max}(1 - \exp(-\epsilon_1 t))$$

and

(4.30)

$$\dot{\lambda} = -\epsilon_1 \lambda + \epsilon_1 \lambda_{max}$$

$$\lambda(0) \geq \epsilon_1 \lambda_{max}$$

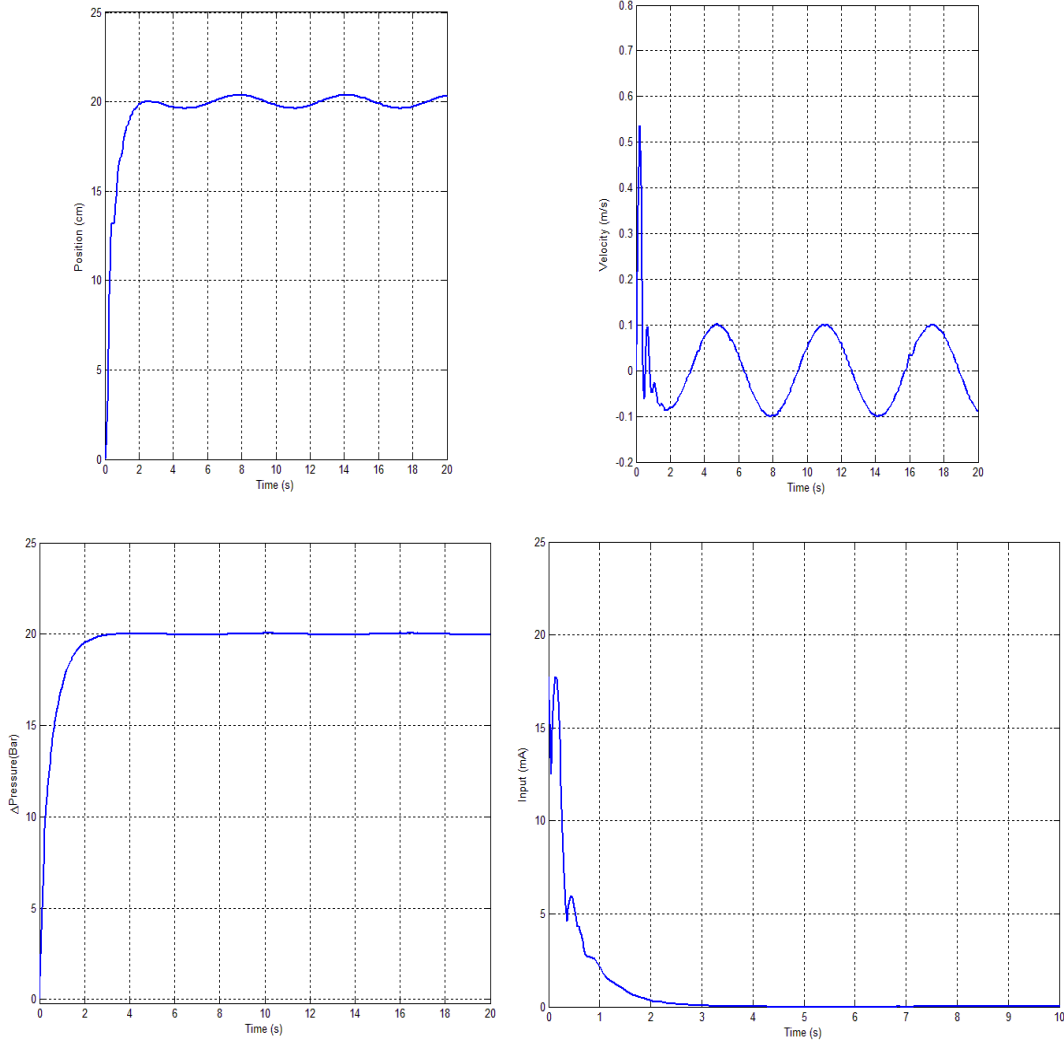


Figure 4.3: Backstepping controller with constant feedback gain, using constant reference ($r = 20\text{cm}$) and under sinusoidal disturbance ($d(t) = 0.1\sin(t)$)

Let,

$$u = \frac{m_t V_t}{4SBk \min(\sqrt{P_d - \xi_3}, \sqrt{P_d + \xi_3})} v \quad (4.31)$$

and,

$$v = -k_o(\alpha_1 e_1 + \alpha_2 e_2 + \alpha_1 e_2) - (|c_2| + |f_3| + |f_4|) \quad (4.32)$$

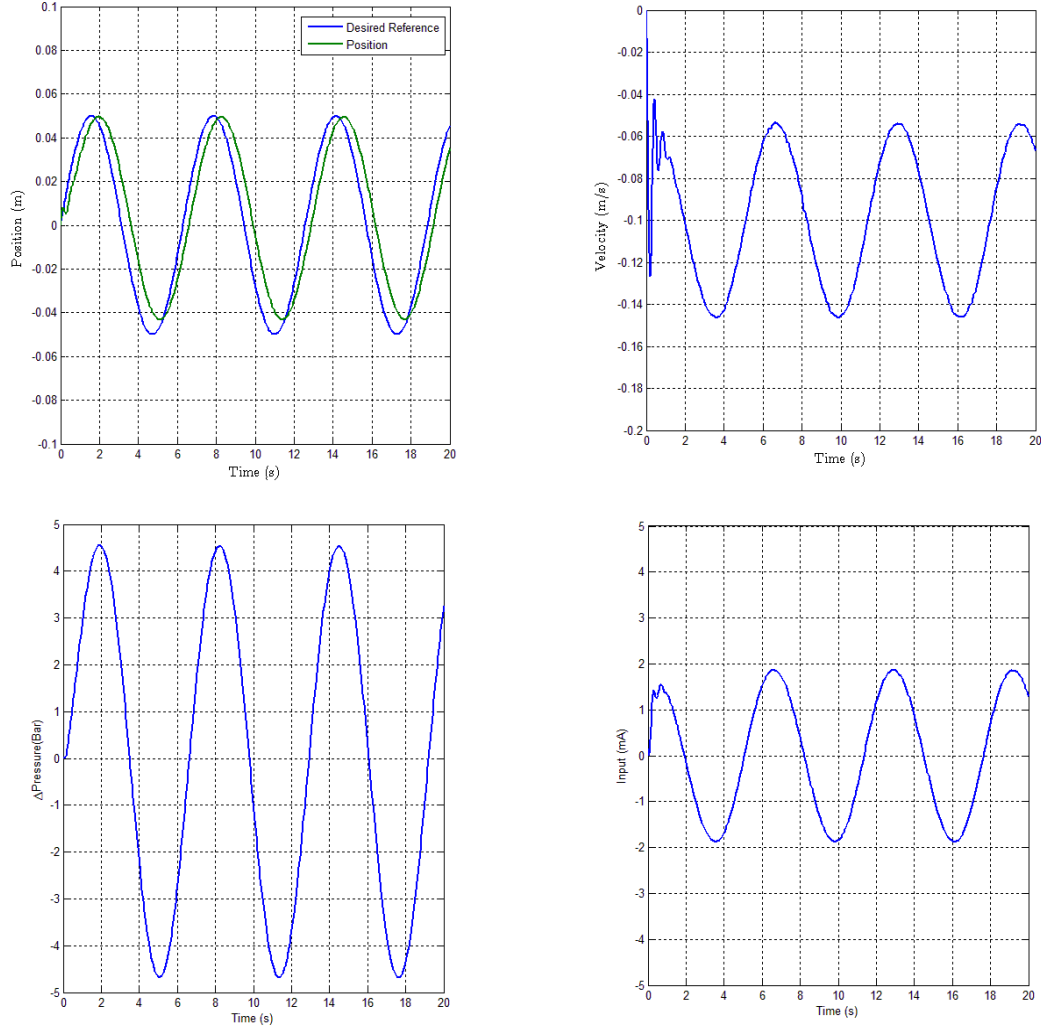


Figure 4.4: Backstepping controller with constant feedback gain, using sinusoidal reference ($r = 0.05\sin(t)\text{m}$) and under constant disturbance ($d(t) = 0.1$)

where

$$\begin{aligned}
f_3 &= e_2 + \lambda e_1 + (1 + \epsilon_1 \lambda_{max} + \frac{1}{2} \lambda^4 + \frac{\epsilon_1}{2} \lambda_{max} \lambda + \lambda) e_2 - \frac{1}{m_t^2} b(S(\frac{m_t}{S})(e_3 - \ddot{r})) \\
&+ (1 + \lambda + \epsilon_1 \lambda^3 + \frac{\epsilon_1}{2} \lambda_{max}) e_3 - \frac{1}{m_t} \beta(e_2 + \dot{r}) \\
&+ \frac{1}{S}(b(e_2 + \dot{r}) + \beta(e_1 + r)) - b(e_2 + \dot{r}) - \beta(e_1 + r) - \frac{S^2}{m_t}(e_2 + \dot{r}) \\
&- \ddot{r} + (2\lambda^3(-\epsilon_1 \lambda + \epsilon_1 \lambda_{max}) + \frac{\epsilon_1}{2} \lambda_{max}(-\epsilon_1 \lambda + \epsilon_1 \lambda_{max}) - \epsilon_1 \lambda + \epsilon_1 \lambda_{max}) e_1 \\
&+ (-\epsilon_1 \lambda + \epsilon_1 \lambda_{max} + \frac{3}{2} \lambda^2(-\epsilon_1 \lambda + \epsilon_1 \lambda_{max})) e_2;
\end{aligned} \tag{4.33}$$

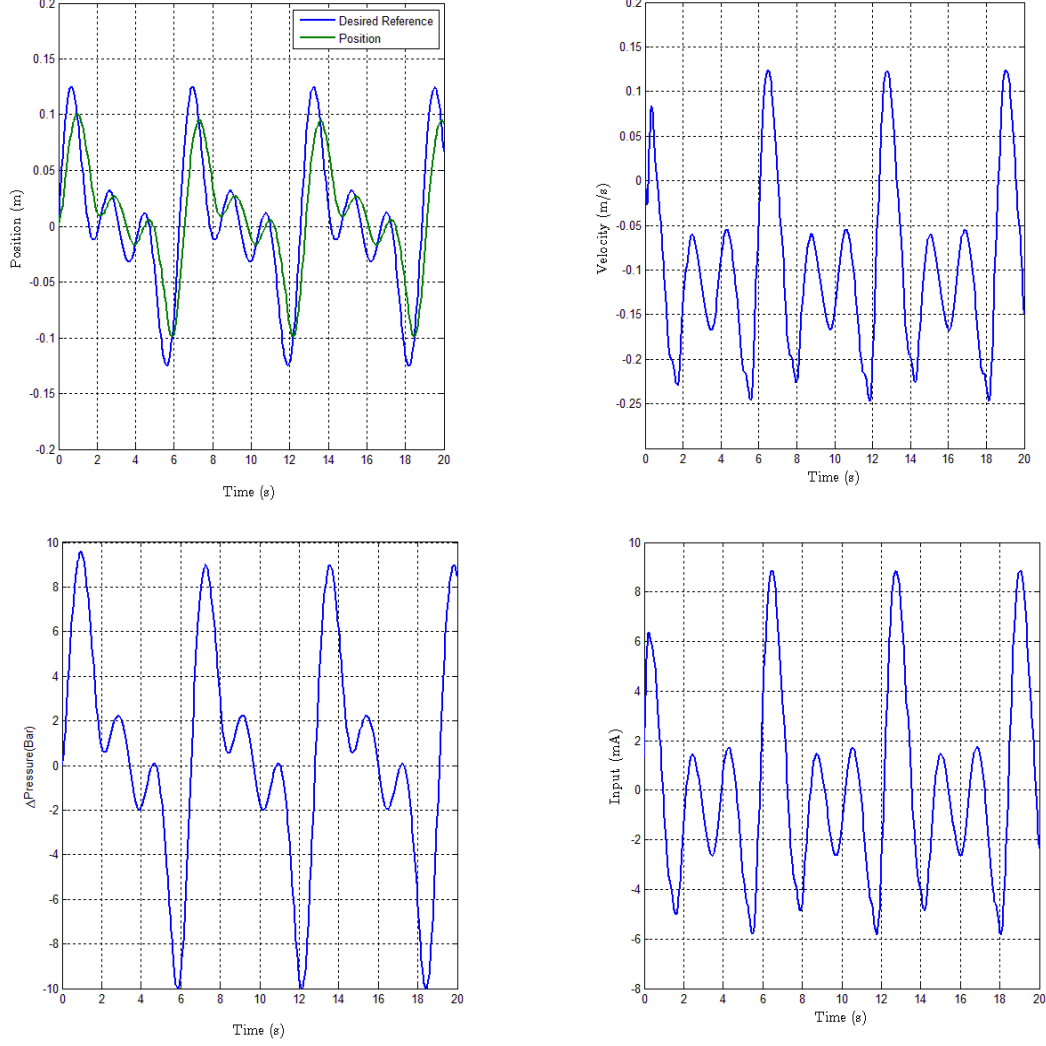


Figure 4.5: Backstepping controller with constant feedback gain, using sinusoidal reference ($r = 0.05(\sin(t) + \sin(2t) + \sin(3t))\text{m}$) and under constant disturbance ($d(t) = 0.1$)

$$f_4 = -\frac{\alpha S}{m_t} \left(\frac{m_t}{S} (e_3 - \dot{r}) + \frac{1}{S} (b(e_2 + \dot{r}) + \beta(e_1 + r)) \right) \quad (4.34)$$

$$c_2 = -\frac{\beta}{m_t} + 1 + \epsilon_1 \lambda_{max} + \frac{1}{2} \lambda^4 + \frac{\epsilon_1}{2} \lambda_{max} \lambda + \lambda \quad (4.35)$$

$$\alpha_1 = 1 + \epsilon_1 \lambda_{max} + \lambda + \frac{1}{2} + \frac{\epsilon_1}{2} \lambda_{max} \lambda + \frac{\lambda^4}{2},$$

$$\alpha_2 = 1 + \lambda + \frac{\lambda^3}{2} + \frac{\epsilon_1}{2} \lambda_{max},$$

$$\alpha_3 = 1$$

Theorem 4.2 *Let $\lambda(t)$ as defined in (4.30), with $0 < \epsilon_1 \leq 1$ and $\lambda_{max} > 0$ two real design parameters, the system with kinematic model (4.3) and controller (4.38)-(4.46) is practically stable and the solution of the error dynamic (4.5) is globally uniformly ultimately bounded with ultimate bound satisfying the following condition $|(\alpha_1 e_1 + \alpha_2 e_2 + \alpha_3 e_3)^2 + (-\frac{\lambda}{2} + \frac{\epsilon_1}{2} \lambda_{max}) e_1^2 + (e_2 + \lambda e_1)^2| \leq \sqrt{\frac{1}{\lambda}} d_{max}^2$*

Proof.

$$V_1 = \frac{1}{2} e_1^2, \tag{4.36}$$

$$\dot{V}_1 = -\lambda e_1^2 + e_1(e_2 + \lambda e_1) + e_1 d$$

Using Young's inequality,

$$e_1 d \leq |e_1| |d| \leq \frac{1}{2\lambda} d^2 + \frac{\lambda}{2} e_1^2 \tag{4.37}$$

$$\dot{V}_1 \leq -\frac{\lambda}{2} e_1^2 + \frac{1}{2\lambda} d^2 + e_1(e_2 + \lambda e_1) \tag{4.38}$$

Let $V_2 = \frac{1}{2}(e_2 + \lambda e_1)^2$, then

$$\begin{aligned} \dot{V}_2 &= (e_2 + \lambda e_1)(\dot{e}_2 + \lambda \dot{e}_1) \\ &= (e_2 + \lambda e_1)[e_3 + \lambda(e_2 + d) + \dot{e}_1] \end{aligned} \tag{4.39}$$

$$\dot{V}_2 = (e_2 + \lambda e_1)(e_3 + \epsilon_1 \lambda_{max} e_1 + \lambda e_2) + \lambda d(e_2 + \lambda e_1) - \epsilon \lambda (e_2 + \lambda e_1) e_1 \quad (4.40)$$

Owing to Young's inequality, one can write

$$\lambda d(e_2 + \lambda e_1) \leq \frac{d^2}{2\lambda} + \frac{\lambda^3}{2}(e_2 + \lambda e_1)^2 \quad (4.41)$$

and

$$-\epsilon_1 \lambda (e_2 + \lambda e_1) e_1 \leq \frac{\epsilon_1}{2} \lambda_{max} e_1^2 + \frac{\epsilon_1}{2} \lambda_{max} (e_2 + \lambda e_1)^2 \quad (4.42)$$

Therefore,

$$\begin{aligned} \dot{V}_2 \leq & (e_2 + \lambda e_1)[e_3 + \epsilon_1 \lambda_{max} e_1 + \lambda e_2] \\ & + \frac{\lambda^3}{2}(e_2 + \lambda e_1) + \frac{\epsilon}{2} \lambda_{max} (e_2 + \lambda e_1)] \\ & + \frac{\epsilon_1}{2} \lambda_{max} e_1^2 + \frac{d^2}{2\lambda} \end{aligned} \quad (4.43)$$

and,

$$\begin{aligned} \dot{V}_1 + \dot{V}_2 \leq & (-\frac{\lambda}{2} + \frac{\epsilon_1}{2} \lambda_{max}) e_1^2 + \frac{1}{\lambda} d^2 + (e_2 + \lambda e_1)[e_3 + \lambda e_2 + e_1 + \epsilon_1 \lambda_{max} e_1 \\ & + \lambda e_2 + \frac{\lambda^3}{2}(e_2 + \lambda e_1) + \frac{\epsilon_1}{2} \lambda_{max} (e_2 + \lambda e_1)] \end{aligned} \quad (4.44)$$

$$\dot{V}_1 + \dot{V}_2 \leq (-\frac{\lambda}{2} + \frac{\epsilon_1}{2} \lambda_{max}) e_1^2 + \frac{1}{\lambda} d^2 - (e_2 + \lambda e_1)^2 + (e_2 + \lambda e_1)[\alpha_1 e_1 + \alpha_2 e_2 + e_3] \quad (4.45)$$

Let $V_3 = \frac{1}{2}(\alpha_1 e_1 + \alpha_2 e_2 + \alpha_3 e_3)^2$, then

$$\begin{aligned} \dot{V} = & \dot{V}_1 + \dot{V}_2 + \dot{V}_3 \\ \leq & (-\frac{\lambda}{2} + \frac{\epsilon_1}{2} \lambda_{max}) e_1^2 + \frac{1}{\lambda} d^2 - (e_2 + \lambda e_1)^2 \\ & + (\alpha_1 e_1 + \alpha_2 e_2 + e_3) ((e_2 + \lambda e_1) + (\alpha_1 \dot{e}_1 + \alpha_2 \dot{e}_2 + \dot{e}_3 + \dot{\alpha}_1 e_1 + \dot{\alpha}_2 e_2)) \end{aligned} \quad (4.46)$$

$$\begin{aligned} \dot{V} \leq & (-\frac{\lambda}{2} + \frac{\epsilon_1}{2} \lambda_{max}) e_1^2 + \frac{1}{\lambda} d^2 - (e_2 + \lambda e_1)^2 \\ & + (\alpha_1 e_1 + \alpha_2 e_2 + e_3)[\alpha_1 e_2 + \lambda e_1 + \dot{e}_1 + \alpha_2 \dot{e}_2 + \dot{e}_3 + \dot{\alpha}_1 e_1 + \dot{\alpha}_2 e_2] \end{aligned} \quad (4.47)$$

Eq. (4.40) can be written in the form given in Eq. (4.41)

$$\begin{aligned} \dot{V} \leq & (-\frac{\lambda}{2} + \frac{\epsilon_1}{2} \lambda_{max}) e_1^2 + \frac{1}{\lambda} d^2 - (e_2 + \lambda e_1)^2 \\ & + (\alpha_1 e_1 + \alpha_2 e_2 + e_3)[g(u) \cdot u + f_3(e) + c_2 d + \frac{f_4}{1+\gamma|u|}] \end{aligned} \quad (4.48)$$

Taking into account that:

$$\frac{1}{1+\gamma|u|} \leq 1; \quad (4.49)$$

$$c_2 d(\alpha_1 e_1 + \alpha_2 e_2 + \alpha_3 e_3) \leq d_{max} |c_2| |\alpha_1 e_1 + \alpha_2 e_2 + \alpha_3 e_3| \quad (4.50)$$

$$(\alpha_1 e_1 + \alpha_2 e_2 + \alpha_3 e_3) f_4 \leq |f_4| |\alpha_1 e_1 + \alpha_2 e_2 + \alpha_3 e_3| \quad (4.51)$$

$$\begin{aligned} \dot{V} \leq & \left(-\frac{\lambda}{2} + \frac{\epsilon_1}{2} \lambda_{max}\right) e_1^2 + \frac{1}{\lambda} d^2 - (e_2 + \lambda e_1)^2 + (\alpha_1 e_1 + \alpha_2 e_2 + \alpha_3 e_3) g(u) \cdot u \\ & + |\alpha_1 e_1 + \alpha_2 e_2 + \alpha_3 e_3| (d_{max} |c_2| + |f_3| + |f_4|) \end{aligned} \quad (4.52)$$

Manipulating Eq. (4.49) - (4.52), leads to

$$\dot{V} \leq \left(-\frac{\lambda}{2} + \frac{\epsilon_1}{2} \lambda_{max}\right) e_1^2 - (e_2 + \lambda e_1)^2 - (\alpha_1 e_1 + \alpha_2 e_2 + \alpha_3 e_3)^2 + \frac{1}{\lambda} d_{max}^2 \quad (4.53)$$

The proof is complete.

4.3 Controller Design using Sliding Mode Control with Discontinuous Surface

In an attempt to benchmark the backstepping based controller using time varying feedback gain with a sliding mode controller (SMC), we took the controller developed in [6]. The authors formulated the controller using two discontinuous sliding surfaces. The surfaces and the controller are given in the Eq. (4.54)- (4.56).

4.3.1 Controller Design using Classical Sliding Surface

The sliding surface was chosen such that the system behaves asymptotically stable when it is confined to the surface. The chosen sliding surface is given in Eq. (4.55)

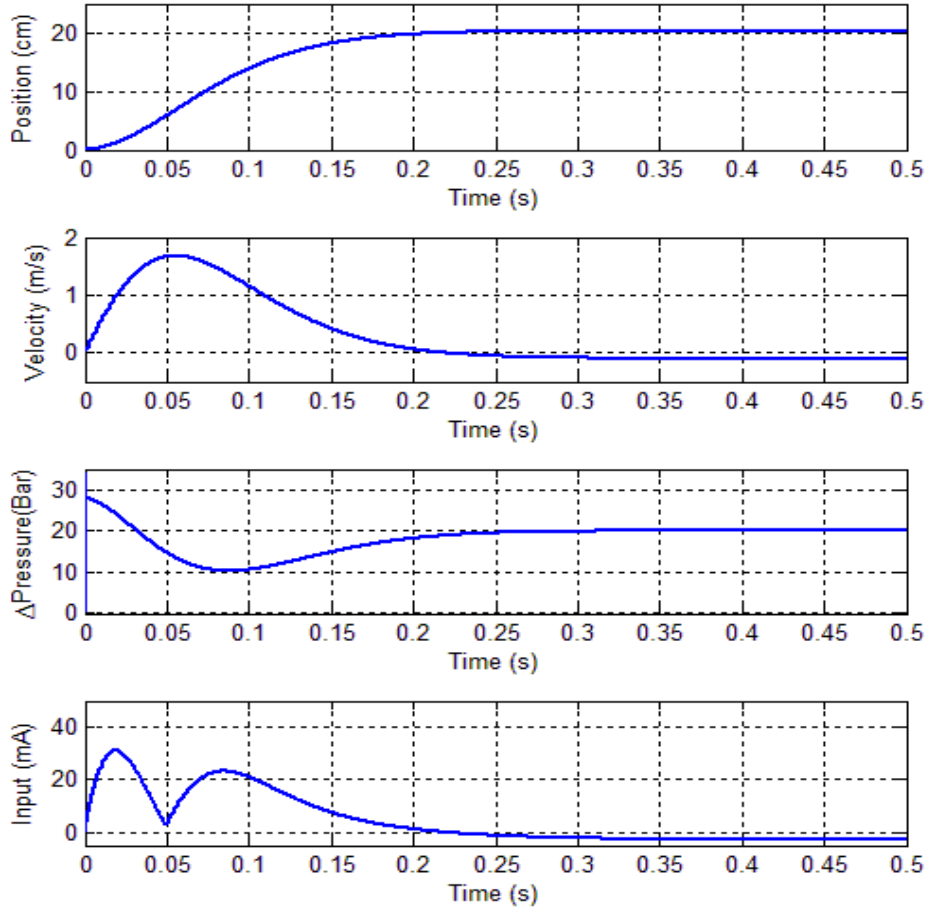


Figure 4.6: Backstepping controller with time-varying feedback gain, using constant reference ($r=0.2\text{m}$) and under constant disturbance ($d(t) = 0.1$)

and the control law is thus given as in Eq. (4.56). Given that:

$$C_2 = 2\lambda_t - b, \tag{4.54}$$

$$C_3 = \lambda^2 m_t - k_l$$

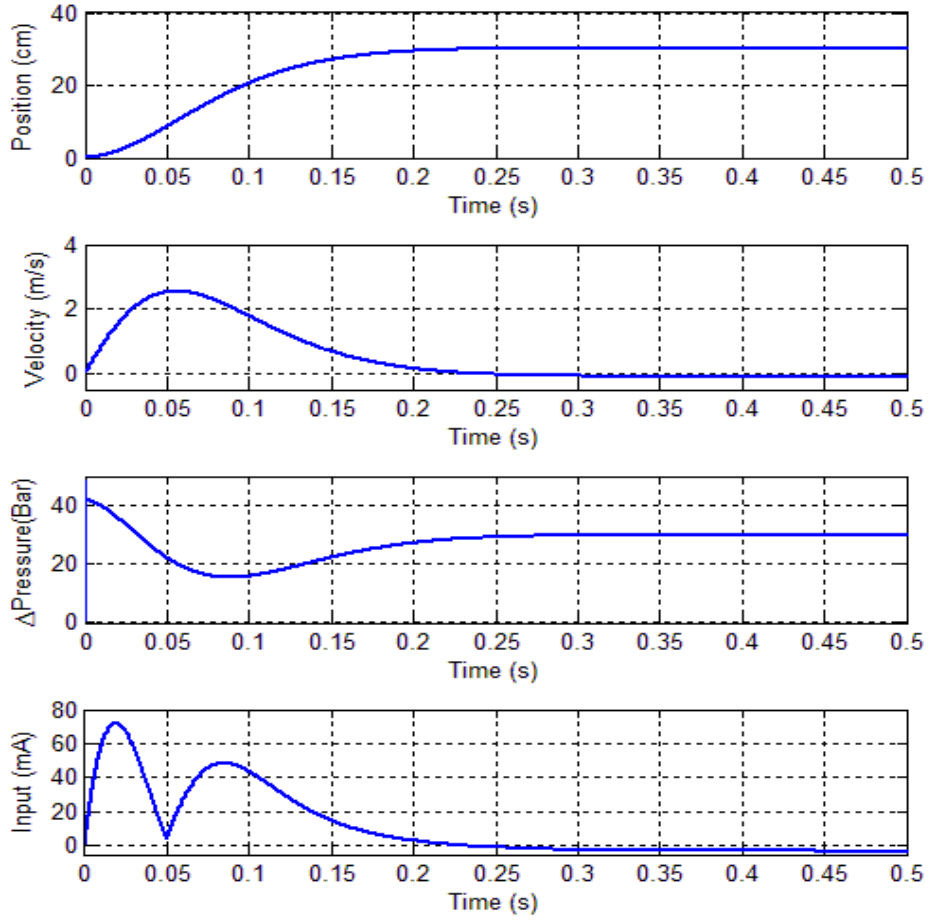


Figure 4.7: Backstepping controller with time-varying feedback gain, using constant reference($r = 0.3\text{m}$) and under constant disturbance($d(t) = 0.1$)

Then the sliding surface ($\sigma(x)$) is

$$\sigma(x) = Sx_1 + C_2x_2 + C_3(x_3 - x_{3ref}) - k_l x_{3ref}; \quad (4.55)$$

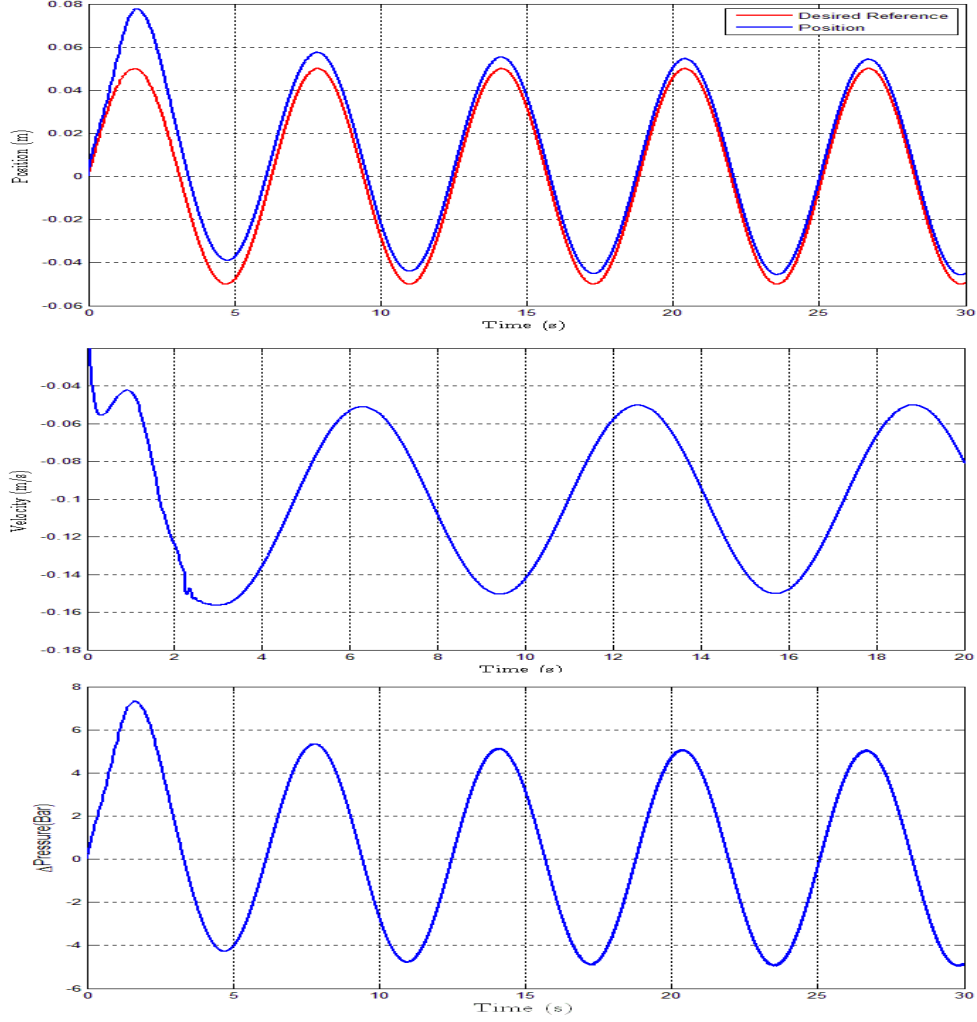


Figure 4.8: Backstepping controller with time-varying feedback gain, for sinusoidal reference ($r = 0.05(\sin(t))\text{m}$) and under constant disturbance ($d(t) = 0.1$)

The control law ($u(x)$) is

$$u(x) = \begin{cases} \frac{-W \text{sign}(\sigma(x)) - \frac{C_2}{m_t}(Sx_1 - bx_2 - k_l x_3) + (\frac{4BS^2}{V_t} - C_3)x_2}{\frac{4BSk}{V_t} \sqrt{P_d - x_1}}, & \text{if } u \geq 0 \\ \frac{-W \text{sign}(\sigma(x)) - \frac{C_2}{m_t}(Sx_1 - bx_2 - k_l x_3) + (\frac{4BS^2}{V_t} - C_3)x_2}{\frac{4BSk}{V_t} \sqrt{P_d + x_1}}, & \text{if } u < 0 \end{cases} \quad (4.56)$$

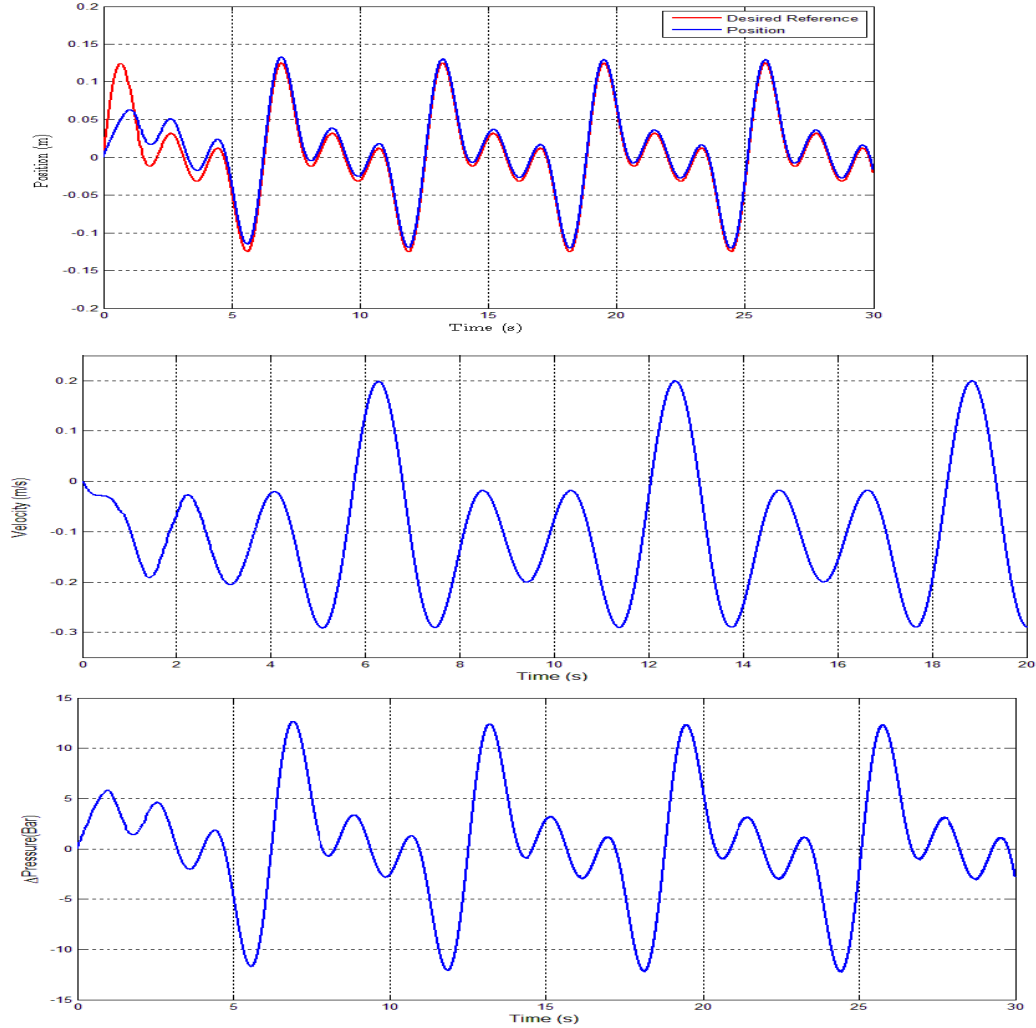


Figure 4.9: Backstepping Controller with time-varying feedback gain, using sum of sinusoids reference ($r = 0.05(\sin(t) + \sin(2t) + \sin(3t))m$) and under constant disturbance ($d(t) = 0.1$)

4.3.2 Controller Design with Discontinuous Surface

In order to improve the efficiency of the controller using classical sliding surface in the foregoing subsection, two discontinuous sliding surfaces are proposed by the authors in [6]. Choosing $W = 10^7$, $W_1 = 100$, $W_2 = 0.15$ & $W_3 = 20$, the following surfaces will be achieved. The sliding surfaces ($\sigma_1(x)$) and ($\sigma(x)$) are

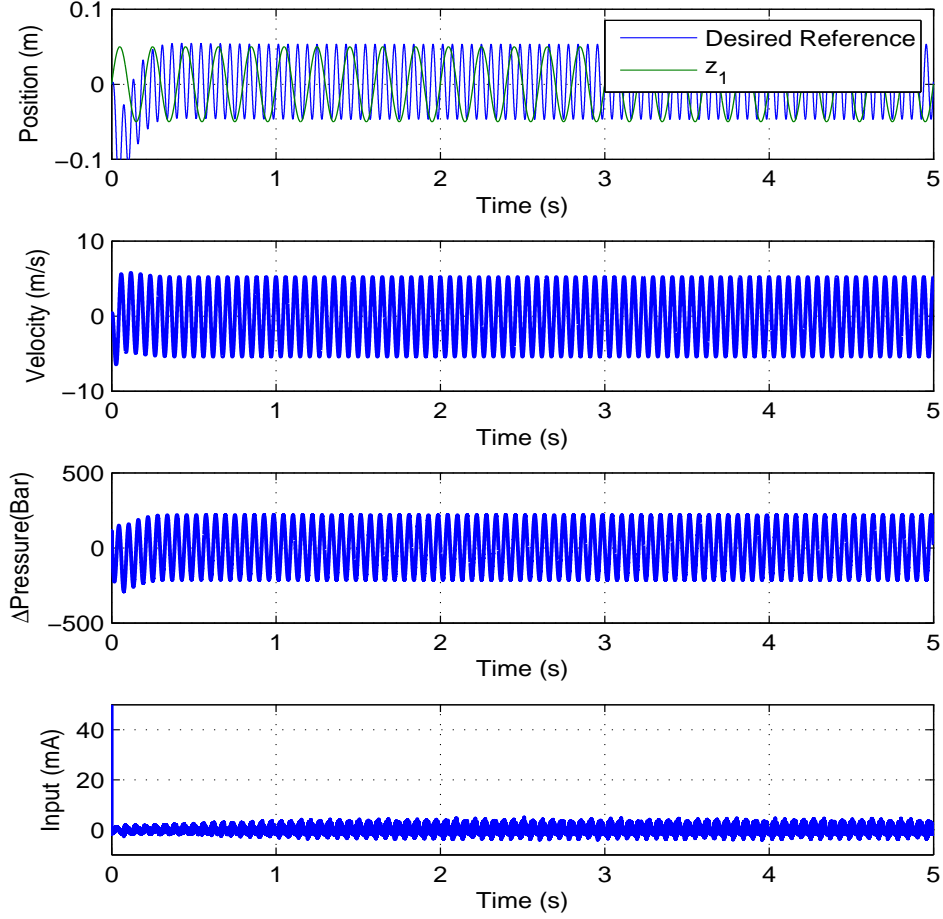


Figure 4.10: Backstepping controller for reference $(0.05\sin(2\pi ft))\text{m}$ with sweep frequency $f=5$ Hz

given as follows.

$$\sigma_1(x_2, x_3) = x_2 + W_3(x_3 - x_{3ref}) + W_2\text{sign}(x_3 - x_{3ref}),$$

$$\sigma(x) = Sx_1 + (m_t W_3 + m_t W_2 \delta(x_3 - x_{3ref}) - b)x_2 - k_l x_3 + m_t W_1 \text{sign}(\sigma_1(x_2, x_3)) \quad (4.57)$$

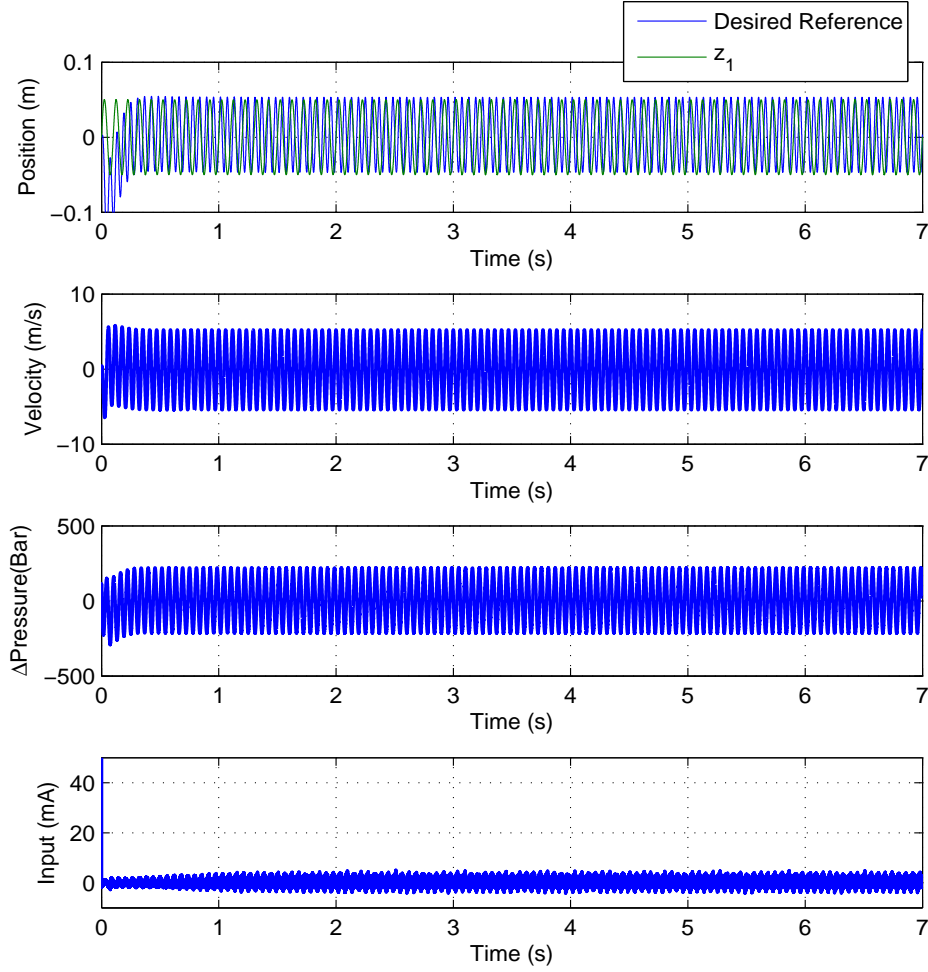


Figure 4.11: Backstepping controller for reference $(0.05\sin(2\pi ft))\text{m}$ with sweep frequency $f=10$ Hz

Here, the control law $(u(x))$ is

$$u(x) = \begin{cases} \frac{-W\text{sign}(\sigma(x)) - m_t W_1 \delta(\sigma_1(x)) + \left(\frac{4BS\alpha}{V_t} + \frac{bS}{m_t} - SW_4\right)x_1 + \left(\frac{4BS^2}{V_t} - \frac{b^2}{m_t} + k_l + bW_3\right)x_2 + \left(k_l W_3 + \frac{bk_l}{m_t}\right)x_3}{\frac{4BSk}{V_t} \sqrt{P_d - x_1}}, & \text{if } u \geq 0 \\ \frac{-W\text{sign}(\sigma(x)) - m_t W_1 \delta(\sigma_1(x)) + \left(\frac{4BS\alpha}{V_t} + \frac{bS}{m_t} - SW_4\right)x_1 + \left(\frac{4BS^2}{V_t} - \frac{b^2}{m_t} + k_l + bW_3\right)x_2 + \left(k_l W_3 + \frac{bk_l}{m_t}\right)x_3}{\frac{4BSk}{V_t} \sqrt{P_d + x_1}}, & \text{if } u < 0 \end{cases}, \quad (4.58)$$

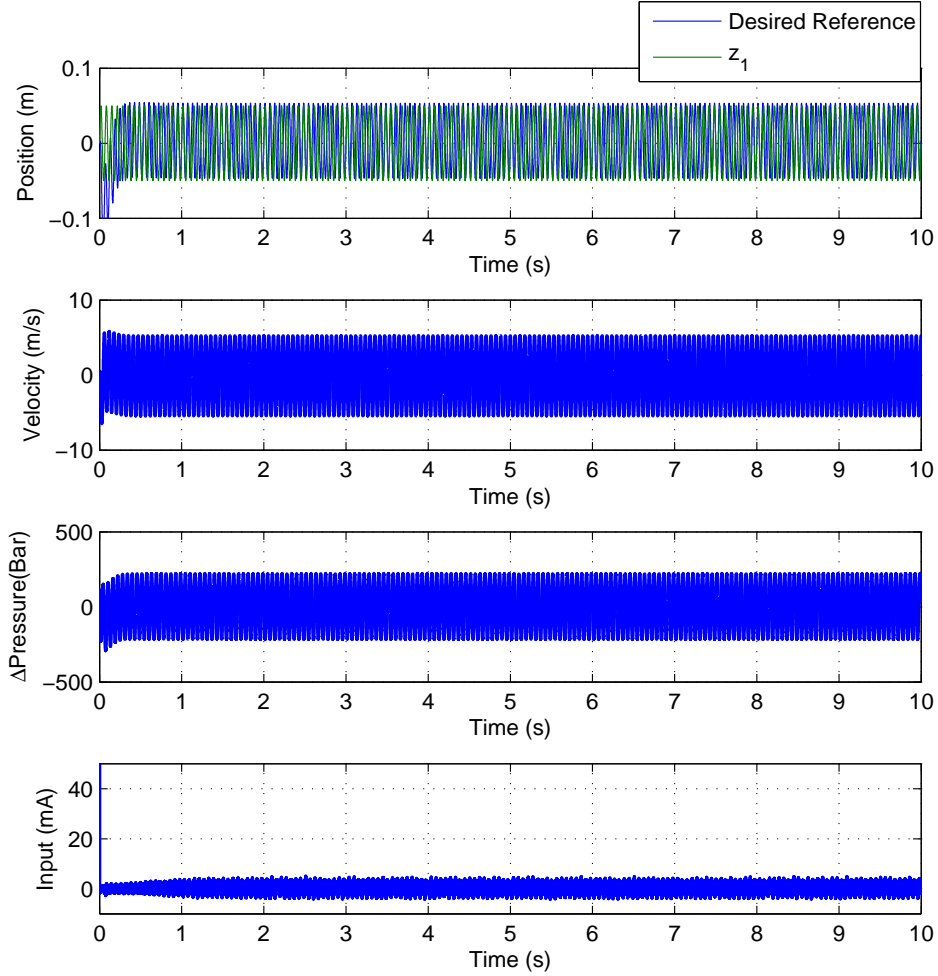


Figure 4.12: Backstepping controller for reference $(0.05\sin(2\pi ft))\text{m}$ with sweep frequency $f=15$ Hz

4.4 Results and Discussion

The numerical values for the parameters used in the simulation are given in Table 4.1. Figures (4.2), (4.3), (4.4) and (4.5) illustrates the response of the system when $\lambda = 20$ using the constant gain controller in Eq. (4.6) under a constant external disturbance. Oscillations of the control input as well as the position are clearly visible. Also, it can easily be observed that time of convergence of the

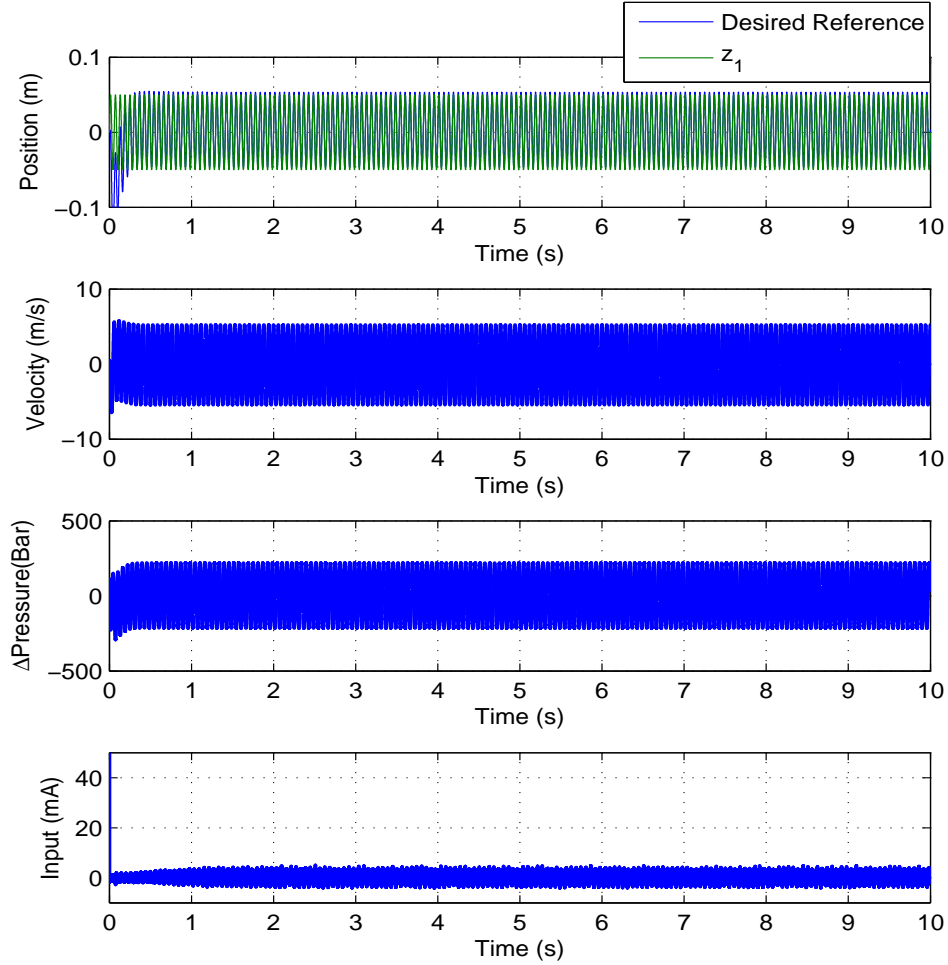


Figure 4.13: Backstepping controller for reference $(0.05\sin(2\pi ft))\text{m}$ with sweep frequency $f=17\text{ Hz}$

position to a steady state value is considerably much especially for applications that require fast responses. This is in contrast with time varying λ , in Figures (4.16), (4.15), (4.8) and (4.9) where the control is smooth and achieves excellent tracking performances. In Figures (4.16) and (4.15), the parameters λ_{max} and ϵ_1 are adjusted to 35 and 0.9 respectively in order to increase both the convergence time and the tracking accuracy. The control easily achieved the desired reference. The results from Figures (4.8) and (4.9) demonstrate the excellent tracking for

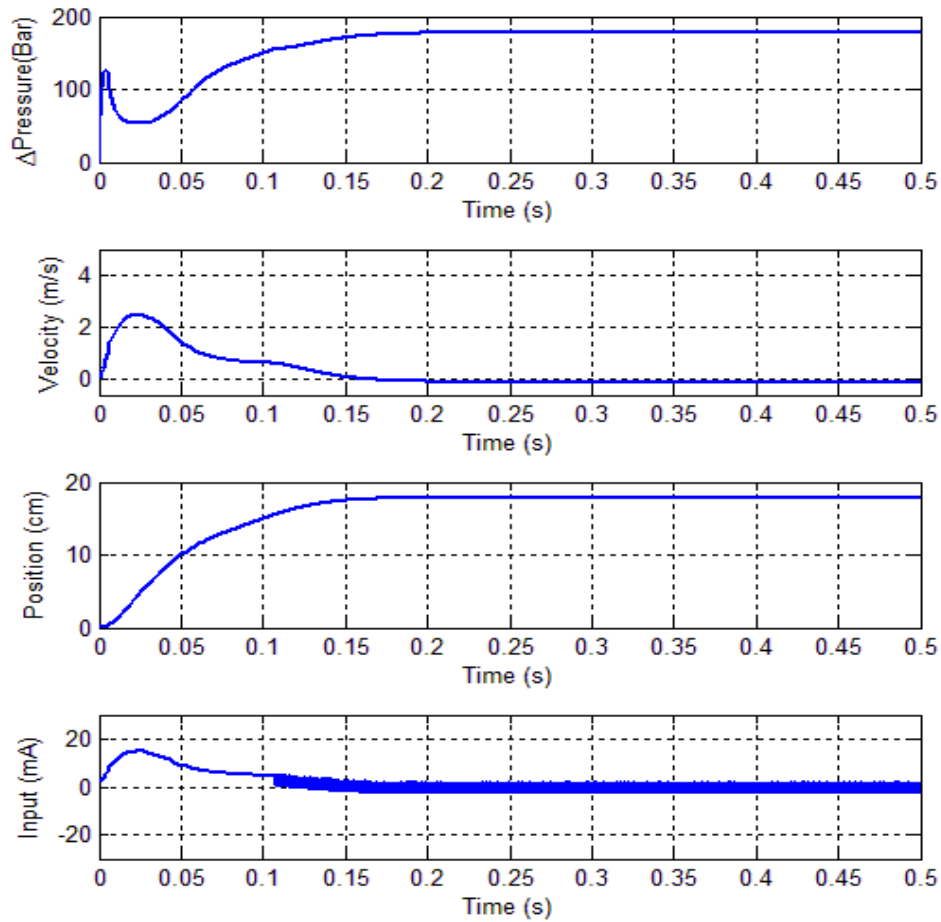


Figure 4.14: SMC under constant disturbance [$d(t) = 0.1$]

a sinusoidal reference input. The control provides a quick convergence of the tracking error to a neighborhood of the origin. It is apparent from Figure (4.17) that both the SMC and Backstepping Controller with time-varying Feedback Gain are very robust against uncertainties and unknown but bounded disturbance. It can be remarked from figure (4.15) that both controllers achieve a good tracking accuracy however, a closer look evidently show that there is chattering in closed-loop system response using the SMC. Besides, the control signal is not smooth

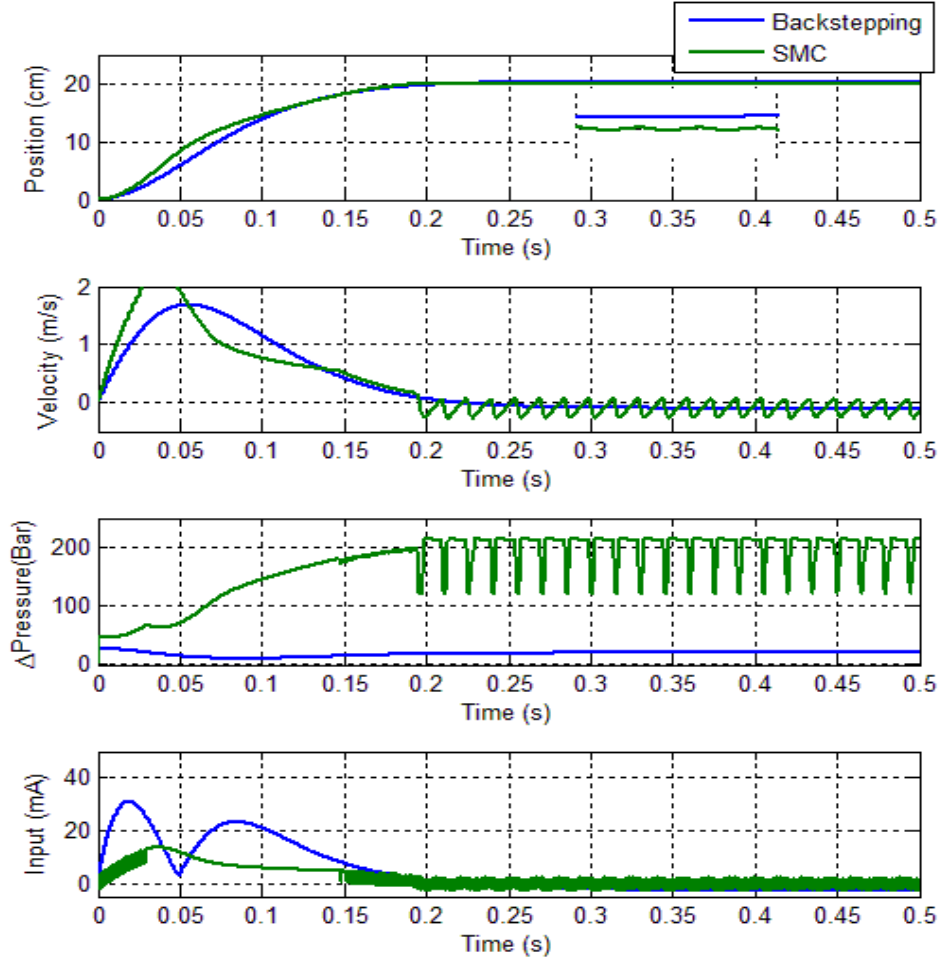


Figure 4.15: SMC and Backstepping controller with time-varying feedback gain, using constant reference ($r = 0.2\text{m}$) and under constant disturbance ($d(t) = 0.1$)

when compared with the Backstepping Controller with time-varying Feedback Gain. In figure (4.16), when the reference input is $r = 0.3\text{m}$, the SMC has a considerable steady state tracking error unlike the backstepping controller which, forces its tracking error to a small neighborhood of zero. Figures (4.10), (4.11), (4.12) and (4.13) correspond to the response of the system to sinusoidal reference ($0.05\sin(2\pi ft)\text{m}$) with sweep frequencies $f=5, 10, 15$ and 17 Hz respectively. It must be remarked that $\lambda(t)$ has to be fast enough in order to enable the system's

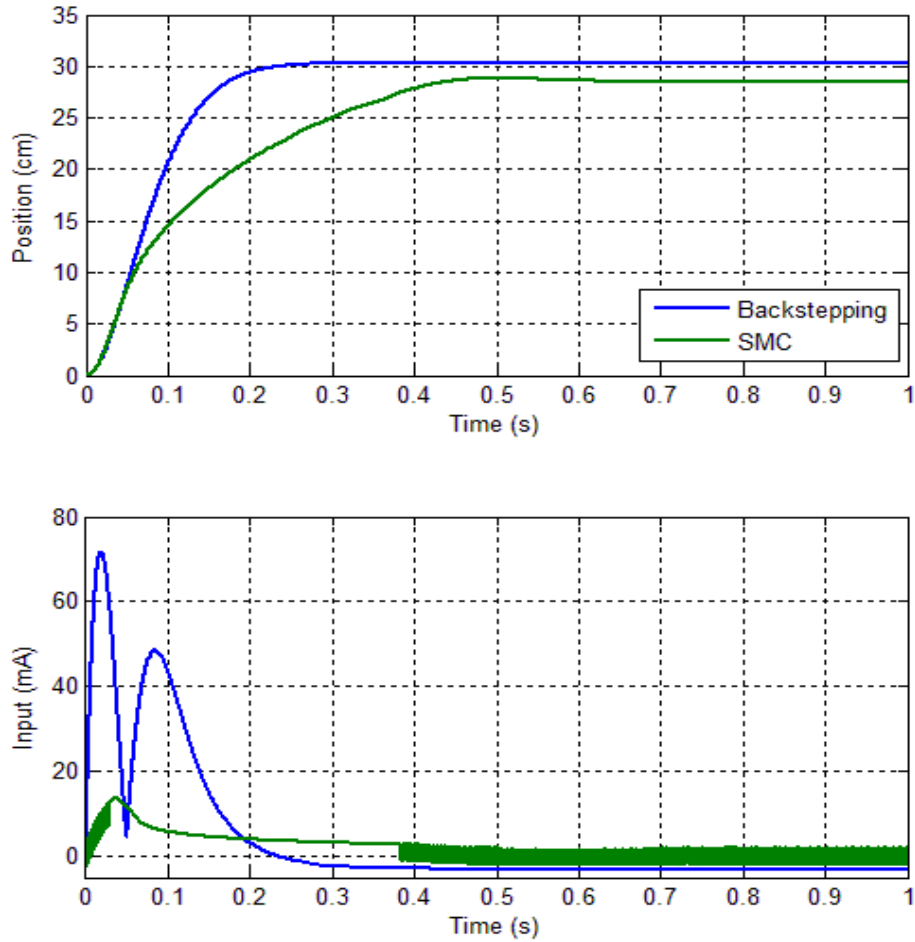


Figure 4.16: SMC and Backstepping controller with time-varying feedback gain, using constant reference ($r = 0.3\text{m}$) and under Constant disturbance($d(t) = 0.1$)

output track a higher frequency reference signals. Tuning ϵ_1 to a value of 3, increases the speed of the control signal and the close loop system is fast enough to achieve a reference with sweep frequency up to 17 Hz.

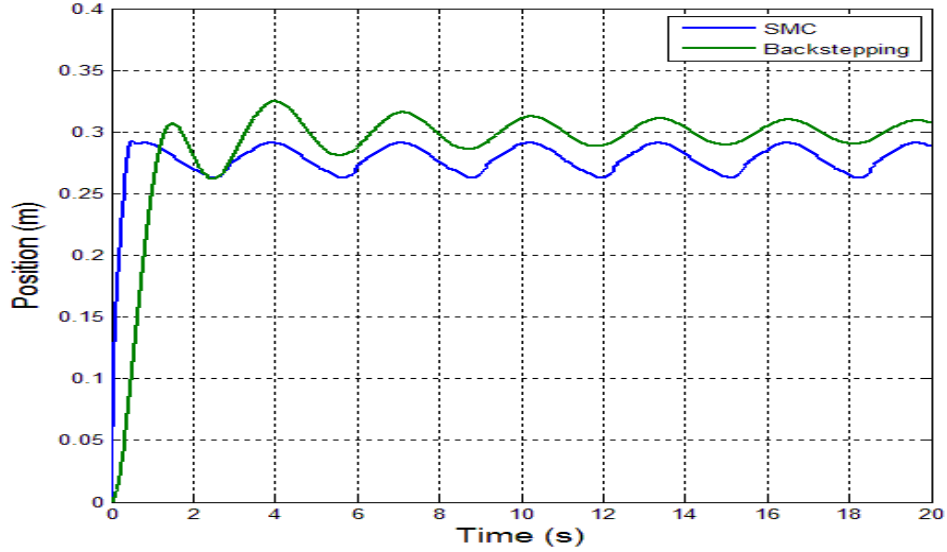


Figure 4.17: SMC and Backstepping controller with time-varying feedback gain, using constant reference ($r = 0.3\text{m}$) and under time-varying disturbance ($d(t) = 0.3\sin(t)$)

Parameters	Value	Units
B	2.2×10^9	Pa
V_t	1×10^{-3}	m^3
γ	8571	s^{-1}
α	4.1816×10^{-12}	$\text{m}^3\text{s}^{-1}\text{Pa}^{-1}$
k	5.12×10^{-5}	$\text{m}^3\text{s}^{-1}\text{A}^{-1}\text{Pa}^{1/2}$
P_s	300×10^5	Pa
P_r	1×10^5	Pa
S	1.5×10^{-3}	m^2
b	590	kg/s
k_l	12500	N/m
Δk_l	2500	N/m
m_t	70	kg

Table 4.1: Numerical value for simulations

CHAPTER 5

OBSERVER DESIGN

The criticality of observer design cannot be exaggerated. Aside the fact that observer reduces the cost of installing sensors, it is also used to monitor the conditions of the system under control and sometimes used in high fault-tolerant applications where sensors are prone to unexpected failure. Some years back, the observer design for nonlinear systems was implemented by using the Luenberger observer design on the linearized version of the system. However, the presence of inherent nonlinearity, friction and deadband make the linearization approach not efficient [33,34]. A nonlinear observer can be used to estimate the immeasurable states and parameter variations can be easily dealt with by implementing an adaptive strategy that estimates the system's parameters online. In the later chapter, an adaptive nonlinear output feedback control for the EHSS will be developed to overcome the problems of variation in parameters.

One of the major drawbacks of all state-feedback control methodologies is that the feedback is dependent on the states of the system under control. In general, accessibility to all the state variables is most times not satisfied and only few of the states are measurable. Practically, availability of the states measurements may

be inconceivable because sometimes either the measurements are impossible or are possible, but too expensive [5]. One way to obtain the nonmeasurable states is to construct an auxiliary system [32]. The role of the auxiliary system is to estimate the missing states knowing only the output of the real system. Feedback control laws can then be formulated using the states estimated by the auxiliary system called the state observer. The real system can intuitively be stabilized if it is ascertained that the estimated states can asymptotically converge to real states which, is not the case most times.

One of the reasons why the stabilization through state observer is not a trivial task is that, the conditions under which stabilizing feedback and observer can be separately designed to obtain an estimated-state feedback control law. In fact, this can easily be tagged as a *separation principle problem*. It must be remarked that the separation principle was well studied in [35] and it was shown that if the control law is continuously differentiable, the same control law formulated from the observed states will also stabilize the real system. Also, [36] generalized the work in [35] by neglecting the differentiability assumptions and focused on continuous control law. In our case, measuring the differential pressure ($\Delta P = \xi_3$) of electro hydraulic system is a costly task and requires high technology procedure to avoid additional leakage [6]. To circumvent this problem, we propose in this section to design a backstepping-based based observer that may estimate the required states and subsequently use them to regulate the position of the rod. The schematic of the observer design is depicted in Figure 5.1

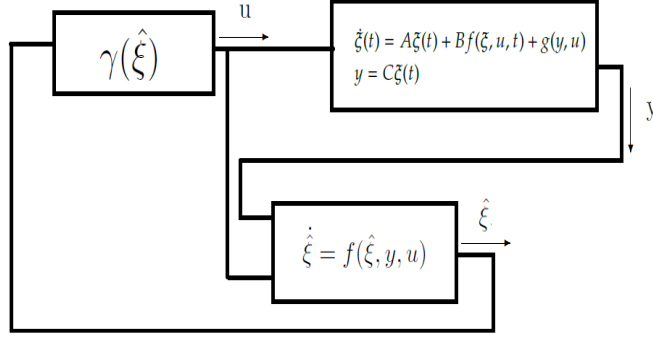


Figure 5.1: Controller using estimated states

5.1 Backstepping based Observer Design

The dynamics of the transformed system is then given in Eq. (5.1)

$$\begin{aligned}
 \dot{\xi}_1 &= \xi_2 + d(t), \\
 \dot{\xi}_2 &= \frac{1}{m_t}(S\xi_3 - b\xi_2 - \beta\xi_1), \\
 \dot{\xi}_3 &= \frac{4B}{V_t}(ku\sqrt{P_d - \text{sign}(u)\xi_3} - \frac{\alpha\xi_3}{1+\gamma|u|} - S\xi_2).
 \end{aligned} \tag{5.1}$$

The system in Eq. (5.1) can be put in the form :

$$\dot{\xi} = f(\xi) + g(\xi)u, \quad y = h(\xi) \tag{5.2}$$

where $f(\xi), g(\xi)$ and $h(\xi)$ are sufficiently smooth in domain $D \subset R^n$.

The relative degree(r) of the system is 3

$$\dot{y} = \frac{\partial h}{\partial \xi}[f(\xi) + g(\xi)u] = L_f h(\xi) + L_g h(\xi)u \tag{5.3}$$

In order to check for the observability of our system, we defined observability matrix as given below:

$$l(\xi_0, u^*) = \begin{pmatrix} h(\xi) \\ L_f h(\xi) \\ L_f^2 h(\xi) \end{pmatrix} = \begin{pmatrix} \xi_1 \\ \xi_2 + d \\ \frac{S\xi_3 - b\xi_2 - (k_l + \Delta k_l)}{m_t} \end{pmatrix} \quad (5.4)$$

$$O(\xi_0, u^*) = \frac{\partial l(\xi_0, u^*)}{\partial \xi} = \begin{pmatrix} 1 & 0 & 0 \\ 0 & 1 & 0 \\ -\frac{k_l + \Delta k_l}{m_t} & -\frac{b}{m_t} & \frac{S}{m_t} \end{pmatrix} \quad (5.5)$$

Since $O(\xi_0, u^*)$ is of full rank, the system is locally observable. Now, considering the following observer model:

$$\begin{aligned} \dot{z}_1 &= z_2 + L_1(\xi_1 - z_1), \\ \dot{z}_2 &= \frac{1}{m_t}(S z_3 - b z_2 - k_l z_1) + L_2(e_1 - \xi_1), \\ \dot{z}_3 &= \frac{4B}{V_t}(k u \sqrt{P_d - \text{sign}(u) z_3} - \frac{\alpha z_3}{1 + \gamma |u|} - S z_2) \\ &\quad + L_3(\xi_1 - z_1). \end{aligned} \quad (5.6)$$

where z_1 , z_2 and z_3 are the states of the observer.

Let the error and the error dynamics be defined as follows:

$$e_1 = \xi_1 - z_1, \quad e_2 = \xi_2 - z_2, \quad e_3 = \xi_3 - z_3. \quad (5.7)$$

$$\begin{aligned}
\dot{e}_1 &= e_2 + d - L_1 e_1, \\
\dot{e}_2 &= \frac{1}{m_t} (S e_3 - b e_2 - k_l e_1 - \Delta k_l \xi_1) - L_2 (e_1 - \xi_1), \\
\dot{e}_3 &= \frac{4Bku}{V_t} ((\sqrt{P_d - \text{sign}(u)\xi_3} - \sqrt{P_d - \text{sign}(u)z_3}) \\
&\quad - \frac{\alpha e_3}{1+\gamma|u|} - S e_2) - L_3 e_1.
\end{aligned} \tag{5.8}$$

Let

$$\alpha_1 = 1 + \frac{k_l}{m_t} + L_2, \tag{5.9}$$

$$\alpha_2 = 1 - \frac{b}{m_t}, \tag{5.10}$$

$$\alpha_3 = \frac{S}{m_t}. \tag{5.11}$$

and

$$\begin{aligned}
g(u, \xi, z) &= \frac{4Bku}{V_t} (\sqrt{P_d - \text{sign}(u)\xi_3} \\
&\quad - \sqrt{P_d - \text{sign}(u)z_3}),
\end{aligned} \tag{5.12}$$

$$c_2 = 1 - \frac{k_l}{m_t} - L_2 \tag{5.13}$$

$$f_6 = -\frac{4\alpha SBk}{m_t V_t} e_3 \tag{5.14}$$

$$f_7 = -\frac{1-\frac{b}{m_t}}{m_t} \xi_1 \tag{5.15}$$

$$L_3 = \frac{m_t}{S}(\alpha_1 e_1 + \alpha_2 e_2 + \alpha_3 e_3 + [d_{max}|c_2| + \Delta k_l |f_7| + |f_6| + |g(u, \xi, z)| \sup_{t \geq 0} |u|]) \quad (5.16)$$

Theorem 5.1 *The system with observer model Eq. (5.6) or equivalently (5.8) with parameters $L_1 \gg \frac{\lambda_0}{2}$, $L_2 = \frac{\Delta k_l}{m_t}$, and let L_3 given by equation(5.16) with (5.9)-(5.15) is practically stable and the solution of the state estimation error is globally uniformly ultimately bounded.*

Proof. In order to prove the stability of the error dynamics, we chose the following Lyapunov candidates:

$$V_1 = \frac{1}{2}e_1^2, \quad (5.17)$$

$$\dot{V}_1 = e_1 e_2 - L_1 e_1^2 + e_1 d.$$

$$\dot{V}_1 \leq (-L_1 + \frac{\lambda_0}{2})e_1^2 + \frac{1}{2\lambda_0}d^2 + e_1 e_2, \quad (5.18)$$

where $L_1 \gg \frac{\lambda_0}{2}$.

Choosing also,

$$V_2 = \frac{1}{2}e_2^2, \quad (5.19)$$

$$\dot{V}_2 = e_2(\frac{1}{m_t}(S e_3 - b e_2 - k_l e_1) - \frac{1}{m_t} \Delta k_l \xi_1 - L_2(e_1 - \xi_1)). \quad (5.20)$$

$$\begin{aligned} \dot{V}_1 + \dot{V}_2 \leq & (-L_1 + \frac{\lambda_a}{2})e_1^2 + \frac{1}{2\lambda_o}d^2 + e_2(\frac{1}{m_t}(Se_3 - be_2 - k_l e_1) \\ & - L_2 e_1 + \xi_1(L_2 - \frac{1}{m_t}\Delta k_l) + e_1). \end{aligned} \quad (5.21)$$

To nullify the effect of Δk_l and ξ_1 , we choose $L_2 = \frac{\Delta k_l}{m_t}$. Therefore,

$$\begin{aligned} \dot{V}_1 + \dot{V}_2 \leq & (-L_1 + \frac{\lambda_a}{2})e_1^2 + \frac{1}{2\lambda_o}d^2 - e_2^2 \\ & + e_2(\frac{1}{m_t}(Se_3 - be_2 - k_l e_1) - L_2 e_1 + e_1 + e_2). \end{aligned} \quad (5.22)$$

Putting Eq. (5.22) in a compact form, we have:

$$\begin{aligned} \dot{V}_1 + \dot{V}_2 \leq & (-L_1 + \frac{\lambda_a}{2})e_1^2 + \frac{1}{2\lambda_o}d^2 - e_2^2 \\ & + e_2(\alpha_1 e_1 + \alpha_2 e_2 + \alpha_3 e_3). \end{aligned} \quad (5.23)$$

with

$$\alpha_1 = 1 + \frac{k_l}{m_t} + L_2,$$

$$\alpha_2 = 1 - \frac{b}{m_t},$$

$$\alpha_3 = \frac{S}{m_t}.$$

Choosing $V_3 = \frac{1}{2}(\alpha_1 e_1 + \alpha_2 e_2 + \alpha_3 e_3)^2$, then,

$$\dot{V} = \dot{V}_1 + \dot{V}_2 + \dot{V}_3 \quad (5.24)$$

$$\begin{aligned} \dot{V} \leq & (-L_1 + \frac{\lambda_o}{2})e_1^2 + \frac{1}{2\lambda_o}d^2 - e_2^2 \\ & + e_2[\alpha_1e_1 + \alpha_2e_2 + \alpha_3e_3] \end{aligned} \quad (5.25)$$

$$+ (\alpha_1e_1 + \alpha_2e_2 + \alpha_3e_3)[\alpha_1\dot{e}_1 + \alpha_2\dot{e}_2 + \alpha_3\dot{e}_3]$$

$$\begin{aligned} \dot{V} \leq & (-L_1 + \frac{\lambda_o}{2})e_1^2 + \frac{1}{2\lambda_o}d^2 - e_2^2 \\ & + (\alpha_1e_1 + \alpha_2e_2 + \alpha_3e_3)[g(u, \xi, z) \cdot u - \frac{S}{m_t}L_3] \\ & + c_2d + \frac{f_6}{1+\gamma|u|} + f_7\Delta k_l \end{aligned} \quad (5.26)$$

Considering that:

$$\frac{1}{1+\gamma|u|} \leq 1; \quad (5.27)$$

$$c_2d(\alpha_1e_1 + \alpha_2e_2 + \alpha_3e_3) \leq d_{max} |c_1| |\alpha_1e_1 + \alpha_2e_2 + \alpha_3e_3| \quad (5.28)$$

$$f_7\Delta k_l(\alpha_1e_1 + \alpha_2e_2 + \alpha_3e_3) \leq \Delta k_l |f_7| |\alpha_1e_1 + \alpha_2e_2 + \alpha_3e_3| \quad (5.29)$$

$$(\alpha_1e_1 + \alpha_2e_2 + \alpha_3e_3)f_6 \leq |f_6| |\alpha_1e_1 + \alpha_2e_2 + \alpha_3e_3| \quad (5.30)$$

$$(\alpha_1e_1 + \alpha_2e_2 + \alpha_3e_3)g(u, \xi, z)u(t) \leq |g(u, \xi, z)| |\alpha_1e_1 + \alpha_2e_2 + \alpha_3e_3| \sup_{t \geq 0} |u| \quad (5.31)$$

then,

$$\begin{aligned} \dot{V} \leq & (-L_1 + \frac{\lambda_o}{2})e_1^2 + \frac{1}{2\lambda_o}d^2 - e_2^2 \\ & - \frac{S}{m_t}(\alpha_1e_1 + \alpha_2e_2 + \alpha_3e_3)L_3 + |\alpha_1e_1 \\ & + \alpha_2e_2 + \alpha_3e_3|(d_{max}|c_2| \\ & + \Delta k_l|f_7| + |f_6| + |g(u, \xi, z)| \sup_{t \geq 0} |u|) \end{aligned} \quad (5.32)$$

To ensure $\dot{V} \leq 0$, L_3 can be selected as follows:

$$L_3 = \frac{m_t}{S} (\alpha_1 e_1 + \alpha_2 e_2 + \alpha_3 e_3 + [d_{max} |c_2| + \Delta k_l |f_7| + |f_6| + |g(u, \xi, z)| \sup_{t \geq 0} |u|]) \quad (5.33)$$

Using equations (5.27 - 5.31),

$$\begin{aligned} \dot{V} \leq & (-L_1 + \frac{\lambda_o}{2}) e_1^2 + \frac{1}{2\lambda_o} d^2 - e_2^2 \\ & - (\alpha_1 e_1 + \alpha_2 e_2 + \alpha_3 e_3)^2 \end{aligned} \quad (5.34)$$

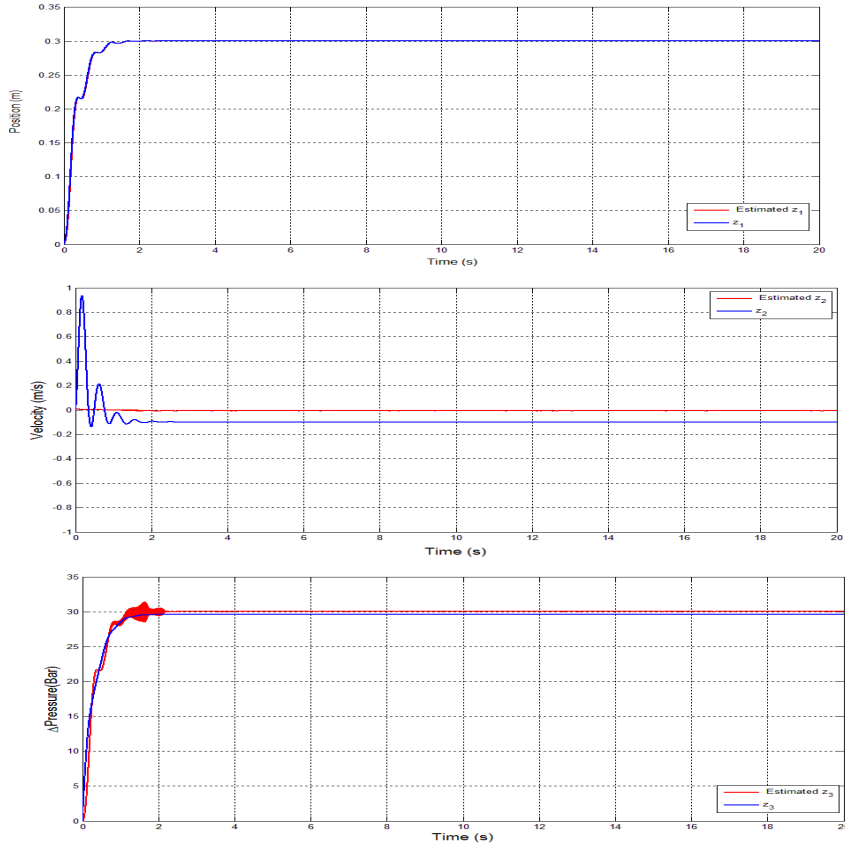


Figure 5.2: Behavior of the observer and hydraulic servo system using a constant feedback gain (λ) and under a constant disturbance

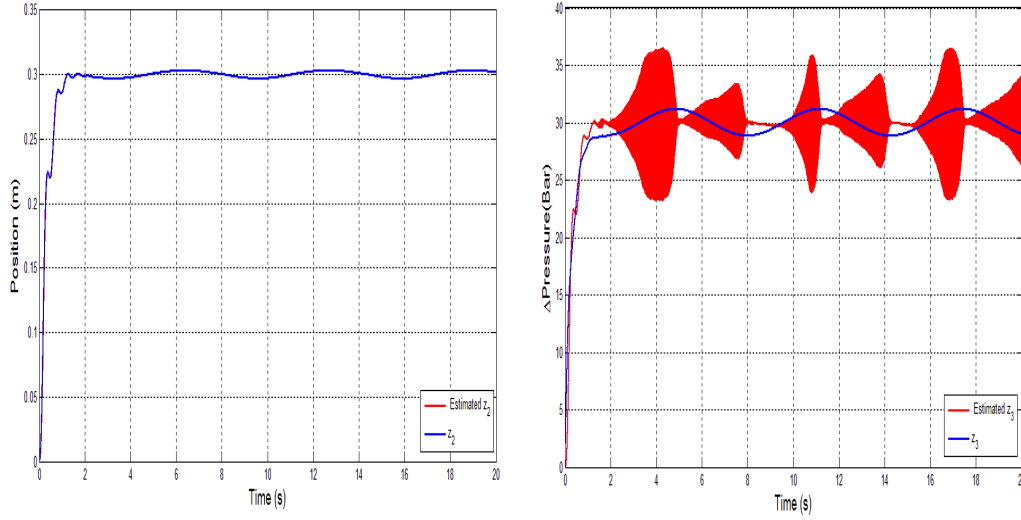


Figure 5.3: Behavior of the observer and hydraulic servo system under a sinusoidal disturbance using a constant feedback gain (λ)

Remark 5.1 *It can be remarked that the tracking error is globally uniformly ultimately bounded with ultimate bound satisfying the following condition $|(-L_1 + \frac{\lambda_o}{2})e_1^2 + e_2^2 + (\alpha_1 e_1 + \alpha_2 e_2 + \alpha_3 e_3)^2| \leq \frac{1}{2\lambda_o} d^2$. The parameter λ_o is also a design parameter introduced in Young's inequality during the proof of stability of the state-observer. Such parameter should be selected as big as possible to decrease the ultimate bound in the tracking error dynamic. The larger is λ_o the more oscillatory is the transient and higher in the control input. In order, to allow λ_o to take large values and avoid transient problems, one may attempt to select λ_o to be function of time rather than a constant. In such case, the design becomes more complicated and separation between the control and the observer is no longer valid.*

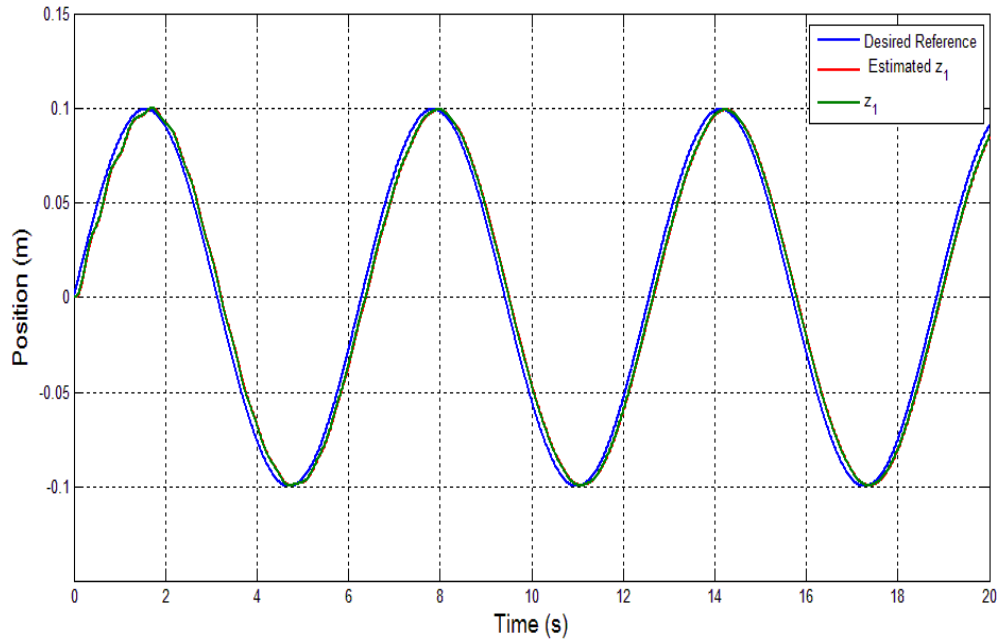


Figure 5.4: Behavior of the observer and hydraulic servo system under a constant disturbance using a constant feedback gain (λ). Reference($r = 10\sin(t)$ cm)

5.2 Results and Discussion

Figure (5.2) shows the performance of the observer. It can be seen that the control easily achieves the desired reference and the observer estimates the states of the system under constant external disturbance with a steady state error converging to a small neighborhood of the origin. When the disturbance is assumed to be time varying ($d(t) = 0.3\sin(t)$) as shown in Figure (5.3), the output of the closed loop system still tracks the reference with small steady state oscillations due to the large amplitude of the sinusoidal external disturbance. Figures (5.4) and (5.5) demonstrate the excellent tracking of sinusoidal reference for both the system and the observer under a constant external disturbance ($d(t) = 0.1$). Even though the observer estimates the position with a very small estimation error in the steady

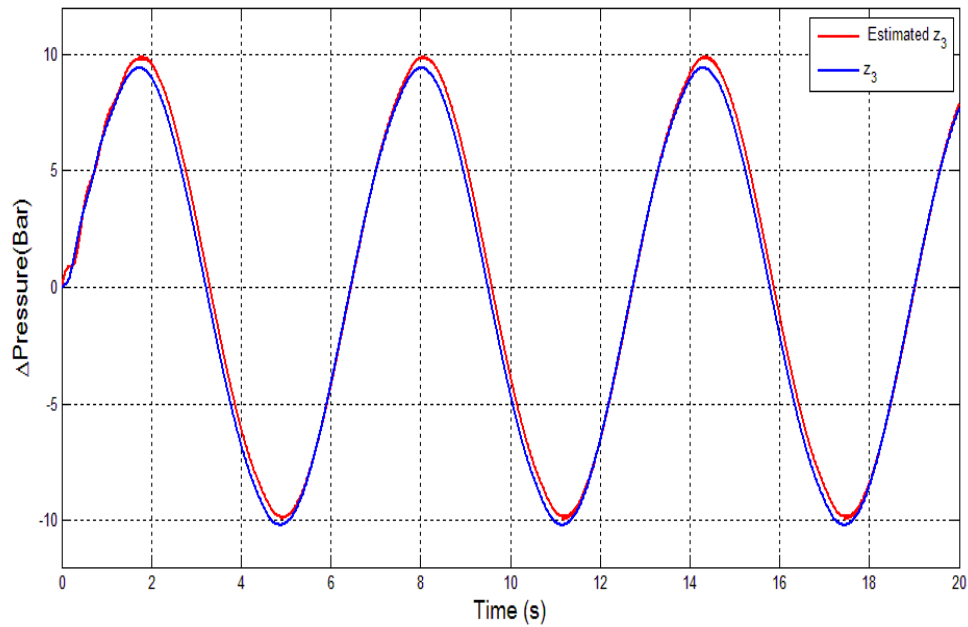


Figure 5.5: Behavior of the observer and hydraulic servo system under a constant disturbance using a constant feedback gain (λ). Reference($r = 10\sin(t)$)cm)

state however, there is a considerable estimation error in the case of the differential pressure. It is also apparent in Figures (5.6) and (5.7) that the control provides a quick convergence of the tracking error to a neighborhood of the origin even when the reference is changed to sum of sinusoids. Whereas, the estimation error is very small for the position, just as observed for sinusoidal reference in Figure (5.4)

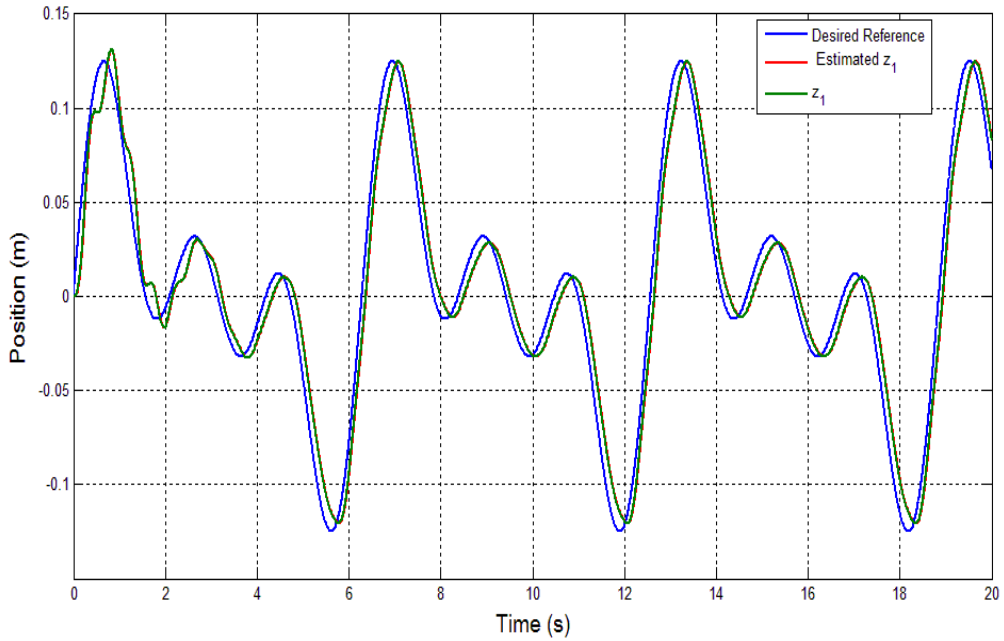


Figure 5.6: Behavior of the observer and hydraulic servo system under a constant disturbance using a constant feedback gain (λ). Reference($r = 0.05(\sin(t) + \sin(2t) + \sin(3t))m$)

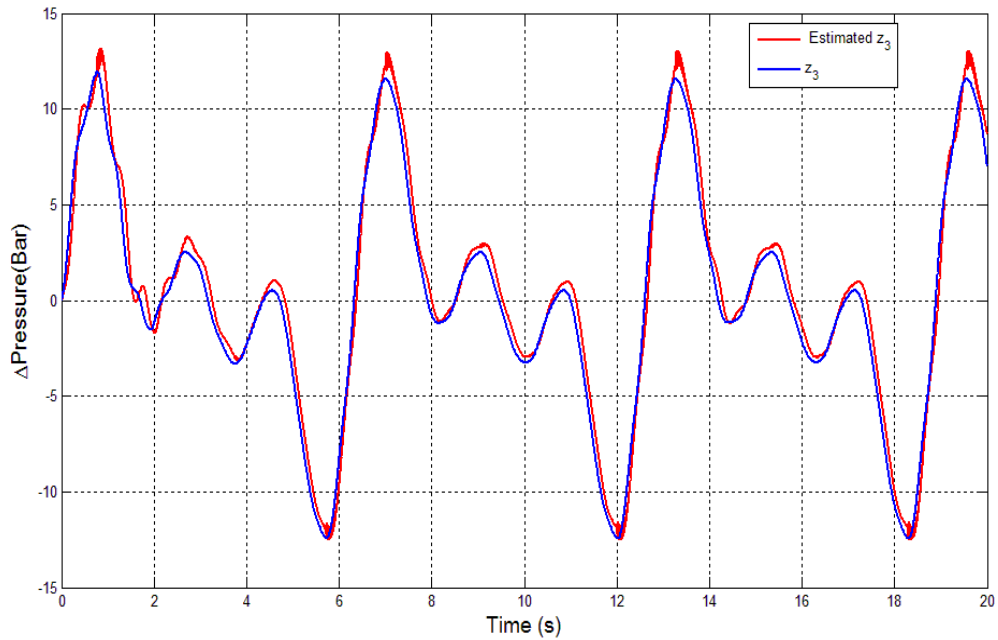


Figure 5.7: Behavior of the observer and hydraulic servo system under a constant disturbance using a constant feedback gain (λ). Reference($r = 0.05(\sin(t) + \sin(2t) + \sin(3t))m$)

CHAPTER 6

ROBUST ADAPTIVE CONTROL DESIGN

Most importantly, EHSS parameters are subject to variation due to temperature rise. For instance, the coefficients such as bulk modulus and viscous friction are prone to variation due to temperature fluctuations. And owing to the fact that backstepping controller design relies on actual system's parameters, the need arises to design a controller that has the capability of adapting to these changes.

To overcome the problem of variation in parameters, adaptive control schemes are generally employed. In controlling EHSS, adaptive schemes suffer a serious setback if the uncertain parameter is the supply pressure difference which happens to appear in a square-root in the dynamics of the system. This setback is because traditional adaptive schemes demand the system to be linear in uncertain parameters.

In this chapter, we present a backstepping based adaptive technique that is robust to uncertainties in the system's parameters and external disturbance. First, we assume the parameters of the load (that is β) and frictional coefficient(b) is unknown but linear and has to be estimated by the adaptive scheme. In the other case, we proposed adaptive scheme that assumes that β and b are nonlinear

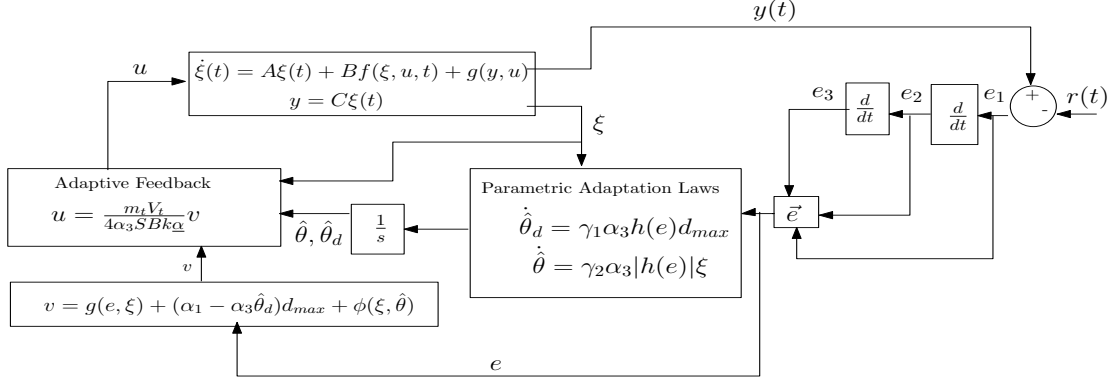


Figure 6.1: Adaptive Control Scheme

function. The schematic of the proposed backstepping based adaptive strategy is shown in Figure 6.1 below

Case 1 Recall Eq. (6.1), and choosing: $A = \frac{4BSk}{m_t V_t}$ and $m(t) = \sqrt{P_d - \text{sign}(u)x_1}$, then the error dynamics satisfy

$$\begin{aligned}
 \dot{e}_1 &= e_2 + d, \\
 \dot{e}_2 &= e_3, \\
 \dot{e}_3 &= \frac{b\beta}{m_t^2} \xi_1 + \left(\frac{-\beta}{m_t} + \frac{b^2}{m_t^2} - \frac{4BS^2}{m_t V_t} \right) \xi_2 + \left(-\frac{bS}{m_t^2} - \frac{4BS\alpha}{m_t V_t (1+\gamma|u|)} \right) \xi_3 \\
 &\quad - \frac{\beta}{m_t} d - \ddot{r} + Am(t)u.
 \end{aligned} \tag{6.1}$$

Let, $\theta_d = \frac{\beta}{m_t}$ and

$$\theta_1 = \frac{b\beta}{m_t^2}, \quad \theta_2 = \frac{-\beta}{m_t} + \frac{b^2}{m_t^2} - \frac{4BS^2}{m_t V_t}, \quad \theta_3 = -\frac{bS}{m_t^2} - \frac{4BS\alpha}{m_t V_t (1+\gamma|u|)}. \tag{6.2}$$

Eq.(6.60) can then be transformed into,

$$\begin{aligned}
 \dot{e}_1 &= e_2 + d, \\
 \dot{e}_2 &= e_3, \\
 \dot{e}_3 &= \theta^T \xi - \theta_d d(t) - \ddot{r} + Am(t)u.
 \end{aligned} \tag{6.3}$$

where, A is a known constant and θ is an unknown parameter vector containing θ_1 , θ_2 and θ_3 . θ_d is unknown parameter associated with the disturbance in the error dynamics. ξ is a state vector comprising of ξ_1 , ξ_2 and ξ_3 . Now, the goal is designing an adaptive feedback such that

$$\lim_{t \rightarrow \infty} |\xi_1 - r(t)| \leq \delta \tag{6.4}$$

where, δ is a sufficiently small positive number. The design task is to make δ as small as possible and at the same time ensuring a control law that is smooth. The following gives the synopsis of the control design schemes.

Theorem 6.1 Let us denote

$$\begin{aligned}
 h(e) &= \alpha_1 e_1 + \alpha_2 e_2 + \alpha_3 e_3, \\
 g(e, \xi) &= \lambda e_1 + (1 + \alpha_1) e_2 + \alpha_2 e_3
 \end{aligned} \tag{6.5}$$

and let the adaptation law be given as

$$\begin{aligned}\dot{\hat{\theta}}_d &= \gamma\alpha_3|h(e)|\mu \\ \dot{\hat{\theta}} &= \gamma\alpha_3|h(e)|\xi\end{aligned}\tag{6.6}$$

and let the adaptive feedback be given as

$$u = \frac{m_t V_t}{4\alpha_3 S B k \underline{\alpha}} \left[|g(e, \xi)| + |\alpha_1 + \alpha_3 \hat{\theta}_d| d_{max} + \phi(\xi, \hat{\theta}) - k_o h(e) \right]\tag{6.7}$$

where, $\underline{\alpha} = \min(\sqrt{P_d - \xi_3}, \sqrt{P_d + \xi_3})$, $\tilde{\theta} = \theta - \hat{\theta}$, $\sup_{t \geq 0} |d(t)| = d_{max}$, $\phi(\xi, \hat{\theta}) = \alpha_3 [|\hat{\theta}^T \xi| + \sup_{t \geq 0} |\ddot{r}|]$ and $\lambda > 0$ is a design parameter

Then, EHSS under the adaptive feedback control law given in (6.7) is practically stable and the solution of the error dynamic (6.1) is globally uniformly ultimately bounded with ultimate bound satisfying the following condition $|\frac{\lambda_c}{2} e_1^2 + (e_2 + \lambda_c e_1)^2 + (\alpha_1 e_1 + \alpha_2 e_2 + \alpha_3 e_3)^2| \leq \sqrt{(\frac{1}{2\lambda} + \frac{1}{2\lambda^5})} d_{max}^2$

Proof. Choosing the lyapunov candidate function as:

$$V_1 = \frac{1}{2} e_1^2,\tag{6.8}$$

Calculating the derivative of $V(x)$ along the trajectories of the perturbed system, we obtain

$$\dot{V}_1 = -\lambda e_1^2 + e_1(e_2 + \lambda e_1) + e_1 d.\tag{6.9}$$

$$\dot{V}_1 \leq -\lambda e_1^2 + e_1(e_2 + \lambda e_1) + \frac{1}{2\lambda} d^2 + \frac{\lambda}{2} e_1^2 \leq -\frac{\lambda}{2} e_1^2 + \frac{1}{2\lambda} d^2 + e_1(e_2 + \lambda e_1).$$

again using the Young's inequality with $\lambda > 0$ [37];

$$e_1 d \leq |e_1| |d| \leq \frac{1}{2\lambda} d^2 + \frac{\lambda}{2} e_1^2 \quad (6.10)$$

Let $V_2 = \frac{1}{2\lambda^4} (e_2 + \lambda e_1)^2$, then

$$\dot{V}_2 = \frac{1}{\lambda^4} (e_2 + \lambda e_1) (e_3 + \lambda (e_2 + d)) \quad (6.11)$$

Therefore,

$$\dot{V}_1 + \dot{V}_2 \leq -\frac{\lambda}{2} e_1^2 + \frac{1}{2\lambda} d^2 + \frac{1}{\lambda^4} (e_2 + \lambda e_1) [e_3 + \lambda e_2 + \lambda^4 e_1 + \lambda d] \quad (6.12)$$

But,

$$\frac{1}{\lambda^3} (e_2 + \lambda e_1) d \leq \frac{1}{\lambda^3} |d| |e_2 + \lambda e_1| \leq \frac{1}{\lambda^3} [\frac{1}{2\lambda^2} d^2 + \frac{\lambda^2}{2} (e_2 + \lambda e_1)^2] \quad (6.13)$$

Inserting Eq. (6.13) into Eq. (6.12), we have

$$\dot{V}_1 + \dot{V}_2 \leq -\frac{\lambda}{2} e_1^2 + (\frac{1}{2\lambda} + \frac{1}{2\lambda^5}) d^2 + (e_2 + \lambda e_1) [\frac{1}{\lambda^4} (e_3 + \lambda e_2 + \lambda^4 e_1) + \frac{\lambda^2}{2} (e_2 + \lambda e_1)]. \quad (6.14)$$

$$\dot{V}_1 + \dot{V}_2 \leq -\frac{\lambda}{2} e_1^2 + (\frac{1}{2\lambda} + \frac{1}{2\lambda^5}) d^2 - (e_2 + \lambda e_1)^2 + (e_2 + \lambda e_1) [\alpha_1 e_1 + \alpha_2 e_2 + \alpha_3 e_3] \quad (6.15)$$

Choosing $V_3 = \frac{1}{2}(\alpha_1 e_1 + \alpha_2 e_2 + \alpha_3 e_3)^2$, then,

$$\begin{aligned} \dot{V}_1 + \dot{V}_2 + \dot{V}_3 \leq & -\frac{\lambda}{2}e_1^2 + \left(\frac{1}{2\lambda} + \frac{1}{2\lambda^5}\right)d^2 - (e_2 + \lambda e_1)^2 + (e_2 + \lambda e_1)[\alpha_1 e_1 + \alpha_2 e_2 + \alpha_3 e_3] \\ & + (\alpha_1 e_1 + \alpha_2 e_2 + \alpha_3 e_3)[\alpha_1 \dot{e}_1 + \alpha_2 \dot{e}_2 + \alpha_3 \dot{e}_3] \end{aligned} \quad (6.16)$$

$$\begin{aligned} \dot{V}_1 + \dot{V}_2 + \dot{V}_3 \leq & -\frac{\lambda}{2}e_1^2 + \left(\frac{1}{2\lambda} + \frac{1}{2\lambda^5}\right)d^2 - (e_2 + \lambda e_1)^2 + (\alpha_1 e_1 + \alpha_2 e_2 + \alpha_3 e_3)[e_2 + \lambda e_1 \\ & + \alpha_1(e_2 + d) + \alpha_2 e_3 + \alpha_3(\tilde{\theta}^T \xi + \hat{\theta}^T \xi - \tilde{\theta}_d d - \hat{\theta}_d d - \ddot{r} + Am(t)u)] \end{aligned} \quad (6.17)$$

$$\begin{aligned} \dot{V}_1 + \dot{V}_2 + \dot{V}_3 \leq & -\frac{\lambda}{2}e_1^2 + \left(\frac{1}{2\lambda} + \frac{1}{2\lambda^5}\right)d^2 - (e_2 + \lambda e_1)^2 \\ & + (\alpha_1 e_1 + \alpha_2 e_2 + \alpha_3 e_3)[\lambda e_1 + (1 + \alpha_1)e_2 + (\alpha_1 - \alpha_3 \hat{\theta}_d)d \\ & - \alpha_3 \tilde{\theta} d + \alpha_3 \tilde{\theta}^T \xi + \alpha_3 \hat{\theta}^T \xi - \alpha_3 \ddot{r} + \alpha_3 Am(t)u] \end{aligned} \quad (6.18)$$

In order to minimize the parametric error, the last candidate is thus chosen as:

$$V_4 = \frac{1}{2\gamma} \tilde{\theta}^T \tilde{\theta} + \frac{1}{2\gamma} \tilde{\theta}_d^2 \quad (6.19)$$

Now,

$$\dot{V} = \dot{V}_1 + \dot{V}_2 + \dot{V}_3 + \dot{V}_4 \quad (6.20)$$

Therefore, the derivative of the lyapunov function is thus given:

$$\begin{aligned} \dot{V} \leq & -\frac{\lambda}{2}e_1^2 + \left(\frac{1}{2\lambda} + \frac{1}{2\lambda^5}\right)d^2 - (e_2 + \lambda e_1)^2 + (\alpha_1 e_1 + \alpha_2 e_2 + \alpha_3 e_3)[\lambda e_1 + (1 + \alpha_1)e_2 \\ & + (\alpha_1 - \alpha_3 \hat{\theta}_d)d - \alpha_3 \tilde{\theta}d + \alpha_3 \tilde{\theta}^T \xi + \alpha_3 \hat{\theta}^T \xi - \alpha_3 \ddot{r} + \alpha_3 Am(t)u] - \frac{1}{\gamma} \tilde{\theta}^T \dot{\hat{\theta}} - \frac{1}{\gamma} \tilde{\theta}_d \dot{\hat{\theta}}_d \end{aligned} \quad (6.21)$$

$$\begin{aligned} \dot{V} \leq & -\frac{\lambda}{2}e_1^2 + \left(\frac{1}{2\lambda} + \frac{1}{2\lambda^5}\right)d^2 - (e_2 + \lambda e_1)^2 - h(e)[g(e, \xi) + (\alpha_1 - \alpha_3 \hat{\theta}_d)d + \alpha_3 \hat{\theta}^T \xi \\ & - \alpha_3 \ddot{r} + \alpha_3 Am(t)u] + \left(-\alpha_3 h(e)d - \frac{1}{\gamma} \hat{\theta}_d \tilde{\theta}_d + \tilde{\theta}^T (\alpha_3 h(e)\xi - \frac{1}{\gamma} \dot{\hat{\theta}})\right) \end{aligned} \quad (6.22)$$

Since the following bounds hold,

$$h(e) \leq |h(e)g(e, \xi)| \leq |h(e)||g(e, \xi)| \quad (6.23)$$

$$h(e)\phi(\xi, \hat{\theta}) \leq \phi(\xi, \hat{\theta})|h(e)| \quad (6.24)$$

$$h(e)(\alpha_1 - \alpha_3 \hat{\theta}_d)d(t) \leq |h(e)||\alpha_1 - \alpha_3 \hat{\theta}_d| \sup_{t \geq 0} |d(t)| \leq |h(e)||\alpha_1 - \alpha_3 \hat{\theta}_d| d_{max} \quad (6.25)$$

By consequence, it is inferred that,

$$\begin{aligned} \dot{V} \leq & -\frac{\lambda}{2}e_1^2 + \left(\frac{1}{2\lambda} + \frac{1}{2\lambda^5}\right)d^2 - (e_2 + \lambda e_1)^2 - h(e)[g(e, \xi) + |\alpha_1 - \alpha_3 \hat{\theta}_d| d_{max} + \phi(\xi, \hat{\theta}) \\ & + \alpha_3 Am(t)u] + \left(-\alpha_3 h(e)d - \frac{1}{\gamma} \hat{\theta}_d \tilde{\theta}_d + \tilde{\theta}^T (\alpha_3 h(e)\xi - \frac{1}{\gamma} \dot{\hat{\theta}})\right) \end{aligned} \quad (6.26)$$

In order to ensure a uniformly ultimately bounded tracking error, we set the adap-

tation laws as given in (6.6) Finally,

$$\dot{V} \leq -\frac{\lambda}{2}e_1^2 + \left(\frac{1}{2\lambda} + \frac{1}{2\lambda^5}\right)d^2 - (e_2 + \lambda e_1)^2 - (\alpha_1 e_1 + \alpha_2 e_2 + \alpha_3 e_3)^2 \quad (6.27)$$

This ends the proof. The external perturbation is bounded whatever the adaptive feedback applied and it must be remarked that the boundedness of $\hat{\theta}$ and $\hat{\theta}_d$ was not addressed in this development. Boundedness of the estimated parameters can be easily achieved by modifying the adaptation law given in (6.6).

6.1 Results Discussion

It must be noted that the proposed adaptive design does not involve the differentiation of $m(t)$ which, is an indication that the scheme can handle the effects of various types of slowly time-varying $m(t)$ and $d(t)$. The problem we solved is a robust adaptive control issue. Using a constant trajectory as seen in Figure (6.18), the adaptive control given in Eq. (6.7) accomplishes a bounded error tracking even in the presence of input nonlinearity, parameter uncertainties and unknown but bounded disturbance. The tracking error depicted in Figure (6.3) is reasonably small and can further be reduced by the choice of λ and ϵ . It must be noted that λ is a design parameter and can be used to reduce the bound of the external disturbance. However, ϵ has to be chosen sufficiently small and its choice is neither dependent on system's parameters nor the bound of the disturbance. Also from Figure (6.18), it can easily be observed that there is a keen compromise between

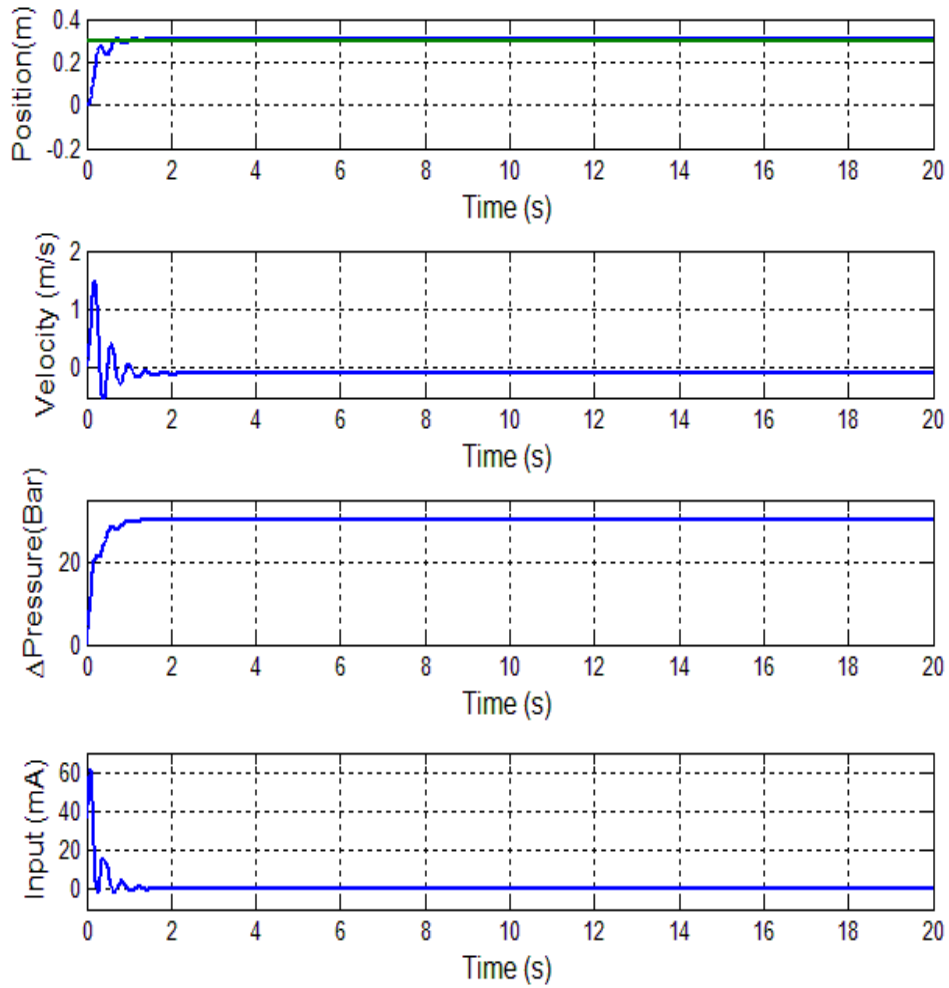


Figure 6.2: Behavior of the hydraulic servo system under a constant disturbance, Reference($r = 30$ cm)

the smoothness of the adaptive control law and the tracking error which, constitutes the main trait of most adaptive strategy. In a nutshell, the proposed solution is robust against parameter uncertainties and disturbance if the ultimate bound satisfies the condition $(\alpha_1 e_1 + \alpha_2 e_2 + \alpha_3 e_3) \leq \sqrt{(\frac{1}{2\lambda_c} + \frac{1}{2\lambda_c^2})} d_{max}$. Figures (6.19,6.5) demonstrate the excellent tracking for a sinusoidal reference input whereas, Figures (6.5,6.20) depict excellent tracking accuracy when the reference is changed to sum of sinusoids. Even though there is a big tracking error in the transient,

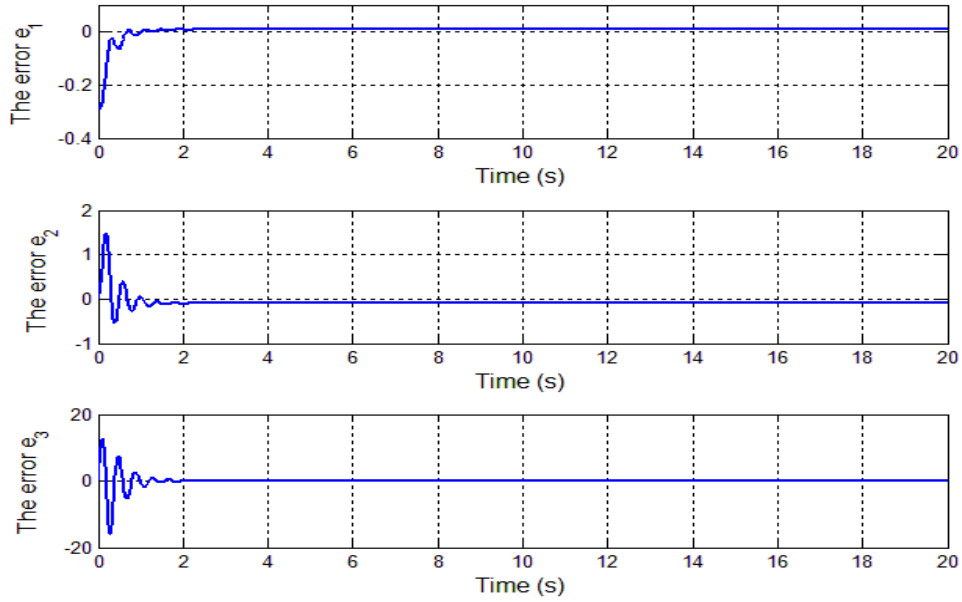


Figure 6.3: The error plots

the error converges to the neighborhood of the origin at the steady states. This phenomenon depicts how robust the adaptive controller is.

6.2 High-Gain Adaptive Observer Design

A nonlinear observer can be used to estimate the immeasurable states and parameter variations can be easily dealt with using adaptive strategy to estimate the system's parameters online. Based on this, we developed an adaptive nonlinear output feedback control for the EHSS that overcomes all these challenges. The schematic of the proposed adaptive output feedback strategy is shown in Figure 6.8 Now, considering the following observer model:

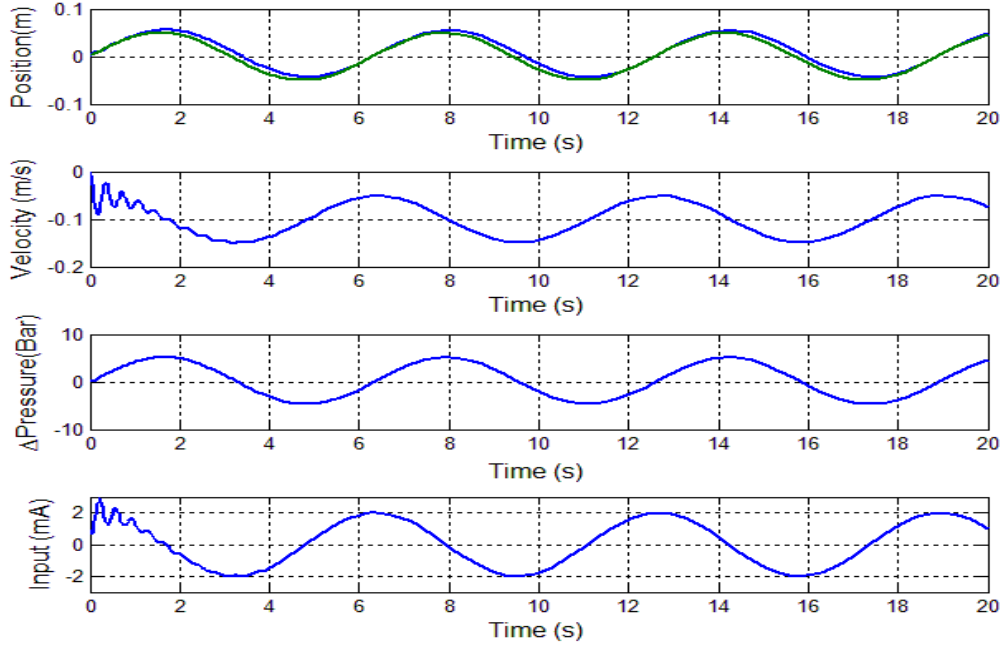


Figure 6.4: Behavior of the hydraulic servo system under a constant disturbance, Reference($r = 10\sin(t)\text{cm}$)

$$\begin{aligned}
 \dot{\hat{\xi}}_1 &= \hat{\xi}_2 + L_1(\xi_1 - \hat{\xi}_1), \\
 \dot{\hat{\xi}}_2 &= \frac{1}{m_t}(S\hat{\xi}_3 - b\hat{\xi}_2 - k_l\hat{\xi}_1) + L_2(\text{breve}\xi_1 - \xi_1), \\
 \dot{\hat{\xi}}_3 &= \frac{4B}{V_t}(ku\sqrt{P_d - \text{sign}(u)\hat{\xi}_3} - \frac{\alpha\hat{\xi}_3}{1+\gamma|u|} - S\hat{\xi}_2) \\
 &\quad + L_3(\xi_1 - \hat{\xi}_1).
 \end{aligned} \tag{6.28}$$

Let the error and the error dynamics be defined as follows:

$$\check{\xi}_1 = \xi_1 - \hat{\xi}_1, \quad \check{\xi}_2 = \xi_2 - \hat{\xi}_2, \quad \check{\xi}_3 = \xi_3 - \hat{\xi}_3. \tag{6.29}$$

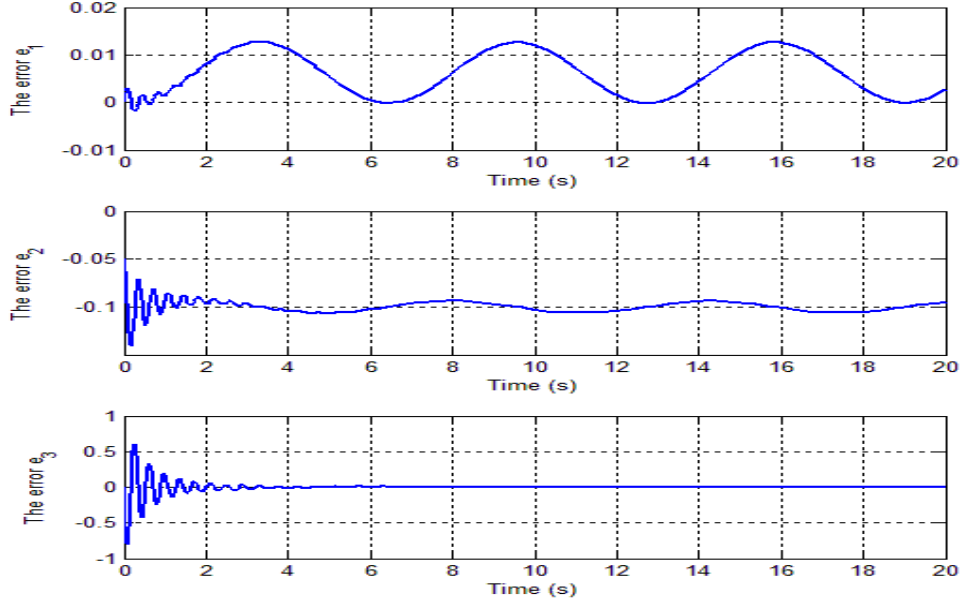


Figure 6.5: The error using Reference($r = 10\sin(t)$ cm)

$$\begin{aligned}
 \dot{\check{\xi}}_1 &= \check{\xi}_2 + d(t) + L_1\check{\xi}_1, \\
 \dot{\check{\xi}}_2 &= \frac{1}{m_t}(S\check{\xi}_3 - b\check{\xi}_2 - \theta\xi_1 - k_l\hat{\xi}_1) - L_2(\check{\xi}_1 - \xi_1), \\
 \dot{\check{\xi}}_3 &= \frac{4B}{V_t}(ku\sqrt{P_d - \text{sign}(u)\xi_3} - \frac{\alpha\xi_3}{1+\gamma|u|} - S\check{\xi}_2) \\
 &\quad - \frac{4B}{V_t}(ku\sqrt{P_d - \text{sign}(u)\hat{\xi}_3}) - L_3\check{\xi}_1.
 \end{aligned} \tag{6.30}$$

Let

$$\alpha_1 = 1 - m_t L_2, \tag{6.31}$$

$$\alpha_2 = 1 - \frac{b}{m_t}, \tag{6.32}$$

$$\alpha_3 = \frac{S}{m_t}. \tag{6.33}$$

$$\tilde{\theta} = \theta - \hat{\theta} \tag{6.34}$$

$$\mu = \sup_{t \geq 0} |d(t)|, \tag{6.35}$$

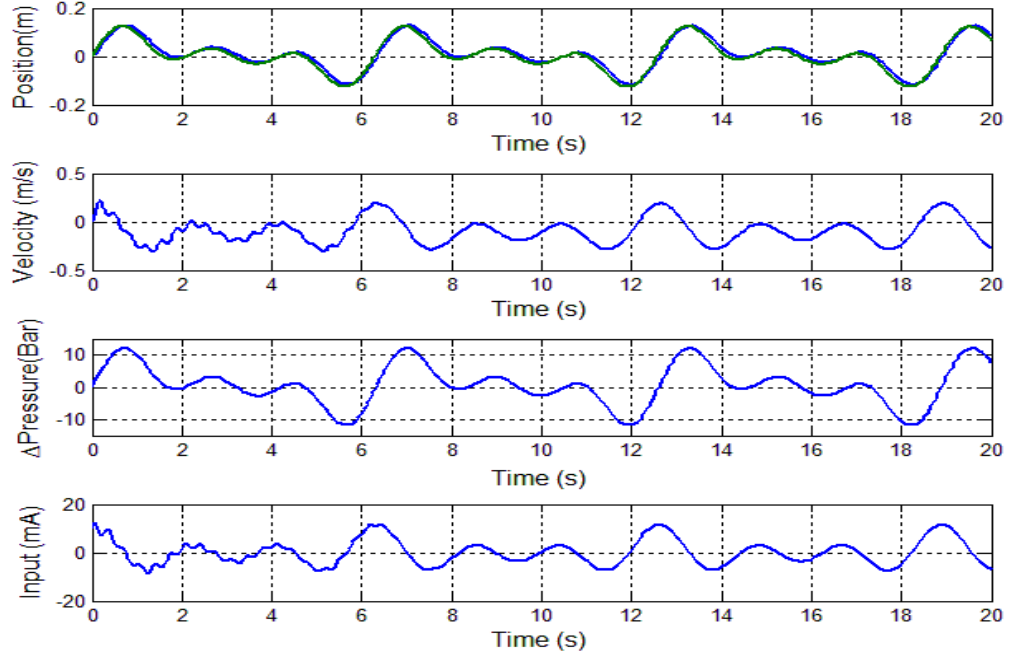


Figure 6.6: Behavior of the hydraulic servo system under a constant disturbance, Reference($r = 0.05(\sin(t) + \sin(2t) + \sin(3t))m$)

$$\begin{aligned}
P(\check{\xi}, \hat{\xi}, \xi) &= \left(\frac{k_l}{m_t}L_1 - \alpha_1 L_1\right)\check{\xi}_1 + \left(1 + \alpha_1 - \frac{\alpha_2 b}{m_t} - \alpha_2 L_2 - \frac{4\alpha_3 BS}{V_t}\right)\check{\xi}_2 \\
&+ \left(\frac{\alpha_2 S}{m_t}\right)\check{\xi}_3 - \frac{\alpha_2 k_l}{m_t}\hat{\xi}_1 + \frac{k_l}{m_t}\hat{\xi}_2 + \alpha_2 L_2 \xi_1
\end{aligned} \tag{6.36}$$

$$h(\check{\xi}, z) = \alpha_1 \check{\xi}_1 + \alpha_2 \check{\xi}_2 + \alpha_3 \check{\xi}_3 - \frac{k_l}{m_t} \hat{\xi}_1,$$

and

$$\begin{aligned}
L_3 &= \frac{1}{\alpha_3} \left(h(\check{\xi}, \hat{\xi}) + |P(\check{\xi}, \hat{\xi})| + \alpha_1 \mu + \frac{\alpha_2}{m_t} |\hat{\theta}| + \frac{4\alpha_3 \alpha B}{V_t} |\check{\xi}_3| \right. \\
&\quad \left. + \frac{4\alpha_3 Bk}{V_t} |g(u, \xi, \hat{\xi})| \sup_{t \geq 0} |u| \right)
\end{aligned} \tag{6.37}$$

Theorem 6.2 *The system with observer model Eq. (6.28) or equivalently (6.30) with parameters $L_1 \gg \frac{\lambda_0}{2}$, $L_2 = \frac{\hat{\theta}}{m_t^2}$, and let L_3 given by equation(6.37) with (6.31)-(6.36) is practically stable and the solution of the state estimation error is globally uniformly ultimately bounded.*

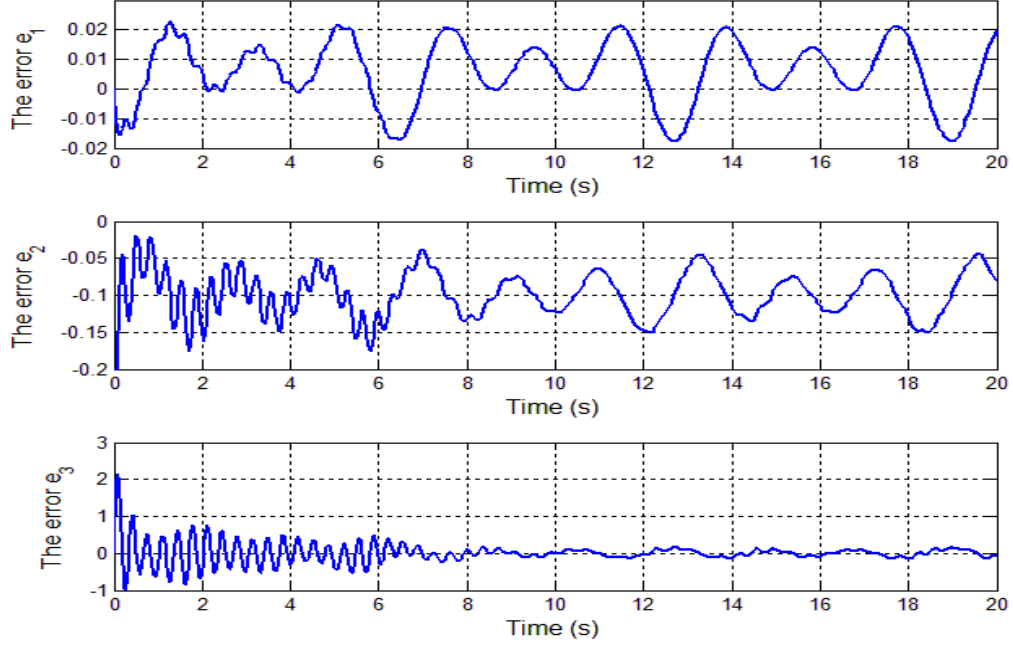


Figure 6.7: The error using Reference($r = 0.05(\sin(t) + \sin(2t) + \sin(3t))m$)

Proof. In order to prove the stability of the error dynamics, we chose the following lyapunov candidates:

$$V_1 = \frac{1}{2}\check{\xi}_1^2, \quad (6.38)$$

$$\dot{V}_1 = \check{\xi}_1\check{\xi}_2 - L_1\check{\xi}_1^2 + \check{\xi}_1d.$$

$$\dot{V}_1 \leq (-L_1 + \frac{\lambda_o}{2})\check{\xi}_1^2 + \frac{1}{2\lambda_o}d^2 + \check{\xi}_1\check{\xi}_2, \quad (6.39)$$

where $L_1 \gg \frac{\lambda_o}{2}$.

Choosing also,

$$V_2 = \frac{1}{2}\check{\xi}_2^2, \quad (6.40)$$

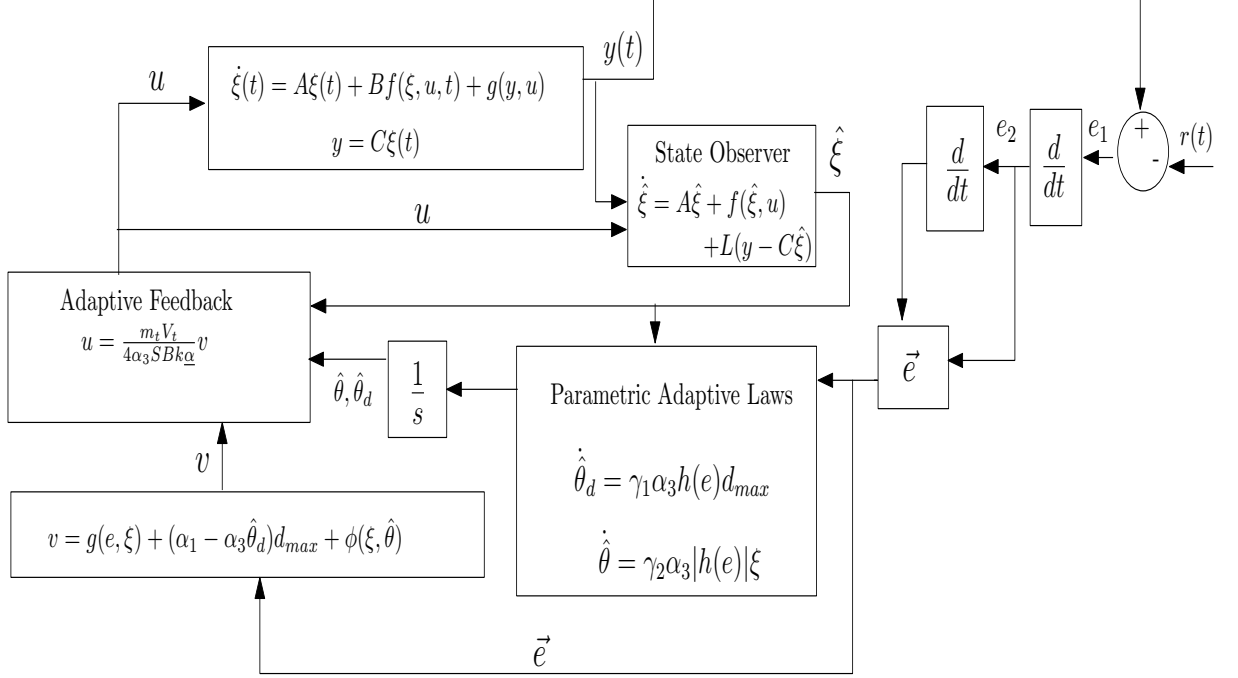


Figure 6.8: Schematic of Adaptive Output Feedback Control.

$$\dot{V}_2 = \check{\xi}_2 \left(\frac{1}{m_t} (S\check{\xi}_3 - b\check{\xi}_2 - \theta\xi_1 - k_l\hat{\xi}_1) - L_2(\check{\xi}_1 - \xi_1) \right). \quad (6.41)$$

$$\begin{aligned} \dot{V}_1 + \dot{V}_2 \leq & (-L_1 + \frac{\lambda_o}{2})\check{\xi}_1^2 + \frac{1}{2\lambda_o}d^2 + \check{\xi}_2 \left(\frac{S}{m_t}\check{\xi}_3 - \frac{b}{m_t}\check{\xi}_2 - \frac{\theta}{m_t}\xi_1 \right. \\ & \left. - \frac{k_l}{m_t}\hat{\xi}_1 - m_t L_2(\check{\xi}_1 - \xi_1) \right) \end{aligned} \quad (6.42)$$

$$\begin{aligned} \dot{V}_1 + \dot{V}_2 \leq & (-L_1 + \frac{\lambda_o}{2})\check{\xi}_1^2 + \frac{1}{2\lambda_o}d^2 + \check{\xi}_2 \left(\frac{S}{m_t}\check{\xi}_3 - \frac{b}{m_t}\check{\xi}_2 - \frac{\hat{\theta}}{m_t}\xi_1 \right. \\ & \left. - \frac{\tilde{\theta}}{m_t}\xi_1 - \frac{k_l}{m_t}\hat{\xi} - m_t L_2(\check{\xi}_1 - \xi_1) \right) \end{aligned} \quad (6.43)$$

$$\begin{aligned} \dot{V}_1 + \dot{V}_2 \leq & (-L_1 + \frac{\lambda_o}{2})\check{\xi}_1^2 + \frac{1}{2\lambda_o}d^2 - \check{\xi}_2^2 - \tilde{\theta} \left[\frac{\xi_1 \check{\xi}_2}{m_t} \right] \\ & + \check{\xi}_2 \left(\check{\xi}_1 + \left(1 - \frac{b}{m_t}\right)\check{\xi}_2 + \frac{S}{m_t}\check{\xi}_3 - \frac{\hat{\theta}}{m_t}\xi_1 \right. \\ & \left. - \frac{k_l}{m_t}\hat{\theta}_1 - m_t L_2(\check{\xi}_1 - \xi_1) \right) \end{aligned} \quad (6.44)$$

Putting Eq. (6.44) in a compact form and choosing $L_2 = \frac{\hat{\theta}}{m_t}$, we have:

$$\begin{aligned} \dot{V}_1 + \dot{V}_2 \leq & (-L_1 + \frac{\lambda_o}{2})\check{\xi}_1^2 + \frac{1}{2\lambda_o}d^2 - \check{\xi}_2^2 \\ & + \check{\xi}_2(\alpha_1\check{\xi}_1 + \alpha_2\check{\xi}_2 + \alpha_3\check{\xi}_3 - \frac{k_l}{m_t}\hat{\xi}_1). \end{aligned} \quad (6.45)$$

Choosing $V_3 = \frac{1}{2}(\alpha_1\check{\xi}_1 + \alpha_2\check{\xi}_2 + \alpha_3\check{\xi}_3 - \frac{k_l}{m_t}\hat{\xi}_1)^2 + \frac{1}{2\gamma_1}\tilde{\theta}^2$, then,

$$\dot{V} = \dot{V}_1 + \dot{V}_2 + \dot{V}_3 \quad (6.46)$$

$$\begin{aligned} \dot{V} \leq & (-L_1 + \frac{\lambda_o}{2})\check{\xi}_1^2 + \frac{1}{2\lambda_o}d^2 - \check{\xi}_2^2 + \tilde{\theta}[-\frac{1}{\gamma_1}\dot{\tilde{\theta}} - \frac{\xi_1}{m_t}\check{\xi}_2] \\ & + \check{\xi}_2[\alpha_1\check{\xi}_1 + \alpha_2\check{\xi}_2 + \alpha_3\check{\xi}_3] \\ & + (\alpha_1\check{\xi}_1 + \alpha_2\check{\xi}_2 + \alpha_3\check{\xi}_3 - \frac{k_l}{m_t}\hat{\xi}_1)[\alpha_1\dot{\check{\xi}}_1 + \alpha_2\dot{\check{\xi}}_2 + \alpha_3\dot{\check{\xi}}_3 - \frac{k_l}{m_t}\dot{\hat{\xi}}_1] \end{aligned} \quad (6.47)$$

$$\begin{aligned} \dot{V} \leq & (-L_1 + \frac{\lambda_o}{2})\check{\xi}_1^2 + \frac{1}{2\lambda_o}d^2 - \check{\xi}_2^2 + \tilde{\theta}[-\frac{1}{\gamma_1}\dot{\tilde{\theta}} - \frac{\xi_1}{m_t}\check{\xi}_2] \\ & + (\alpha_1\check{\xi}_1 + \alpha_2\check{\xi}_2 + \alpha_3\check{\xi}_3 - \frac{k_l}{m_t}z_1)[\check{\xi}_2 + \alpha_1\dot{\check{\xi}}_1 + \alpha_2\dot{\check{\xi}}_2 + \alpha_3\dot{\check{\xi}}_3 - \frac{k_l}{m_t}\dot{\hat{\xi}}_1] \end{aligned} \quad (6.48)$$

$$\begin{aligned} \dot{V} \leq & (-L_1 + \frac{\lambda_o}{2})\check{\xi}_1^2 + \frac{1}{2\lambda_o}d^2 - \check{\xi}_2^2 + \tilde{\theta}[-\frac{1}{\gamma_1}\dot{\tilde{\theta}} - \frac{\xi_1}{m_t}\check{\xi}_2 - \frac{\alpha_2}{m_t}\xi_1 h(\check{\xi}, \hat{\xi})] \\ & + h(\check{\xi}, \hat{\xi})(P(\check{\xi}, \hat{\xi}) + \alpha_1 d - \frac{\alpha_2}{m_t}\hat{\theta}\xi_1 - \frac{4\alpha_3\alpha_B}{V_t(1+\gamma|u|)}\check{\xi}_3) \\ & + \frac{4\alpha_3 Bk}{V_t}g(u, \xi, \hat{\xi}) \cdot u - \frac{S}{m_t}L_3\check{\xi}_1 h(\check{\xi}, \hat{\xi}) \end{aligned} \quad (6.49)$$

Considering that:

$$\frac{1}{1+\gamma|u|} \leq 1; \quad (6.50)$$

$$\alpha_1 h(\check{\xi}, \hat{\xi})d(t) \leq \alpha_1 |h(\check{\xi}, \hat{\xi})|\mu \quad (6.51)$$

$$P(\check{\xi}, \hat{\xi})h(\check{\xi}, \hat{\xi}) \leq |P(\check{\xi}, \hat{\xi})| |h(\check{\xi}, \hat{\xi})| \quad (6.52)$$

$$\frac{\alpha_2}{m_t} \hat{\theta} \xi_1 h(\check{\xi}, \hat{\xi}) \leq \frac{\alpha_2}{m_t} |h(\check{\xi}, \hat{\xi})| |\hat{\theta}| |\xi_1| \quad (6.53)$$

$$\frac{4\alpha_3 Bk}{V_t(1+\gamma|u|)} \check{\xi}_3 \leq \frac{4\alpha_3 Bk}{V_t} |\check{\xi}_3| \quad (6.54)$$

$$\frac{4\alpha_3 Bk}{V_t} h(\check{\xi}, \hat{\xi}) g(u, \xi, \hat{\xi}) u(t) \leq \frac{4\alpha_3 Bk}{V_t} |g(u, \xi, \hat{\xi})| |h(\check{\xi}, \hat{\xi})| \sup_{t \geq 0} |u| \quad (6.55)$$

then, To ensure $\dot{V} \leq 0$, L_3 is selected as given in (6.37) and also using equations (6.21 - 6.50),

$$\begin{aligned} \dot{V} \leq & (-L_1 + \frac{\lambda_o}{2}) \check{\xi}_1^2 + \frac{1}{2\lambda_o} d^2 - \check{\xi}_2^2 \\ & - (\alpha_1 \check{\xi}_1 + \alpha_2 \check{\xi}_2 + \alpha_3 \check{\xi}_3 - \frac{k_t}{m_t} \hat{\xi}_1)^2 \end{aligned} \quad (6.56)$$

Remark 6.1 *This is similar to the remark in Chapter 5. The parameter λ_o is a design parameter introduced in Young's inequality during the proof of stability of the state-observer. Such parameter should be selected as big as possible to make decrease the ultimate bound in the tracking error dynamic. The larger is λ_o the more oscillatory is the transient and higher in the control input.*

6.3 Simulation Results for the High-Gain Adaptive Observer Design

The parameters in Table 6.2 are used for simulating the results of Figures (6.9-6.16).

Design parameter	Value
Design parameter ϵ	0.0001
Adaptation Gain γ_1	8

Table 6.1: Numerical value for simulating the high gain adaptive observer

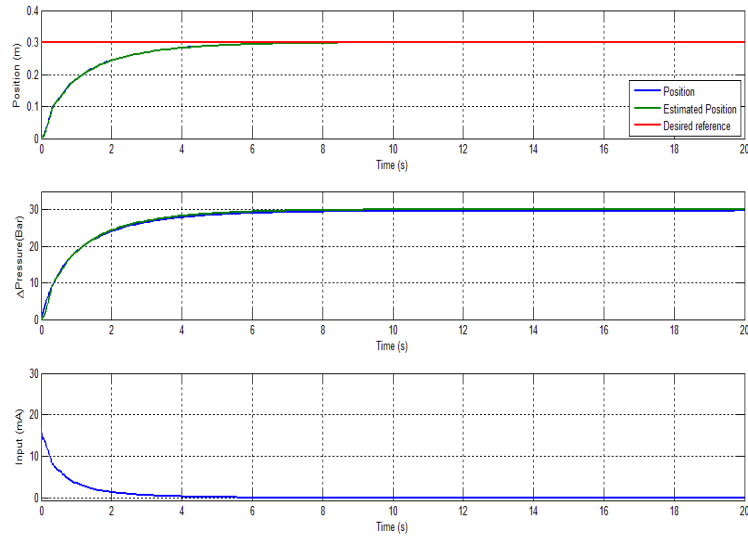


Figure 6.9: Behavior of the observer and hydraulic servo system under a constant disturbance using a constant feedback gain (λ). Reference($r = 0.3m$)

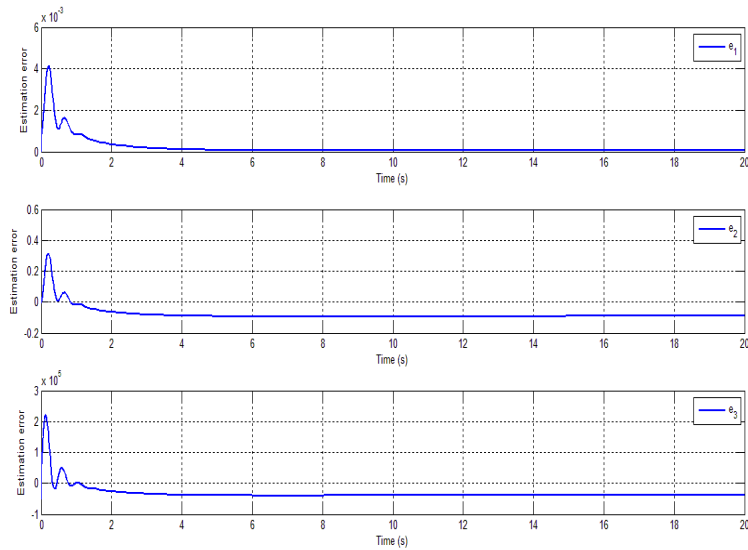


Figure 6.10: Estimation error when $r = 0.3m$

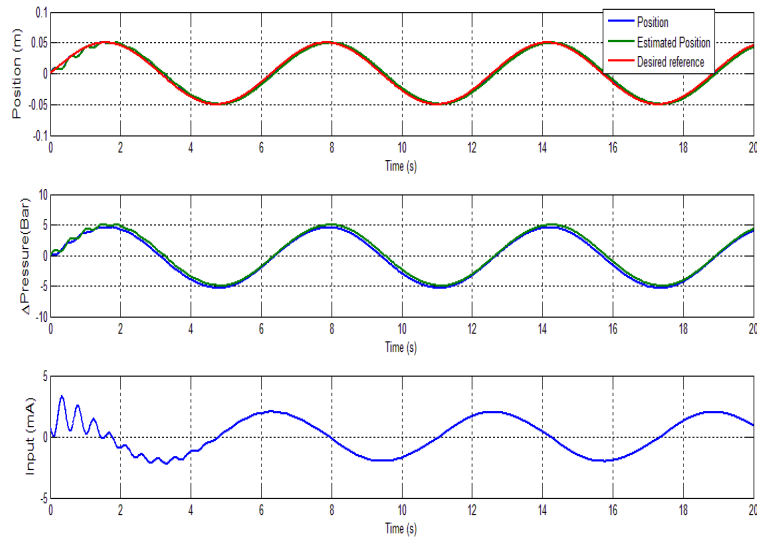


Figure 6.11: Behavior of the observer and hydraulic servo system under a constant disturbance using a constant feedback gain (λ). Reference($r = 10\sin(t)cm$)

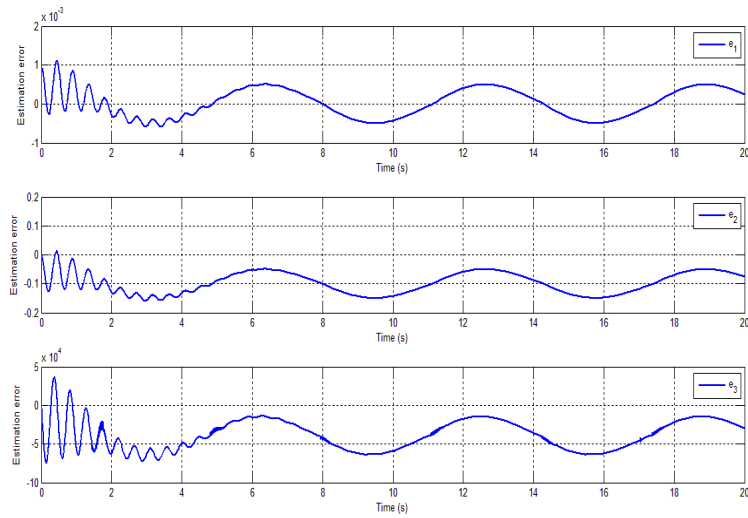


Figure 6.12: Estimation error when $r = 10\sin(t)cm$

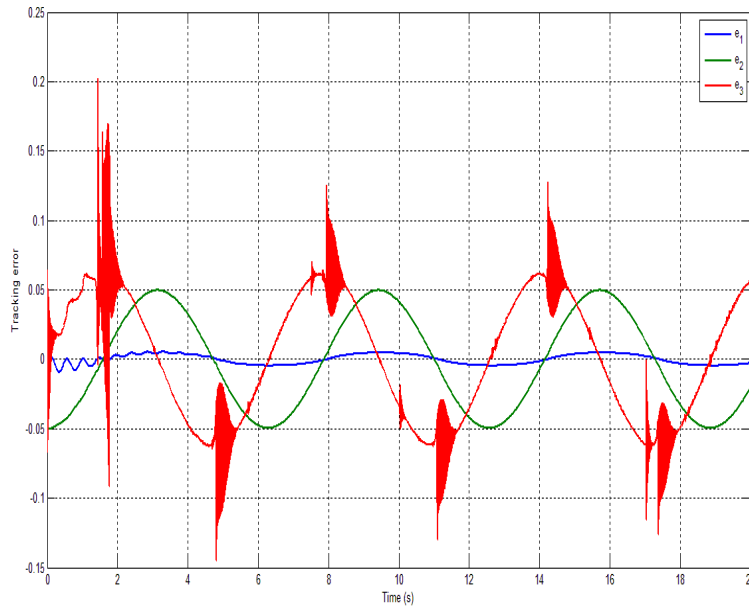


Figure 6.13: Tracking error when $r = 10\sin(t)\text{cm}$

6.3.1 Results Discussion

Figures (6.9) and (6.10) show the performance of the observer and the estimation error respectively. It can be seen that the control easily achieves the desired reference and the observer estimates the states of the system under constant external disturbance with a steady state error converging to a small neighborhood of the origin. When the reference was changed to sinusoidal trajectories as shown in Figure (6.14) respectively, the output of the closed loop system still tracks the reference with small steady state bias due to the large amplitude external disturbance as shown in (6.16). Also, it was observed that the estimated parameters were fairly accurate despite the parametric uncertainties and external disturbance.

Case 2 *We also considered a scenario whereby a more complicated vibrator-ground model can result due to the non-ideal contact stiffness that exists at the*

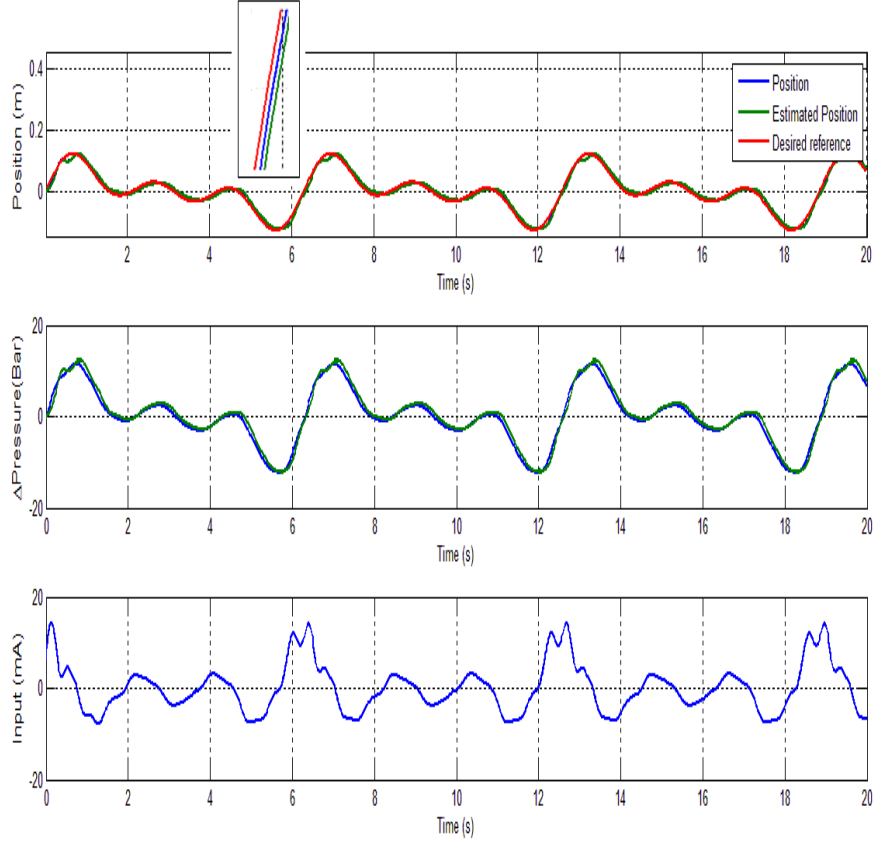


Figure 6.14: Behavior of the observer and hydraulic servo system under a constant disturbance using a constant feedback gain (λ). Reference($r = 0.05(\sin(t) + \sin(2t) + \sin(3t))\text{m}$)

boundary interaction between the vibrator's baseplate and ground as depicted in

Fig. 6.17. In order to achieve this, we replaced β and b as given in Eq. (6.57)

$$\beta = \gamma_1 \xi_1^2 + \gamma_2 \xi_2^2 + \gamma_3 \xi_3^2 = \theta^T \phi(\xi) \quad (6.57)$$

$$b = b_0 + \Delta f(\xi, b_0)$$

where $\Delta f(\xi, b_0)$ is unknown but bounded nonlinear function that satisfies

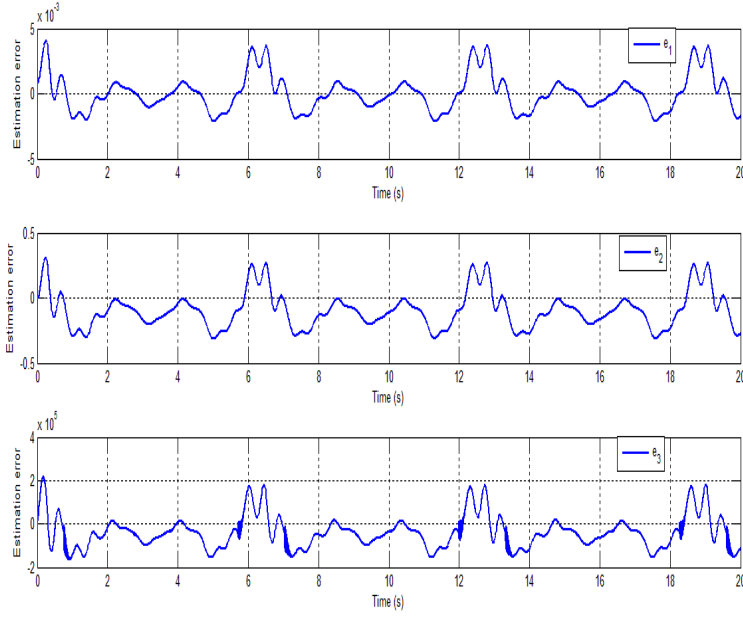


Figure 6.15: Estimation error when $(r = 0.05(\sin(t) + \sin(2t) + \sin(3t))\text{m})$

Eq. (6.58)

$$\sup_{t \geq 0} |\Delta f(\xi, b_0)| \leq F_{max} \quad (6.58)$$

$$\dot{e}_1 = e_2 + d,$$

$$\dot{e}_2 = e_3,$$

$$\begin{aligned} \dot{e}_3 = & \frac{b_0}{m_t^2} \theta^T \phi(\xi) \xi_1 + \left(-\frac{1}{m_t} \theta^T \phi(\xi) + \frac{b_0^2}{m_t^2} - \frac{4BS^2}{m_t V_t} \right) \xi_2 + \left(-\frac{b_0 S}{m_t^2} - \frac{4BS\alpha}{m_t V_t (1+\gamma|u|)} \right) \xi_3 \\ & + \frac{\Delta f(\xi, b_0)}{m_t^2} \theta^T \phi(\xi) \xi_1 + \left(\frac{1}{m_t} (2b_0 \Delta f(\xi, b_0) + \Delta f^2(\xi, b_0)) \right) \xi_2 - \left(\frac{S}{m_t} \Delta f(\xi, b_0) \right) \xi_3 \\ & - \theta_d^T \phi(\xi) d(t) - \ddot{r} + Am(t)u. \end{aligned} \quad (6.59)$$

where, $\theta_d^T \phi(\xi) = \frac{\beta}{m_t}$

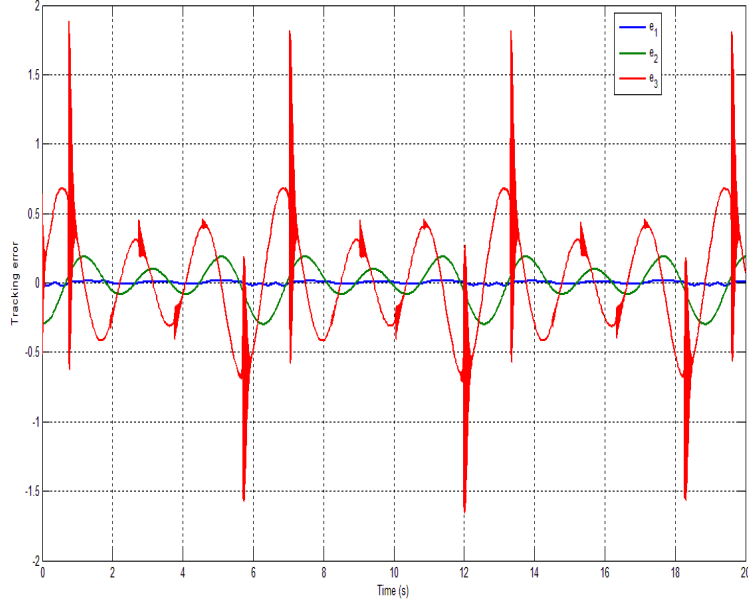


Figure 6.16: Tracking error when $(r = 0.05(\sin(t) + \sin(2t) + \sin(3t)))m$

Let,

$$\begin{aligned}\Delta F_1 &= \frac{\Delta f(\xi, b_0)}{m_t^2} \leq F_{max} \\ \Delta F_2 &= \frac{1}{m_t^2}(2b_0\Delta f(\xi, b_0) + \Delta f^2(\xi, b_0)) \leq F_{max}^3 \\ \Delta F_3 &= \frac{S}{m_t} \Delta f(\xi, b_0) \leq F_{max}\end{aligned}\tag{6.60}$$

Now, the error dynamics are given as:

$$\begin{aligned}\dot{e}_1 &= e_2 + d, \\ \dot{e}_2 &= e_3, \\ \dot{e}_3 &= \frac{b_0}{m_t^2} \theta^T \phi(\xi) \xi_1 + \left(-\frac{1}{m_t} \theta^T \phi(\xi) + \frac{b_0^2}{m_t^2} - \frac{4BS^2}{m_t V_t}\right) \xi_2 + \left(-\frac{b_0 S}{m_t^2} - \frac{4BS\alpha}{m_t V_t(1+\gamma|u|)}\right) \xi_3 \\ &\quad + \Delta F_1 \theta^T \phi(\xi) \xi_1 + \Delta F_2 \xi_2 - \Delta F_3 \xi_3 - \theta_d^T \phi(\xi) d(t) - \ddot{r} + Am(t)u.\end{aligned}\tag{6.61}$$

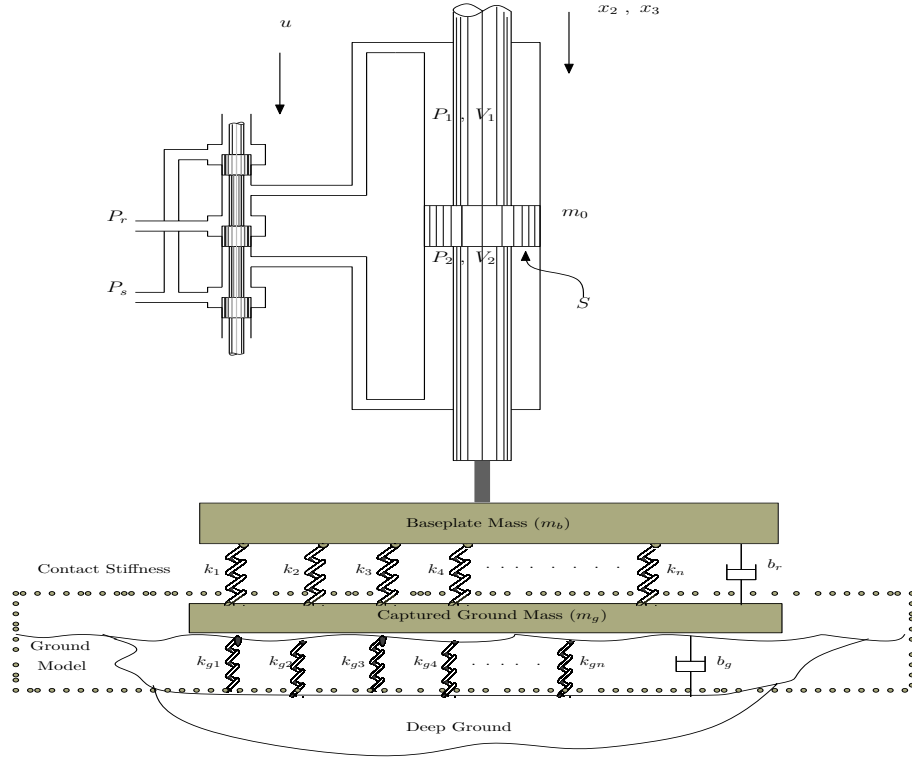


Figure 6.17: A more detailed vibrator-ground model prototype [1].

Now, to prove the boundedness of the error dynamics, we again choose the Lyapunov functions as follows:

$$V_1 = \frac{1}{2}e_1^2, \quad (6.62)$$

Calculating the derivative of $V(x)$ along the trajectories of the perturbed system, we obtain

$$\dot{V}_1 = -\lambda e_1^2 + e_1(e_2 + \lambda e_1) + e_1 d. \quad (6.63)$$

$$\dot{V}_1 \leq -\lambda e_1^2 + e_1(e_2 + \lambda e_1) + \frac{1}{2\lambda}d^2 + \frac{\lambda}{2}e_1^2 \leq -\frac{\lambda}{2}e_1^2 + \frac{1}{2\lambda}d^2 + e_1(e_2 + \lambda e_1).$$

again using the Young's inequality with $\lambda > 0$;

$$e_1 d \leq |e_1| |d| \leq \frac{1}{2\lambda} d^2 + \frac{\lambda}{2} e_1^2 \quad (6.64)$$

Let $V_2 = \frac{1}{2\lambda^4} (e_2 + \lambda e_1)^2$, then

$$\dot{V}_2 = \frac{1}{\lambda^4} (e_2 + \lambda e_1) (e_3 + \lambda (e_2 + d)) \quad (6.65)$$

Therefore,

$$\dot{V}_1 + \dot{V}_2 \leq -\frac{\lambda}{2} e_1^2 + \frac{1}{2\lambda} d^2 + \frac{1}{\lambda^4} (e_2 + \lambda e_1) [e_3 + \lambda e_2 + \lambda^4 e_1 + \lambda d] \quad (6.66)$$

But,

$$\frac{1}{\lambda^3} (e_2 + \lambda e_1) d \leq \frac{1}{\lambda^3} |d| |e_2 + \lambda e_1| \leq \frac{1}{\lambda^3} [\frac{1}{2\lambda^2} d^2 + \frac{\lambda^2}{2} (e_2 + \lambda e_1)^2] \quad (6.67)$$

Inserting Eq. (6.67) into Eq. (6.66), we have

$$\dot{V}_1 + \dot{V}_2 \leq -\frac{\lambda}{2} e_1^2 + (\frac{1}{2\lambda} + \frac{1}{2\lambda^5}) d^2 + (e_2 + \lambda e_1) [\frac{1}{\lambda^4} (e_3 + \lambda e_2 + \lambda^4 e_1) + \frac{\lambda^2}{2} (e_2 + \lambda e_1)]. \quad (6.68)$$

$$\dot{V}_1 + \dot{V}_2 \leq -\frac{\lambda}{2} e_1^2 + (\frac{1}{2\lambda} + \frac{1}{2\lambda^5}) d^2 - (e_2 + \lambda e_1)^2 + (e_2 + \lambda e_1) [\alpha_1 e_1 + \alpha_2 e_2 + \alpha_3 e_3] \quad (6.69)$$

Choosing $V_3 = \frac{1}{2}(\alpha_1 e_1 + \alpha_2 e_2 + \alpha_3 e_3)^2$, then,

$$\begin{aligned} \dot{V}_1 + \dot{V}_2 + \dot{V}_3 \leq & -\frac{\lambda}{2}e_1^2 + \left(\frac{1}{2\lambda} + \frac{1}{2\lambda^5}\right)d^2 - (e_2 + \lambda e_1)^2 + (e_2 + \lambda e_1)[\alpha_1 e_1 + \alpha_2 e_2 + \alpha_3 e_3] \\ & + (\alpha_1 e_1 + \alpha_2 e_2 + \alpha_3 e_3)[\alpha_1 \dot{e}_1 + \alpha_2 \dot{e}_2 + \alpha_3 \dot{e}_3] \end{aligned} \quad (6.70)$$

where,

$$\begin{aligned} \alpha_1 &= \frac{3}{2} + \lambda, \\ \alpha_2 &= 1 + \frac{1}{\lambda^3} + \frac{1}{2\lambda}, \\ \alpha_3 &= \frac{1}{\lambda^4}. \end{aligned} \quad (6.71)$$

$$\begin{aligned} \dot{V}_1 + \dot{V}_2 + \dot{V}_3 \leq & -\frac{\lambda}{2}e_1^2 + \left(\frac{1}{2\lambda} + \frac{1}{2\lambda^5}\right)d^2 - (e_2 + \lambda e_1)^2 \\ & + (\alpha_1 e_1 + \alpha_2 e_2 + \alpha_3 e_3)[e_2 + \lambda e_1 + \alpha_1(e_2 + d) + \alpha_2 e_3 + \alpha_3 \left(\frac{b_0}{m_t^2} \theta^T \phi(\xi)\xi_1\right. \\ & + \left(-\frac{1}{m_t} \theta^T \phi(\xi) + \frac{b_0^2}{m_t^2} - \frac{4BS^2}{m_t V_t}\right)\xi_2 + \left(-\frac{b_0 S}{m_t^2} - \frac{4BS\alpha}{m_t V_t(1+\gamma|u|)}\right)\xi_3 + \Delta F_1 \theta^T \phi(\xi)\xi_1 \\ & \left. + \Delta F_2 \xi_2 - \Delta F_3 \xi_3 - \theta_d^T \phi(\xi)d(t) - \ddot{r} + Am(t)u] \end{aligned} \quad (6.72)$$

Setting,

$$\begin{aligned} h(e) &= \alpha_1 e_1 + \alpha_2 e_2 + \alpha_3 e_3 \\ g(e, \xi) &= e_2 + \lambda e_1 + \alpha_1 e_2 + \alpha_2 e_3 + \alpha_3 \left(\frac{b_0^2}{m_t^2} - \frac{4BS^2}{m_t V_t}\right)\xi_2 + \frac{b_0 S}{m_t} \xi_3 \end{aligned} \quad (6.73)$$

Now,

$$\begin{aligned}
\dot{V}_1 + \dot{V}_2 + \dot{V}_3 &\leq -\frac{\lambda}{2}e_1^2 + \left(\frac{1}{2\lambda} + \frac{1}{2\lambda^5}\right)d^2 - (e_2 + \lambda e_1)^2 + (\alpha_1 e_1 + \alpha_2 e_2 + \alpha_3 e_3)[g(e, \xi)] \\
&\quad + \alpha_3 \frac{\alpha_3 b_0}{m_t^2} \theta^T \phi(\xi) \xi_1 + \left(-\frac{\alpha_3}{m_t} \theta^T \phi(\xi) \xi_2 - \frac{4BS\alpha\alpha_3}{m_t V_t(1+\gamma|u|)}\right) \xi_3 + \alpha_1 d + \alpha_3 \Delta F_1 \theta^T \phi(\xi) \xi_1 \\
&\quad + \alpha_3 \Delta F_2 \xi_2 - \alpha_3 \Delta F_3 \xi_3 - \alpha_3 \theta_d^T \phi(\xi) d(t) - \alpha_3 \ddot{r} + \alpha_3 Am(t)u]
\end{aligned} \tag{6.74}$$

Let $A_1 = \frac{\alpha_3 b_0}{m_t^2}$, $A_2 = \frac{\alpha_3}{m_t}$ and $A_3 = \frac{4BS\alpha\alpha_3}{m_t V_t}$

$$\begin{aligned}
\dot{V}_1 + \dot{V}_2 + \dot{V}_3 &\leq -\frac{\lambda}{2}e_1^2 + \left(\frac{1}{2\lambda} + \frac{1}{2\lambda^5}\right)d^2 - (e_2 + \lambda e_1)^2 + (\alpha_1 e_1 + \alpha_2 e_2 + \alpha_3 e_3)[g(e, \xi)] \\
&\quad + A_1 \theta^T \phi(\xi) \xi_1 - A_2 \theta^T \phi(\xi) \xi_2 - \frac{A_3}{1+\gamma|u|} \xi_3 + \alpha_1 d + \alpha_3 \Delta F_1 \theta^T \phi(\xi) \xi_1 \\
&\quad + \alpha_3 \Delta F_2 \xi_2 - \alpha_3 \Delta F_3 \xi_3 - \alpha_3 \theta_d^T \phi(\xi) d(t) - \alpha_3 \ddot{r} + \alpha_3 Am(t)u]
\end{aligned} \tag{6.75}$$

Since, $\tilde{\theta} = \theta - \hat{\theta}$

$$\begin{aligned}
\dot{V}_1 + \dot{V}_2 + \dot{V}_3 &\leq -\frac{\lambda}{2}e_1^2 + \left(\frac{1}{2\lambda} + \frac{1}{2\lambda^5}\right)d^2 - (e_2 + \lambda e_1)^2 + (\alpha_1 e_1 + \alpha_2 e_2 + \alpha_3 e_3)[g(e, \xi)] \\
&\quad + A_1 \tilde{\theta}^T \phi(\xi) \xi_1 + A_1 \hat{\theta}^T \phi(\xi) \xi_1 - A_2 \tilde{\theta}^T \phi(\xi) \xi_2 - A_2 \hat{\theta}^T \phi(\xi) \xi_2 - \frac{A_3}{1+\gamma|u|} \xi_3 + \alpha_1 d \\
&\quad + \alpha_3 \Delta F_1 \tilde{\theta}^T \phi(\xi) \xi_1 + \alpha_3 \Delta F_1 \hat{\theta}^T \phi(\xi) \xi_1 + \alpha_3 \Delta F_2 \xi_2 - \alpha_3 \Delta F_3 \xi_3 - \alpha_3 \tilde{\theta}_d^T \phi(\xi) d(t) \\
&\quad - \alpha_3 \hat{\theta}_d^T \phi(\xi) d(t) - \alpha_3 \ddot{r} + \alpha_3 Am(t)u]
\end{aligned} \tag{6.76}$$

$$\text{Let } V_4 = \frac{1}{2\gamma_1} \tilde{\theta}^T \tilde{\theta} + \frac{1}{2\gamma_2} \tilde{\theta}_d^2$$

$$\dot{V} = \dot{V}_1 + \dot{V}_2 + \dot{V}_3 + \dot{V}_4 \quad (6.77)$$

Therefore, the derivative of the lyapunov function is thus given:

$$\begin{aligned} \dot{V} \leq & -\frac{\lambda}{2} e_1^2 + \left(\frac{1}{2\lambda} + \frac{1}{2\lambda^5}\right) d^2 - (e_2 + \lambda e_1)^2 + (\alpha_1 e_1 + \alpha_2 e_2 + \alpha_3 e_3) [g(e, \xi) \\ & + A_1 \tilde{\theta}^T \phi(\xi) \xi_1 + A_1 \hat{\theta}^T \phi(\xi) \xi_1 - A_2 \tilde{\theta}^T \phi(\xi) \xi_2 - A_2 \hat{\theta}^T \phi(\xi) \xi_2 - \frac{A_3}{1+\gamma|u|} \xi_3 + \alpha_1 d + \alpha_3 \Delta F_1 \tilde{\theta}^T \phi(\xi) \xi_1 \\ & + \alpha_3 \Delta F_1 \hat{\theta}^T \phi(\xi) \xi_1 + \alpha_3 \Delta F_2 \xi_2 - \alpha_3 \Delta F_3 \xi_3 - \alpha_3 \tilde{\theta}_d^T \phi(\xi) d(t) - \alpha_3 \hat{\theta}_d^T \phi(\xi) d(t) - \alpha_3 \ddot{r} + \alpha_3 A m(t) u] \\ & - \frac{1}{\gamma_1} \tilde{\theta}^T \dot{\hat{\theta}} - \frac{1}{\gamma_2} \tilde{\theta}_d \dot{\hat{\theta}}_d \end{aligned} \quad (6.78)$$

In order to annihilate the parametric error, the update laws are chosen as given in Eq. (6.79)

$$\begin{aligned} \dot{\hat{\theta}} &= \gamma_1 (A_1 h(e) \phi(\xi) \xi_1 - A_2 h(e) \phi(\xi) \xi_2 + \alpha_3 F_{max} |\xi_1| \phi(\xi)) \\ \dot{\hat{\theta}}_d &= -\gamma_2 \alpha_3 \phi(\xi) d_{max} \end{aligned} \quad (6.79)$$

The following bounds hold given that $F_{max} = \sup_{t \geq 0} |\Delta F_1|$ and $d_{max} = \sup_{t \geq 0} |d(t)|$,

$$\begin{aligned} \Phi(\xi, \hat{\theta}) &= A_1 |\hat{\theta}^T \phi(\xi)| |\xi_1| + A_2 |\hat{\theta}^T \phi(\xi)| |\xi_2| + \alpha_3 F_{max} |\hat{\theta}^T \phi(\xi)| |\xi_1| + \alpha_3 \sup_{t \geq 0} |\ddot{r}| \\ &\geq A_1 \hat{\theta}^T \phi(\xi) \xi_1 - A_2 \hat{\theta}^T \phi(\xi) \xi_2 + \alpha_3 \Delta F_1 \hat{\theta}^T \phi(\xi) \xi_1 + \alpha_3 \ddot{r} \end{aligned} \quad (6.80)$$

$$\alpha_3 h(e) \Delta F_2 \xi_2 \leq \alpha_3 |h(e)| \sup_{t \geq 0} |\Delta F_2| |\xi_2| \leq \alpha_3 |h(e)| |\xi_2| F_{max}^3 \quad (6.81)$$

$$\alpha_3 h(e) \Delta F_3 \xi_3 \leq \alpha_3 |h(e)| \sup_{t \geq 0} |\Delta F_3| |\xi_3| \leq \alpha_3 |h(e)| |\xi_3| F_{max} \quad (6.82)$$

$$\frac{A_3 h(e)}{1 + \gamma |u|} \xi_3 \leq A_3 |h(e)| |\xi_3|$$

To ensure a uniformly ultimately bounded tracking error, we choose "u" as:

$$u = \left(\frac{m_t V_t}{4 \alpha_3 S B k \min(\sqrt{P_d - \xi_3}, \sqrt{P_d + \xi_3})} \right) v \quad (6.83)$$

where,

$$v = |g(e, \xi)| + |\alpha_1 + \alpha_3 \hat{\theta}_d^T \phi(\xi)| d_{max} + \Phi(\xi, \hat{\theta}) + \alpha_3 |\xi_3| F_{max} + \alpha_3 |\xi_2| F_{max}^3 - k_o h(e) \quad (6.84)$$

Ultimately,

$$\dot{V} \leq -\frac{\lambda}{2} e_1^2 + \left(\frac{1}{2\lambda} + \frac{1}{2\lambda^5} \right) d^2 - (e_2 + \lambda e_1)^2 - (\alpha_1 e_1 + \alpha_2 e_2 + \alpha_3 e_3)^2 \quad (6.85)$$

6.4 Results and Discussion

The numerical values for the parameters used in the simulation are given in Table 6.2. It must be noted that the proposed adaptive design does not involve the differentiation of $m(t)$ which, is an indication that the scheme can handle the effects of various types of slowly time-varying $m(t)$ and $d(t)$. The problem we solved is a robust adaptive control issue. Using a constant trajectory as seen in Fig-

Parameters	Value	Units	Parameters	Value	Units
B	2.2×10^9	Pa	P_r	1×10^5	Pa
V_t	1×10^{-3}	m^3	S	1.5×10^{-3}	m^2
γ	8571	s^{-1}	b	590	kg/s
Δk_l	2500	N/m	k_l	12500	N/m
P_s	300×10^5	Pa	m_t	70	kg
k	$5.12 \times 10^{-9} m^3 s^{-1} A^{-1} Pa^{1/2}$		α	$4.1816 \times 10^{-12} m^3 s^{-1} Pa^{-1}$	

Table 6.2: Numerical values for simulations

ure (6.18), the adaptive control given in Eq. (6.7) accomplishes a bounded error tracking even in the presence of input nonlinearity, parameter uncertainties and unknown but bounded disturbance. The tracking error depicted in Figure (6.18 b) is reasonably small and can further be reduced by the choice of λ and ϵ . It must be noted that λ is a design parameter and can be used to reduce the bound of the external disturbance. However, ϵ has to be chosen sufficiently small and its choice is neither dependent on system's parameters nor the bound of the disturbance. Also from Figure (6.18), it can easily be observed that there is a keen compromise between the smoothness of the adaptive control law and the tracking error, which constitutes the main trait of most adaptive strategy. In a nutshell, the proposed solution is robust against parameter uncertainties and disturbance if the ultimate bound satisfies the condition $(\alpha_1 e_1 + \alpha_2 e_2 + \alpha_3 e_3) \leq \sqrt{(\frac{1}{2\lambda_c} + \frac{1}{2\lambda_c^5})} d_{max}$. Figure (6.19) demonstrate the excellent tracking for a sinusoidal reference input whereas, Figure (6.20) depict excellent tracking accuracy when the reference is changed to sum of sinusoids. Figure (6.21) presents the case when non-ideal contact stiffness exists at the boundary interaction between the vibrator's baseplate

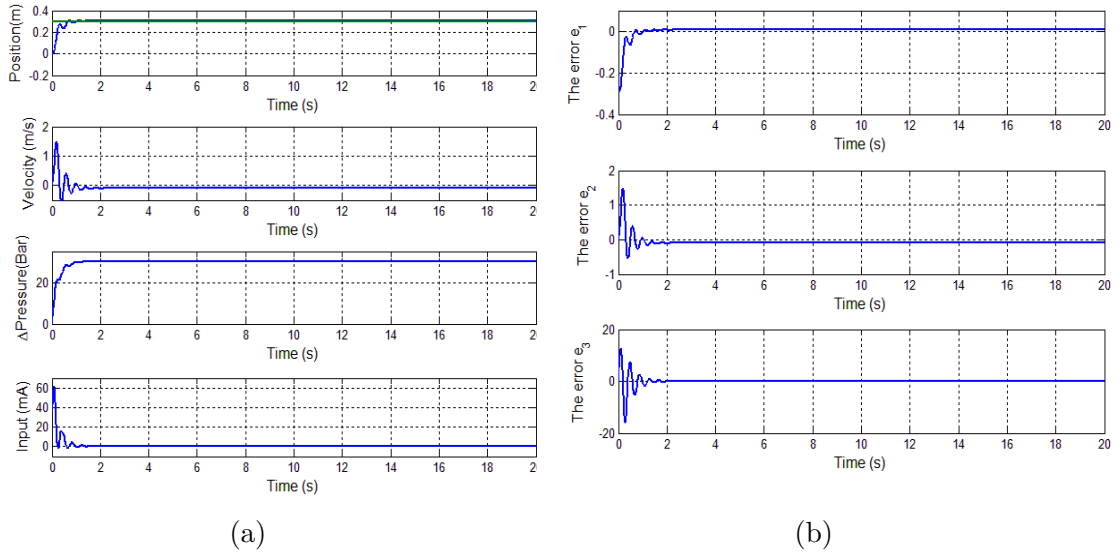


Figure 6.18: Behavior of the hydraulic servo system with $r = 30cm$

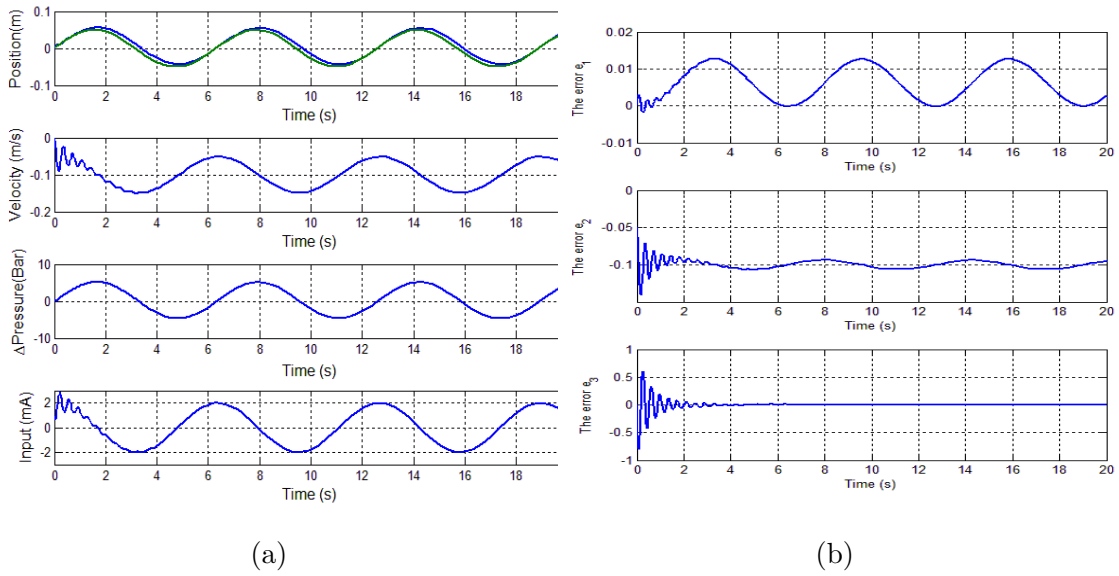


Figure 6.19: Behavior of the hydraulic servo system with $r = 10\sin(t)cm$

and ground and β is replaced by a nonlinear function of the states to better make the vibrator-ground model more complicated. Even though there is a big tracking error in the transient, the error converges to the neighborhood of the origin at the steady states. This phenomenon depicts how robust the adaptive controller is.

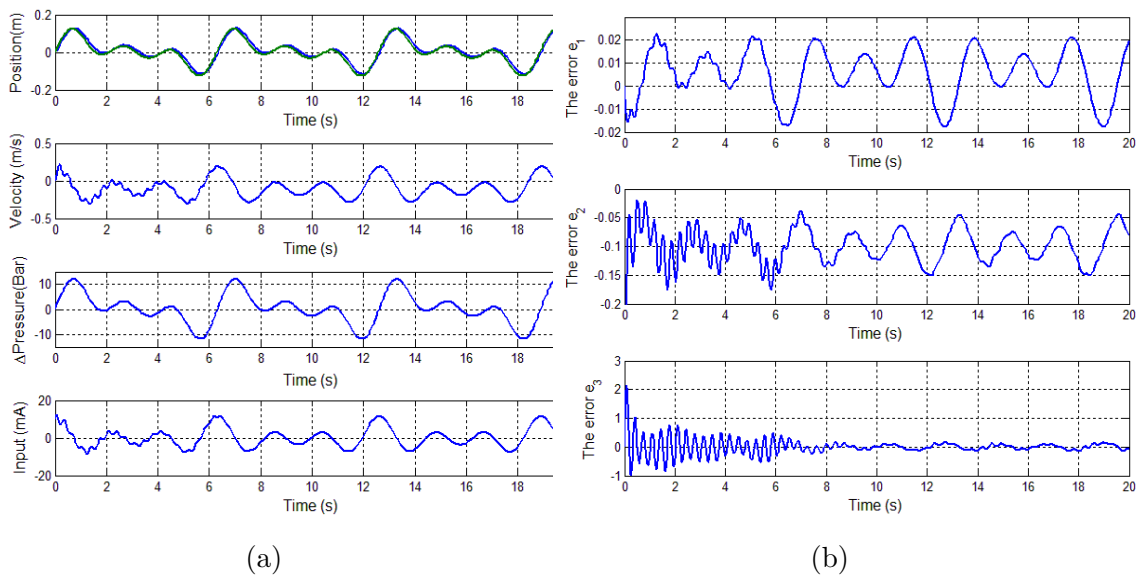
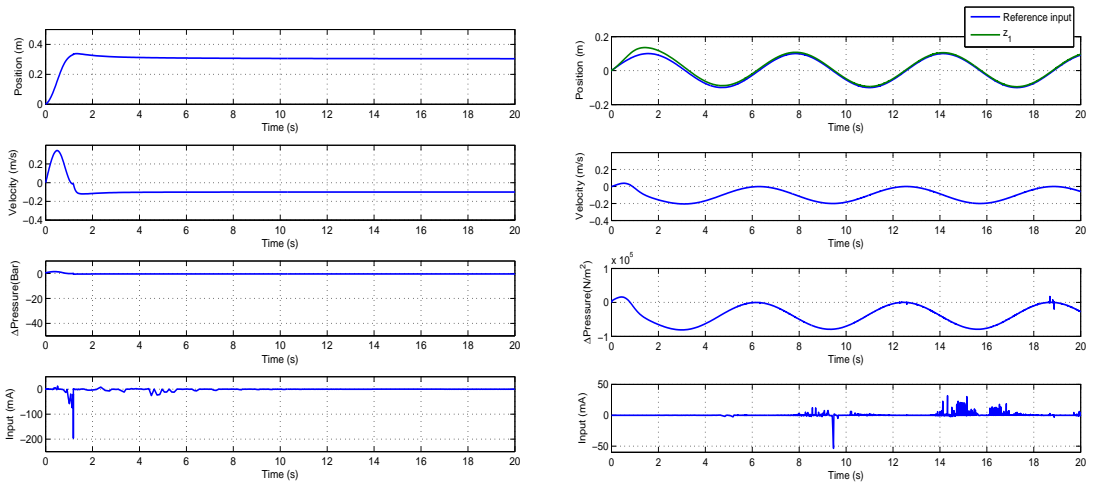
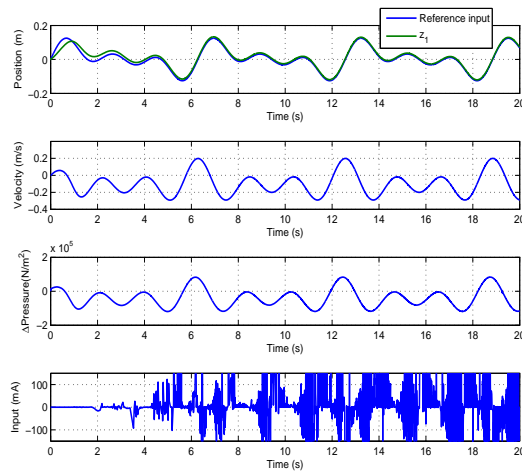


Figure 6.20: Behavior of the hydraulic servo system $r = 0.05(\sin(t) + \sin(2t) + \sin(3t))\text{m}$



(a) $r = 0.3\text{m}$

(b) $r = 0.1\sin(t)\text{m}$



(c) $r = 0.05(\sin(t) + \sin(2t) + \sin(3t))\text{m}$

Figure 6.21: Behavior of the perturbed hydraulic servo system under an adaptive control with time-varying gain.

CHAPTER 7

CONCLUSIONS AND FUTURE WORK

In this thesis, backstepping-based controller was developed for hydraulic servo system subject to uncertain parameters and unknown but bounded disturbance. The work is basically organized in three main folds. In the first part, both constant and time varying gain controller were developed using backstepping technique while, the second part dealt with constructing state observer to estimate the states of the system. Lastly, an adaptive controller is developed to handle parameter variations.

7.1 Conclusions

The mathematical model of the electro-hydraulic system used in this thesis reflects the real behavior of the system. The model takes into consideration leakages which were most times neglected in theoretical analysis. Having employed a proper model for the system, we proposed a backstepping-based robust adaptive controller for the hydraulic servo system rod subject to uncertainty in parameters and to an unknown but bounded disturbance. The controller compasses a design parameter that can be tuned to ensure close convergence of the tracking error to

a vicinity of zero. By using Lyapunov approach with the assumptions that all the states are measurable, the controller is practically stable and the tracking error is globally uniformly ultimately bounded. Also, we studied the problem of stabilization using estimated states by constructing a high gain observer to estimate the unavailable states and subsequent use the estimates in the feedback. We again showed that under mild conditions, the stabilizing controller built using estimated states will also stabilize the system in question. Hence, the EHSS is observable if we only measure the displacement of the piston. Finally, we overcame the problem of variation in parameters by using a backstepping based adaptive control schemes that is robust to uncertainties in the system's parameters and external disturbance.

7.2 Future works

The design of a high observer pose a number of open issues. First, the construction of this observer is based on the exact knowledge of system's parameters and this limits its area of application. In the event of any parameter changes, its performance deteriorates. Choosing high gain to attenuate the effect of parametric uncertainties may lead to large estimation errors due to noise and jumps in measured signal. Secondly, if there is parameter mismatch in nominal model and actual system, then the observer with fixed parameters can lead to large transient state estimation errors. Solving this problem with an adaptive observer will be a welcome idea. Lastly, developing control laws for the system in order to handle

frequency sweeps higher than 17 Hz will be a very interesting problem.

REFERENCES

- [1] Z. Wei, “Modelling and modal analysis of seismic vibrator baseplate,” in *Geophysical Prospecting*, vol. 58. Stafford TX: EAGE, November 2010, p. 1931.
- [2] H. Angue-Mintsa, R. Venugopal, J. Kenne, and C. Belleau, “Feedback linearization-based position control of an electrohydraulic servo system with supply pressure uncertainty,” in *IEEE Transactions on Control Systems Technology*, vol. 20, no. 4. IEEE, July 2012, pp. 1092–1099.
- [3] I. Beresnev, “Ground force orplate displacement based vibrator control,” *Journal of Sound and Vibration*, vol. 331, pp. 1715–1721, 2012.
- [4] C. Bagaini, T. Dean, J. Quigley, and G. Tite, “Systems and methods for enhancing low-frequency content in vibroseis acquisition,” Jun. 14 2007, uS Patent App. 11/299,411. [Online]. Available: <http://www.google.je/patents/US20070133354>
- [5] S. Ibrir, “On observer design for nonlinear systems,” *International Journal of Systems Science*, vol. 37, no. 15, pp. 1097–1109, 2006.

- [6] E. Kolsi-Gdoura, M. Feki, and N. Derbel, "Position control of a hydraulic servo system using sliding mode with discontinuous surface," in *International Multi-Conference on Systems, Signals and Devices*. Barcelona: IEEE, February 2014, pp. 1–6.
- [7] C. Kaddiddi, J. Kenne, and M. Saad, "Indirect adaptive control of an electrohydraulic servo system based on nonlinear backstepping," in *IEEE International Symposium on Industrial Electronics*. Montreal, Que: IEEE, Sept 2006, pp. 3147–3153.
- [8] T. Ling, M. Rahmat, A. Husain, and R. Ghazali, "System identification of electro-hydraulic actuator servo system," in *4th International Conference on Mechatronics (ICOM)*, vol. 58. Kuala Lumpur, Malaysia: IEEE, May 2011, pp. 1–7.
- [9] H. Hao and L. Huihu, "Modeling and simulation of flow field of main spool in servo valve," in *International Conference on Electronic & Mechanical Engineering and Information Technology*, vol. 2. Heilongjiang, China: IEEE, August 2011, pp. 867–870.
- [10] S. Hutamarn and P. Pratumswan, "Neuro-fuzzy based on support vector machine friction compensator in servo hydraulic system," in *IEEE Conference on Industrial Electronics and Applications*. Singapore: IEEE, July 2012, pp. 2118–2122.

- [11] X. Wang and S. Wang, “High performance adaptive control of mechanical servo system with lugre friction model:identification and compensation,” *Journal of Dynamic Systems, Measurement, and Control*, vol. 134, no. 1, pp. 1–7, 2012.
- [12] A. Bonchis, P. Corke, D. Rye, and Q. Ha, “Variable structure methods in hydraulic servo system control,” *Automatica*, vol. 37, no. 4, pp. 589–595, 2001.
- [13] J. Shao, Z. Wang, J. Lin, and G. Han, “Model identification and control of electro-hydraulic position servo system,” in *International Conference on Intelligent Human-Machine Systems and Cybernetics*, vol. 1. Hangzhou, Zhejiang: IEEE, August 2009, pp. 210–213.
- [14] T. Lim, “Pole placement control of an electrohydraulic servo motor,” in *International Conference on Power Electronics and Drive Systems*, vol. 1. IEEE, May 1997, pp. 350–356.
- [15] M. Ahmed, N. Lachhab, and F. Svaricek, “Non-model based adaptive control of electrohydraulic servo systems using prefilter inversion,” in *9th International Multi-Conference on Systems, Signals and Devices*. Chemnitz: IEEE, March 2012, pp. 1–6.
- [16] R. Xiang and Z. Yinyin, “Electro-hydraulic position synchronization control system based on auto-disturbances rejection and feedback,” in *World Automation Congress*. Puerto Vallarta, Mexico: IEEE, June 2012, pp. 1–4.

- [17] H. Angue-Mintsa, R. Venugopal, J. Kenne, and C. Belleau, "Adaptive position control of an electrohydraulic servo system with load disturbance rejection and friction compensation," *Journal of Dynamic Systems, Measurement, and Control*, vol. 133, no. 6, pp. 1–7, 2011.
- [18] L. Lai, "A synchronization position control method based on dynamic particle swarm optimization algorithm in electro-hydraulic servo system," in *IET International Conference on Smart and Sustainable City*. Shanghai: IEEE, August 2013, pp. 23–26.
- [19] H. Chen, J. Renn, and J. Su, "Sliding mode control with varying boundary layers for an electro-hydraulic position servo system," *The international Journal of Advanced Manufacturing Technology*, vol. 26, no. 1, pp. 117–123, 2005.
- [20] R. Tang and Q. Zhang, "Dynamic sliding mode control scheme for electrohydraulic position servo system," *Procedia Engineering*, vol. 24, pp. 28–32, 2011.
- [21] L. Xinliang, J. Shan, Z. Jing, and X. Wang, "Adaptive sliding mode position control of electro-hydraulic servo system with single rod actuators," in *IEEE International Symposium on Robotic and Sensors Environments*. Washington, DC: IEEE, October 2013, pp. 220–225.
- [22] S. Rozali, M. Kamarudin, M. Rahmat, and A. Husain, "Asymptotic tracking position control for nonlinear systems using backstepping technique," *Proce-*

dia Engineering, vol. 53, pp. 255–263, 2013.

- [23] K. I. K. M and P. Kokotovic, *Nonlinear and Adaptive Control Design*, 1995.
- [24] Z. Dashti, M. Gholami, M. Jafari, and M. Shoorehdeli, “Neural-adaptive control based on backstepping and feedback linearization for electro hydraulic servo system,” in *Iranian Conference on Intelligent Systems*. Bam: IEEE, February 2014, pp. 1–6.
- [25] H. Yanada and K. Furuta, “Adaptive control of an eletrohydraulic servo system utilizing online estimate of its natural frequency,” in *International Conference on Power Electronics and Drive Systems*, vol. 17, no. 6. Elsevier, July 2007, pp. 337–343.
- [26] Z. Zhang and W. Chen, “Adaptive output feedback control of nonlinear systems with actuator failures,” *Information Sciences*, vol. 179, no. 24, pp. 4249–4260, 2009.
- [27] G. Tao, S. Chen, and S. Joshi, “An adaptive control scheme for systems with unknown actuator failures,” *Automatica*, vol. 38, no. 6, pp. 1027–1034, 2002.
- [28] H. Mintsu, J. Kenne, and R. Venugopal, “Adaptive control of an electrohydraulic position servo system,” in *AFRICON*. Nairobi: IEEE, Sept 2009, pp. 1–6.
- [29] M. Choux, H. Karimi, G. Hovland, M. Hansen, M. Ottestad, and M. Blanke, “Robust adaptive backstepping control design for a nonlinear hydraulic-

- mechanical system,” in *Joint 48th IEEE Conference on Decision and Control*. Shanghai, China: IEEE, December 2009, pp. 2460–2468.
- [30] F. Ursu, I. Ursu, and E. Munteanu, “Adaptive backstepping type control for electrohydraulic servos,” in *Mediterranean Conference on Control and Automation*. Athens: IEEE, June 2007, pp. 1–6.
- [31] J. J. Sallas, “How do hydraulic vibrators work? a look inside the black box,” in *Geophysical Prospecting*, vol. 58. Plano, TX: EAGE, August 2010, pp. 3–17.
- [32] M. Feki, “Synthese de commandes et d observateurs pour les systemes non-lineaires: Application aux systemes hydrauliques,” Ph.D. dissertation, Universite de Metz, Metz-France, June 2001.
- [33] A. Mohanty, S. Gayaka, and B. Yao, “An adaptive robust observer for velocity estimation in an electro-hydraulic system,” *International journal of adaptive control and signal processing*, vol. 26, no. 10, pp. 1076–1089, 2012.
- [34] J. Hedrick, R. Rajamani, and K. Yi, “Observer design for electronic suspension applications.” *Vehicle System Dynamics*, vol. 23, no. 1, p. 413440, 1994.
- [35] M. Vidyasagar, “on the stabilization of nonlinear systems using state detection,” *IEEE Transaction on Automatic Control*, vol. 25, no. 3, p. 504509, 1980.

- [36] J. Tsiniias, "A generalization of vidyasagars theorem on stabilizability using state detection," *Systems & Control Letters*, vol. 17, no. 1, p. 3742, 1991.
- [37] F. Chen and W. Zhang, "Lmi criteria for robust chaos synchronization of a class chaotic system," *Nonlinear Analysis*, vol. 67, no. 12, pp. 3384–3393, 2007.

Vitae

- Name: Ayinde Babajide Odunitan
- Nationality: Nigerian
- Date of Birth: 31/07/1985
- Email: *jideayinde07@gmail.com*
- Permanent Address: AX2A Surulere Street, Isokun, Ilesa, Osun State, Nigeria.
- B.Sc degree from Obafemi Awolowo University (Nigeria) in Electronic and Electrical Engineering (2010).
- Texas A&M University (USA)-Credits Transferred (2013).
- MS degree from KFUPM (Saudi Arabia) in Systems and Control Engineering (2015).

Refereed Journal Papers:

- S. Ferik, **B. Ayinde**, S. Ibrir and M. Feki, "Backstepping-based Robust Adaptive Output Feedback Control of Electrohydraulic Servo System", submitted to International Journal of Control, Feb. 2015, under revision.

- S. Ferik, **B. Ayinde**, S. Ibrir and M. Feki, "Robust Adaptive Backstepping Control of Electro Hydraulic Actuator", submitted to Journal of Sound and Vibration, Nov. 2014, under revision.

Refereed Conference Papers:

- **B. Ayinde** and A. Barnawi, "Differential Evolution Based Deployment of Wireless Sensor Network", to appear in ACS/IEEE International Conference on Computer Systems and Applications, Pg. 131-137, 2014.
- **B. Ayinde**, S. Ferik, S. Ibrir and M. Feki, "Backstepping Control of an Electro-hydraulic Servo System Subject to Disturbance and Parameter Uncertainty", to appear in 8th IEEE GCC Conference and Exhibition, Oman, 2015.
- S. Ferik, **B. Ayinde**, S. Ibrir and M. Feki, "Backstepping-based Output Feedback Control of an Electro-hydraulic Servo System", to appear in International Conference on Systems, Analysis and Automatic Control, Tunisia, 2015.